



universität
wien

MASTERARBEIT / MASTER'S THESIS

Titel der Masterarbeit / Title of the Master's Thesis

„Effects of Low-Dose Hypericin-PDT on Murine BMDCs
and Subsequent Induction of Regulatory T Lymphocytes“

verfasst von / submitted by

Nicole Maeding

angestrebter akademischer Grad / in partial fulfilment of the requirements for the degree of
Master of Science (MSc)

Wien, 2017 / Vienna 2017

Studienkennzahl lt. Studienblatt /
degree programme code as it appears on
the student record sheet:

A 066 830

Studienrichtung lt. Studienblatt /
degree programme as it appears on
the student record sheet:

Molekulare Mikrobiologie, Mikrobielle Ökologie und
Immunbiologie / Molecular Microbiology, Microbial
Ecology and Immunobiology

Betreut von / Supervisor:

Univ.-Prof. Dr. Barbara Krammer

:

Declaration of Authorship

Herewith I declare that this thesis was written on my own. I confirm that no sources other than those specified in this thesis have been used. Furthermore, I announce that parts of the introduction of this thesis have been published in form of a review under my first authorship in advance. Parts to which this applies have been indicated and the original manuscript can be found in Appendix V.

Nicole Maeding

Wals-Siezenheim, June 25th, 2017

Acknowledgements

I thank everyone who helped me in developing and conducting this study for their teaching, their support and above all their encouragement.

Mum, this is for you. Thank you for always believing in me.

Abstract

Photodynamic therapy (PDT) is a cancer treatment modality which is based on three components: a non-toxic photosensitizer (PS), visible light and molecular oxygen. After accumulation of the PS in the target cells and irradiation with light, reactive oxygen species are generated causing cytotoxicity. Destruction of tumor cells as a result of PDT treatment happens either directly or indirectly by e.g. PDT-stimulated immune reactions against the lesion. In the latter case the tumor cells can be targeted by the immune system as a consequence of the induction of an inflammatory response and the initiation of tumor-specific immune reactions. In this context, generation of memory immunity *in vivo* and a requirement for dendritic cells (DC) for PDT efficiency has been shown. However, tumors are known to generate a tolerogenic environment to evade immune recognition, including the induction of regulatory T cells (Treg). In order to enable a tumor-specific immune response and generate memory immunity, tolerance towards the tumor must have been breached at some point due to the treatment. We hypothesized that PDT treatment might skew DC-mediated induction of Treg in the tumor microenvironment towards effector T cell differentiation, thereby promoting recognition and elimination of the tumor.

Since information about the direct effects of PDT on DCs is rare, this study was designed to evaluate two aspects: Part 1 was designed to assess direct effects of PDT using hypericin as PS on DCs, while the second part evaluated the capacity of treated DCs to induce Treg and effector T cells in a co-culture system of PDT-DCs and naive OVA antigen specific T lymphocytes. DCs showed increased proliferation at concentrations up to 100 nM hypericin and a cytotoxic effect at concentrations higher than 200 nM in response to PDT (irradiation with a fluence of 1.1 J/cm^2 at 610 nm). Additionally, expression of proinflammatory IL-12 was upregulated and anti-inflammatory TGF- β was downregulated with low-dose treatment (80 nM). In contrast, at 300 nM hypericin expression of IL-12 and IL-6 was downregulated while TGF- β was similar to untreated controls. Induction of Treg by PDT-DCs displayed a tendency towards reduced Treg levels in response to low-dose treatment. Secretion of IFN- γ and IL-17 showed similar IFN- γ levels across all treatment conditions and increased IL-17 levels in co-cultures with 300 nM hypericin-PDT treated DCs and high doses of antigen.

In summary, this study shows a beneficial effect of low-dose hypericin-PDT on DC viability and proinflammatory capacity. Furthermore, it points to diminished induction of Treg by PDT-DCs and maintenance of normal effector T cell induction comparable to that seen with untreated DCs.

List of Abbreviations

aa	amino acids
Ab	antibody
ACK	ammonium-chloride-potassium complex
APC	antigen presenting cell
ATP	adenosintriphosphate
BMDC	bone marrow-derived dendritic cell
bp	basepairs
BPD	Benzoporphyrin derivative
BSA	bovine serum albumin
β-ME	beta-Mercaptoethanol
CD	cluster of differentiation
cDNA	complementary DNA
CRT	calreticulin
CSN	Conditioned supernatant
Ct	Cycle threshold
CTLA-4	cytotoxic T-lymphocyte-associated protein 4
CTL	cytotoxic T lymphocyte
Cq	Cycle of quantification
CXCL	Chemokine (C-X-C) ligand
CXCR	Chemokine (C-X-C) receptor
DAMP	Damage-associated molecular pattern
DC	Dendritic cell
DEPC	Diethylpyrocarbonate
DMEM	Dulbecco's Modified Eagle's Medium
DMSO	Dimethylsulfoxide
DNA	Deoxyribonucleicacid
dNTPs	Deoxynucleotide triphosphates
FACS	Fluorescence activated cell sorting
FCS	fetal calf serum
FITC	Fluoresceinisothiocyanate
FoxP3	forkhead box protein 3
FSC	Forward scatter
GM-CSF	granulocyte macrophage-colony stimulating factor
g	Gram
G418	genitacin
h	Hour
H ₂ O	Water
HMGB1	High-mobility group box 1 protein
HPRT	hypoxanthine phosphoribosyltransferase 1
HSP	Heat-shock protein
ICAM-1	intracellular adhesion molecule 1
ICD	Immunogenic cell death
IFN	Interferon
IL	Interleukin
i.v.	intravenously
J	Joule

kg	kilogram
LD	lethal dose
LDL	Low-density lipoprotein
LPS	Lipopolysaccharide
MEM	Minimal Essential Medium
MHC	Major histocompatibility complex
MIP	Macrophage inflammatory protein
mg	milligram
μg	microgram
mM	millimolar (millimol per liter)
μM	Micromolar (micromol per liter)
mRNA	messenger RNA
MTT	3-[4,5-dimethylthiazol-2-yl]-2,5-diphenyltetrazolium bromide
mW	Milli-Watt
NaAc	Sodiumacetate
NK cells	Natural killer cells
nM	nanomolar (nanomol per liter)
nm	nanometer
OVA	Ovalbumin
PBS	Phosphate buffered saline
PCR	Polymerase chain reaction
PDT	Photodynamic therapy
PE	Phycoerythrine
PS	Photosensitizer
pTreg	peripheral Treg
qRT-PCR	quantitative real time reverse transcriptase PCR
RFU	relative fluorescence unit
RNA	Ribonucleic acid
ROR _γ t	RAR-related orphan receptor gamma
ROS	Reactive oxygen species
rpm	rounds per minute
RPMI	Roswell Park Memorial Institute
RT	Room temperature
s	Second
s.c.	subcutaneously
SEM	standard error of the mean
SFM	serum-free medium
SSC	Sideward scatter
TAE	Tris-acetate-EDTA
TAM	Tumor-associated macrophage
TCR	T cell receptor
TDLN	Tumor-draining lymph node
TGF-β	Transforming growth factor beta
Th1	T helper cell type 1
Th2	T helper cell type 2
TME	Tumor microenvironment
TNF	Tumor necrosis factor
Treg	regulatory T cell
tTreg	thymic Treg

o.n.	Over night
V	Volt

Table of Contents

1. Introduction.....	1
1.1 Photodynamic Therapy (PDT).....	1
1.2 Physicochemical Basis of PDT.....	2
1.3 Photosensitizer Properties and Delivery.....	3
1.4 Biological Consequences of PDT.....	6
1.4.1 Cell Death.....	6
1.4.2 Stimulation of Innate Immunity.....	7
1.4.2.1 Cytokine Release.....	8
1.4.2.2 Neutrophils.....	9
1.4.3 Specific Anti-Tumor Immunity.....	10
1.4.3.1 CD4 ⁺ T Helper Cells.....	12
1.4.3.2 CD8 ⁺ Cytotoxic T Lymphocytes (CTL).....	14
1.4.3.3 Regulatory T Cells (Treg).....	14
1.4.3.4 Dendritic Cells.....	16
2. Aim of the Study.....	17
3. Materials and Methods.....	19
3.1 Cell Culture.....	19
3.1.1 Thawing and Maintenance of Cells.....	19
3.1.2 GM-CSF Cell Culture and Generation of GM-CSF-conditioned Supernatant.....	19
3.1.3 Production of IL-6-conditioned Supernatant.....	21
3.1.4 Culture of GK1.5 and N418 Cells.....	22
3.1.5 Bone Marrow-Derived Dendritic Cells.....	23
3.1.5.1 Isolation of Bone Marrow Cells from Mouse Femur.....	23
3.1.5.2 Generation of Dendritic Cells from Bone Marrow Cells.....	23
3.1.6 BMDC-T-cell Co-Culture.....	24
3.1.6.1 General Co-Culture Protocol.....	25
3.1.6.2 BMDC-Splenocyte Co-Culture.....	25
3.1.6.3 BMDC-T-Lymphocyte Co-Culture.....	26
3.2 Assays and Treatments.....	26
3.2.1 Dark Cytotoxicity.....	26
3.2.2 Phototoxicity Assay.....	26
3.2.3 PDT Treatment, Maturation and Antigen Loading of BMDCs for Co-Culture....	27
3.2.4 MTT Assay.....	28
3.2.5 RNA Isolation.....	29

3.2.6	cDNA Generation.....	29
3.2.7	Quantitative Real-Time PCR.....	30
3.2.7.1	Primer Design.....	30
3.2.7.2	qRT-PCR.....	31
3.2.8	FACS Analysis.....	32
3.2.9	Sandwich ELISA.....	34
3.3	List of Chemicals, Reagents and Equipment.....	36
4.	Results.....	42
4.1	Dark Cytotoxicity.....	42
4.2	Light-dependent Cytotoxicity.....	43
4.3	Induction of Cell Death in Tumor Cell Lines with Low-Dose Treatment.....	44
4.4	Expression of Cytokine mRNA in BMDCs in Response to PDT.....	46
4.4.1	Expression of IL-1 β and IL-6.....	46
4.4.2	Expression of IL-12 and TGF- β	48
4.5	Secretion of IL-6 by BMDCs in Response to PDT.....	50
4.6	Titration of OVA Peptide Dose.....	52
4.7	Induction of Regulatory T Cells by PDT-treated BMDCs in Response to OVA.....	54
4.8	Cytokine Secretion by T Cells in the Co-Culture.....	55
4.8.1	IFN γ in the Co-Culture Supernatant.....	55
4.8.2	IL-17A in the Co-Culture Supernatant.....	55
5.	Discussion.....	59
6.	Conclusion.....	70
7.	References.....	72
	Appendix I: Summary.....	81
	Appendix II: Zusammenfassung.....	82
	Appendix III: List of Figures.....	83
	Appendix IV: List of Tables.....	84
	Appendix V: Published Review ‘Boosting Tumor-Specific Immunity Using PDT’.....	85

1. Introduction

In the past century cancer has emerged as one of the major health threats we are facing, with a global incidence of 14.1 million new cases per year (2012, cancerresearchuk.org). Due to intensive research, there are a variety of treatment options available by now, which have proven to be successful in controlling the primary tumor or even metastases.

A shortcoming of those options lies within the nature of the employed treatment methods: two of the three classical therapies, namely chemotherapy and radiotherapy, are toxic to the host. Specifically, they cause severe bystander damage to non-malignant tissue and the hematopoietic system. Bone marrow hypoplasia and aplasia are quite common, leading to decreasing blood cell counts. This includes immune cells, thus inhibiting the host's ability to mount efficient immune responses against recurring tumors and developing metastases as well as pathogens. Especially if repeated treatment cycles are required the bone marrow increasingly loses its capacity for self-renewal. Another risk of those therapies is that emergence of other cancer types can be promoted by the treatment itself. More recent approaches which are less harmful to the patient show different limitations: targeted antibody therapies like with trastuzumab against HER2/neu in breast cancer prove to be successful. Unfortunately, they are only applicable for patients carrying the corresponding mutation of the target and this usually pertains to the minority of cases. Additionally, resistances against targeted therapies are increasingly emerging. Thus, there is a substantial need for treatment modalities that show good control of primary tumors, boost the host's immune system to enable effective anti-tumor immunity and that constitute a therapeutic option for the majority of patients.

1.1 Photodynamic Therapy (PDT)

An alternative treatment within the field of cancer therapies is photodynamic therapy (PDT). PDT is a clinically approved cancer treatment which is used for treatment of early staged disease, superficial cancer types and as palliative easement in terminal/late staged cancers. It offers the advantage of minimal side effects for the patient while maintaining high efficiency¹⁻³. Additionally, it is simple and cost effective. PDT employs a light-sensitive photosensitizer (PS) and visible light of appropriate wavelength to excite the PS. After local or systemic application the PS accumulates in a tumor-specific manner and is subsequently photo-

activated. In the presence of molecular oxygen this leads to generation of reactive oxygen species (ROS) which induces target cell destruction by apoptotic and necrotic cell death ⁴. Furthermore, indirect effects facilitate tumor destruction, i.e. vascular shut-down and induction of an inflammatory response and immune reactions targeted against the tumor (see below) ^{1,5}. A major benefit of PDT is that, despite its tumor-selective accumulation, it is a non-targeted therapy. Therefore it does in general not induce resistances and offers a strategy to overcome inter- and intra-tumoral heterogeneity. Since commonly used PS do not enter the nucleus, mutagenic transformation can be excluded as well.

1.2 Physicochemical Basis of PDT

PDT requires three basic components: a light-sensitive PS, a light source of appropriate wavelength and a molecule in the triplet state to take up the energy from the excited PS. The only molecule in the body naturally occurring in the triplet state is molecular oxygen. Upon excitation with light the PS is promoted from its energetic ground state S_0 to the instable S_1 level (Fig. 1). From this state the molecule can either directly revert back to the ground state by emitting the surplus energy as fluorescence or it can undergo a so-called intersystem crossing. The emission of fluorescence can be detected and – due to preferential accumulation of the PS in the tumor – is used for diagnostic use. The intersystem crossing, which results in reversal of the spin of the excited electron so that both electrons have the same spin, is the first step of the subsequent processes that make PS suitable for therapeutic use: Firstly, the excited molecule can lose the surplus energy via emitting it as phosphorescence without involvement of other molecules. Secondly, the excited PS can react with surrounding molecules via electron or hydrogen transfer (type I reaction). This results in transition of the PS to its ground state and production of reactive oxygen species (ROS; O_2^- , H_2O_2 , OH^\cdot). Thirdly, singlet oxygen 1O_2 can be produced by direct energy transfer from the PS to ground-state molecular oxygen 3O_2 (type II reaction). ROS are highly reactive molecules and they are known to have various harmful effects on cells. These include DNA damage, lipid peroxidation, oxidation of amino acids in proteins and oxidative deactivation of enzymes by oxidation of co-factors. More importantly, exposition to excessive amounts of ROS result in cell death via apoptosis, autophagy and necrosis ⁴.

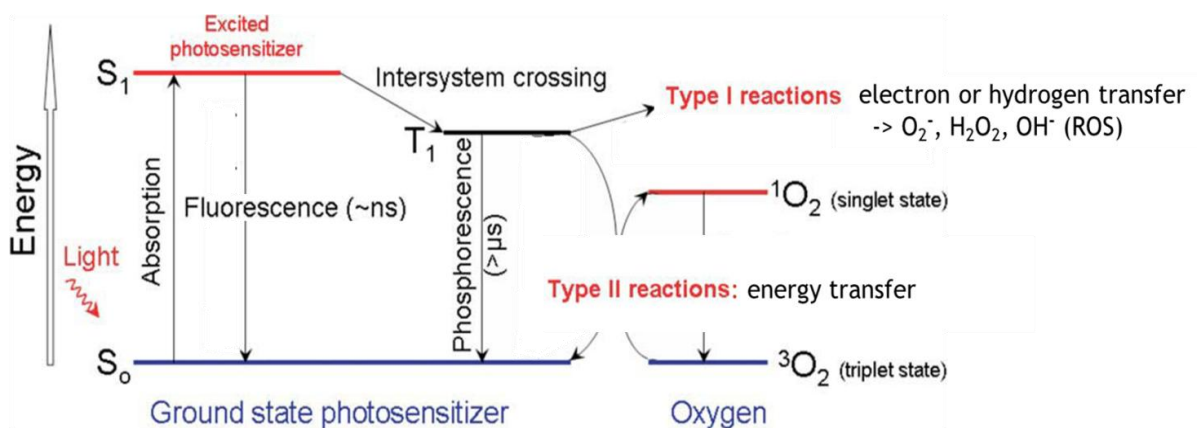


Figure 1: Photochemical Reactions upon Excitation of a PS with Light. Jablonski diagram modified from Agostinis et al ¹.

1.3 Photosensitizer Properties and Delivery

The ideal photosensitizer would foremost fulfill the following requirements: preferential accumulation in the target tissue, an absorption peak between 600 and 800 nm to allow for maximal treatment depth and no dark cytotoxicity and rapid clearance from normal tissue to avoid collateral damage from phototoxic side effects ¹.

Obviously, selective targeting of the tumor tissue is a desirable feature of any anti-cancer agent to maximize specificity of the therapy and spare healthy tissue. It is well established that PSs predominantly accumulate in tumor tissue, a feature which makes it possible to employ them for either diagnostic use (detection of emitted fluorescence to verify localization and extension of the tumor) or therapeutic intervention (destruction of tumor cells via direct and indirect effects) ^{1,4}. Although the underlying mechanisms for their localization may vary among different PS, there are a number of hypotheses concerning this important property. These include binding of the PS to low-density lipoprotein (LDL) for which the receptor has been shown to be upregulated on tumor cells, retention of PS within tumors by tumor-associated macrophages (TAM) which can contain high levels of PS due to their naturally increased phagocytic capacity and accumulation of PS within the tumor mass as a result of incomplete construction of the stroma (e.g. by loss of E-cadherin leading to accumulation of hypericin in the tumor ⁶), leaky tumor vessels and diminished lymphatic drainage (enhanced permeability and retention effect) ⁷. However, albeit most systemically applied PS show

preferential accumulation in tumor tissue, some of it will remain in normal tissue and this can result in unintended damage of varying degree, e.g. upon exposure to scattered light or sunlight ³. To improve target specificity, efforts are being made to couple the PS to molecules which have a high affinity and / or specificity for corresponding molecules on specific tumors (e.g. certain receptors). Vehicles in question for this include LDL, proteins, peptides, monoclonal antibodies and antibody fragments ⁸. Especially the eradication of circulating tumor cells by PDT could benefit from such an approach: efforts are being made to target these cells with antibody-conjugated PS and conduct extracorporeal illumination of the blood afterwards to destroy the aberrant cells ⁹.

After application, the PS has to be photoactivated by illumination. To do so, the light has to penetrate the tissue deep enough to reach the treatment area which is only possible for light in the range of 600 to 1200 nm. However, the penetrating light has to have sufficient energy to result in a photodynamic reaction and generate $^1\text{O}_2$. This is only achievable with light of up to 800 nm. Therefore, useful PS need to have an absorption peak between 600 and 800 nm. To circumvent the limitations arising from this (restriction of applicability by tumor site accessibility, penetration depth and tumor size) the past years have seen several efforts to develop advanced protocols: for the treatment of solid tumors and lesions in parenchymal organs interstitial PDT and self-illuminated PDT are under investigation. The first approach employs optical fibres as a light source which are implanted in the tumor whereas the second uses bioluminescent quantum dots as an internal light source for the PS ^{10–13}.

Naturally, harmful phototoxic side effects are undesirable and need to be avoided. Hence, PS used for treatment should display minimal to no dark toxicity and rapid clearance from normal tissue. Additionally, it has been proposed that photobleaching (light-mediated destruction) of the PS might be a beneficial feature since overtreatment would be avoided. Furthermore, this would reduce the risk of phototoxic side effects generated by PS which had been released from dying tumor cells and localized elsewhere ^{3,14}.

Table 1 gives an overview of clinically approved PS and their applications. A detailed review on the properties, advantages and disadvantages of these PS is given by Allison and Sibata ³. A PS not on this list is hypericin. Hypericin is an active constituent of *Hypericum perforatum* (St. John's wort) and a naturally occurring photosensitizer. Chemically it is a naphthodianthrone, a lipophilic anthraquinone derivative with antibacterial, antiviral and antidepressant activity ¹. It is successfully used in fluorescence guided detection of cancerous tissue due to its high tumor selectivity. Besides the pronounced tumor selectivity, hypericin

shows minimal dark cytotoxicity and is photoactivated at a wavelength of 610 nm within cells. Moreover, it is the only PS so far which has been shown to induce all major hallmarks of immunogenic cell death, an immunogenic form of cell death leading to the generation of a tumor-specific immune response ^{15,16}. Taken together, these factors make hypericin a very promising candidate for therapeutic use. However, it is still not a clinically approved PS. This might be – at least partially – due to economic reasons: as a naturally occurring substance hypericin cannot be patented which inherently limits interest from pharmaceutical companies – despite the attention it gains from academic research. Furthermore, it was shown that hypericin can induce anti-inflammatory processes and even result in resistance to PDT under certain circumstances ^{17–19}. Therefore, meticulous research on the precise parameters when and how to use hypericin in PDT for cancer treatment would be needed to change the status of this promising PS from experimental to clinically approved.

Table 1: Clinically Approved Photosensitizers and Their Indications

Trade Name	Drug	Indications	Approval
Foscan®	Meso-tetrahydroxy-phenyl chlorine	Head and neck Cancer	EU, Iceland, Norway
Laserphyrin®	Mono-L-aspartyl chlorine e6	Lung cancer	Japan
Levulan®	Aminolevulinic acid	Actinic keratosis, esophageal dysplasia	EU, USA
Metvixia®	Methyl aminolevulinate	Actinic keratosis, basal cell carcinoma, non-melanoma skin cancer	Australia, EU, New Zealand, USA
Photofrin®	Hematoporphyrin derivative	Bladder cancer, lung cancer, cervical dysplasia and cervical cancer, gastric cancer, esophageal cancer, Barrett's esophagus	Canada, Denmark, EU, Finland, Japan, UK, USA
Photosense®	Sulfonated aluminum	Various cancers	Russia

phthalocyanine			
Visudyne®	Benzoporphyrin derivative monoacid	Wet age-related macular degeneration, pathologic myopia, histoplasmosis	Canada, EU, Japan, USA

1.4 Biological Consequences of PDT (Published as Part of the Review ‘Boosting Tumor-Specific Immunity Using PDT’²⁰)

The destruction of tumor cells as a result of PDT treatment happens either directly or indirectly. As a direct effect, the oxidation of proteins, lipids and DNA by ROS leads to stimulation of signaling processes which culminate in apoptosis and necrosis. Indirectly, tumor cells are killed by the vascular shutdown caused by the damage of endothelial cells and the vascular basement membrane. Subsequently, this leads to blood flow stasis, tissue hemorrhages and oxygen deprivation. Additionally, the tumor cells can be targeted by the immune system as a consequence of the induction of an inflammatory response and the initiation of tumor-specific immune reactions. This contributes to fighting off primary and secondary disease manifestations^{5,20}.

1.4.1 Cell Death

In general, PDT is able to result in apoptosis, necrosis, the so-called immunogenic cell death (ICD), and autophagy. Apoptosis is traditionally considered as a programmed form of cell death which is immunologically silent. The remnants of these “physiologically” dying cells are quickly removed afterwards by phagocytes. Therefore, cells undergoing apoptosis normally do not elicit a strong immune response or a detectable response at all, for that matter. In contrast to that, necrosis is the result of an insult or trauma that leads to rapid cell death. This form of cell death characteristically involves the uncontrolled release of cellular products and the initiation of an inflammatory response in the surrounding tissue, which can lead to severe bystander damage. Although an inflammatory response is necessary for the induction of the immune response, this process can be detrimental for the host when it cannot be resolved by

the immune system. In light of these definitions, one would assume that necrotic cells or a mixture of necrotic and apoptotic cells should be more efficient in facilitating the development of a distinct immune response than apoptotic cells. Contrasting this, there are numerous reports demonstrating that apoptotic cells are superior to necrotic cells in inducing antitumor immunity^{15,21–26}. Intensive research in the field of cell death in the following years led to the fairly new concept of ICD. ICD describes an immunogenic form of apoptosis or necrosis. Since the emergence of the concept of ICD it has been shown that tumor cells undergoing immunogenic apoptosis are more potent inducers of antitumor immune responses than cell dying via necrosis or nonimmunogenic apoptosis. Thus, it would be favorable to use and develop PSs which predominantly cause ICD in cancer cells for future approaches. Importantly, so far hypericin is the only PS shown to induce all major molecular and immunological hallmarks of ICD. This includes surface expression of CRT, HSP70, and HSP90 and secretion of ATP—four DAMPs crucial in ICD^{15,16}.

1.4.2 Stimulation of Innate Immunity

The local trauma inflicted by PDT treatment on the tumor cells, the vasculature, and the surrounding tissue causes induction and release of various mediators leading to an inflammatory reaction to initiate an immune response. The oxidative stress due to the excessive generation of ROS results in surface expression and secretion of damage-associated molecular patterns (DAMPs) as well as inflammatory mediators which are released from dying and damaged cells. DAMPs are molecules derived from host cells to signal cell injury or death. They predominantly comprise nuclear or cytosolic proteins which become released from the cell or exposed on its surface and serve in the initiation of a noninfectious immune response. Recognition of DAMPs via engagement with their respective receptors on infiltrating immune cells (so-called pattern recognition receptors, PRRs) aids in signaling the nature of the underlying threat to the immune system and enabling the appropriate immune response. DAMPs reported to be necessary for the generation of antitumor immunity and induced upon PDT include surface calreticulin (CRT), heat shock protein (HSP) 70, HSP90, ATP, and high-mobility group box 1 protein (HMGB1)^{27,28}. Inflammatory mediators include cytokines and chemokines. Cytokines are small, secreted proteins produced mostly by immune cells, but also by endothelial and stromal cells as well as fibroblasts. Their main function is to promote or inhibit proliferation, activation, and differentiation of immune cells, thus they are commonly divided

into proinflammatory and anti-inflammatory or immunosuppressive cytokines. Prominent examples for proinflammatory cytokines are interleukin (IL)-12 and IL-4, which are necessary for the differentiation of T helper cells type 1 (Th1) and type 2 (Th2), respectively. Classical anti-inflammatory or immunosuppressive cytokines include IL-10 and transforming growth factor (TGF)- β . IL-10 effectively inhibits expression of Th1 cytokines and major histocompatibility complex (MHC) II and macrophage activation. TGF- β inhibits cell proliferation and induces differentiation of regulatory T cells (Treg), an immunosuppressive subtype of T helper cells. Chemokines are small cytokines which build up gradients in the affected area and serve as chemoattractants. They are essential for directing the migration and activation of phagocytes and lymphocytes in the course of an inflammatory reaction. Guided by chemotactic gradients, inflammatory immune cells enter the affected region to launch an immune reaction and remove the source of the threat.

1.4.2.1 Cytokine Release

Elevated levels of a variety of cytokines have been shown in animal as well as human studies. Increased production of IL-6 appears to be a frequent event after PDT^{29–33}. IL-6 is considered to be a proinflammatory cytokine which stimulates the immune response, the induction of fever, and acute-phase proteins. However, results on the impact or function of IL-6 in PDT outcome differ. In a system of EMT6 tumors treated with Photofrin®-PDT, blocking of IL-6 with respective antibodies significantly reduced PDT-induced neutrophilia at 2 hours and 8 hours post-treatment³⁴. Contrasting this, another study found no effect of anti-IL-6 treatment on intratumoral neutrophil levels after PDT³⁰. Those contradictory findings may be attributed to the different photosensitizers used, evaluation of blood neutrophil levels vs intratumoral neutrophil numbers, and different treatment protocols and evaluation time points. Another prominent cytokine elevated after PDT is IL-1 β . In a model of rat rhabdomyosarcoma it was shown that increased IL-1 β preceded PDT-induced neutrophilia³⁵. In subsequent studies, other groups were able to demonstrate that IL-1 β is indeed a crucial mediator in PDT outcome and neutrophilia since blocking of this cytokine led to a significantly decreased rate of tumor cures and neutrophils in the tumor-draining lymph nodes (TDLN) in response to treatment^{36,37}. Other cytokines that have been reported to be elevated post PDT include tumor necrosis factor (TNF)- α and interferon (IFN)³⁸. The chemokines CXCL1 (chemokine (C-X-C) ligand 1 or keratinocyte chemoattractant, KC) and CXCL2 (macrophage inflammatory protein-2,

MIP-2) were also shown to be increased after PDT treatment in a murine model of EMT6 carcinoma. These two chemokines are known for possessing neutrophil chemoattractant activity. However, only CXCL2 was shown to be necessary for neutrophil migration into the tumors in this setting³⁰. In a rather recent report, Brackett et al. found induction of the cytokine IL-17 after treatment. This cytokine proved its importance by acting upstream of IL-1 β to regulate its expression levels. Thereby, it indirectly controlled the expression of CXCL2 which was dependent on IL-1 β . Diminished levels were found for TGF- β in the sera of CT26 colon carcinoma-bearing mice after PDT treatment with benzoporphyrin derivative (BPD)³⁹. Additionally, blockade of immunosuppressive cytokines TGF- β and IL-10 has been shown to greatly enhance PDT-mediated tumor cure rates in C3H/HeN mice with subcutaneous FsaR fibrosarcomas⁴⁰.

1.4.2.2 Neutrophils

The importance of neutrophils in PDT efficiency has been proven in numerous studies. Neutrophils pose the first line of defense against pathogens and inflammatory insults to the host. In order to do so they secrete leukotrienes, prostaglandins, and cytokines to initiate the development of the inflammatory response. Furthermore, they are able to directly kill pathogens and they have been reported to be able to present antigens via MHC class II under certain circumstances. This raises the possibility that neutrophils could aid in the activation of CD4⁺ T helper cells. Increased levels of neutrophils following PDT have been reported frequently^{36,37,41–43}. Moreover, Korbelik et al. showed that depletion of neutrophils led to a drop in mice cured from EMT6 tumors to 30%, with tumors recurring after 2–3 weeks⁴⁴. In line with this are findings from Kousis and coworkers demonstrating that neutrophil depletion resulted in diminished numbers of activated cytotoxic T lymphocytes (CTL) in the TDLN and the tumor tissue⁴⁵. In a different approach using blockade of neutrophil migration by administering anti-ICAM1 (intercellular adhesion molecule 1) the group of Sun demonstrated complete abrogation of the curative outcome of their treatment regimen. Additionally, this work showed an impairment of the curative effect following administration of anti-IL-1 β ³⁶. This finding was further highlighted by studies from Brackett et al.³⁷. In their setting, neutrophil entry into TDLN post-PDT was mediated by CXCR2–CXCL2 interaction, with CXCL2 induction being dependent on IL-17A and IL-1 β . Interestingly, the degree of neutrophil infiltration appears to be governed by the treatment regimen applied. Work from Shams et al. revealed that the high-

est degree of neutrophil influx into tumor tissue and TDLN was achieved with a treatment regimen delivering a low fluence at a low fluence rate. This was further accompanied by a substantial increase in activated CTL⁴⁶. A previous study already demonstrated the highest degree of induction of proinflammatory cytokines IL-6, MIP-1, and MIP-2 under these treatment conditions compared to regimens delivered at higher fluence and/or higher fluence rate³³.

1.4.3 Specific Anti-Tumor Immunity

The first evidence for induction of a tumor-specific immune response following PDT came from Canti et al. in 1994. This group demonstrated that normal mice cured from MS-2 fibrosarcoma by PDT were able to resist a rechallenge with tumor cells in a tumor-specific manner. In contrast to this, immunosuppressed counterparts were not able to resist the rechallenge⁴⁷. Since then, several studies have shown that an intact immune system—specifically the adaptive arm of the immune response—is crucial for PDT outcome. Korbelik et al. demonstrated that treatment of BALB/c mice bearing EMT6 mammary carcinomas with PDT resulted in complete cures, whereas SCID mice did not elicit the same antitumor response with the identical PDT regimen⁴². Since SCID mice lack mature T lymphocytes, they are not able to mount a cellular adaptive immune response. Likewise, the group of Preise successfully treated BALB/c mice with a vascular-targeted PDT approach from CT26 tumors with cure rates of more than 70%. When the same experiments were carried out in BALB/nude or SCID mice, cure rates dropped to 18% and 11% respectively⁴⁸. Similar findings were repeatedly reported from other groups as well over the years^{38,49,50}. Induction of systemic and memory immunity following PDT treatment has also been verified in numerous studies. Systemic immunity is reflected by the extension of the locally induced immune response to distant nontreated areas. A study by Kabingu and coworkers demonstrated the destruction of lung metastases indicative of an ongoing systemic immune response: mice were inoculated subcutaneously (s.c.) and intravenously (i.v.) with EMT6 tumor cells to generate a primary tumor (s.c.) and lung tumors mimicking metastases (i.v.). Treatment of the primary tumor with Photofrin®-PDT led to 90%–100% of tumor ablation, and analysis of lung metastases 10 days after PDT revealed a significant reduction of lung tumors compared to nontreated controls⁴⁹. Likewise, Mroz et al. reported regression of distant untreated tumors. In their model, mice bearing bilateral s.c. CT26.CL25 tumors were treated with BPD-PDT on one side while

the contralateral tumor was left untreated. In a total of seven out of nine mice, this approach led to complete and permanent regression of the contralateral tumor³⁸. Recent publications by other groups further support those findings^{46,50}. Additionally, clinical observations report the regression of lesions outside the treatment field after PDT-treatment as well, thus indicating the generation of systemic immunity in human patients^{51–53}.

Recurring disease can only be prevented when memory immunity is successfully generated. In experimental models of cancer, generation of such a memory immunity can be evaluated by resistance of previously cured subjects to rechallenge with the same type of cancer cells. The first study indicating the induction of tumor-specific immune memory was published by Korblick et al. in 1999: this work showed the ability of SCID mice to resist tumor cell rechallenge after they were cured from EMT6 tumors by a combination approach of adoptive transfer of tumor-sensitized splenocytes and PDT treatment⁵⁴. The group of Preiss demonstrated long-lasting protection against rechallenge in immunocompetent mice cured from primary tumors using a vascular-targeted approach of PDT. Interestingly, this approach even resulted in partial cross-protection against a different type of tumor cell used for rechallenge. However, the mechanism underlying this observation still remains to be elucidated⁴⁸. In another study by Sanovic et al., BALB/c mice bearing a s.c. CT26 colon carcinoma were treated with hypericin–PDT, and this treatment yielded a striking 100% of tumor cures, which lasted until the end of the study. Additionally, i.v. challenge of those cured mice with viable CT26 cells showed no development of new tumors, thereby indicating existence of systemic memory immunity. Notably, these results were obtained with a protocol using a low PS dose delivered at a low fluence and low fluence rate⁵⁵. Similar findings were reported by Mroz et al. who demonstrated 95% of cured mice resisting tumor development upon subsequent rechallenge³⁸. Reginato and coworkers achieved 90% of cures with a treatment protocol employing BPD and Treg depletion using cyclophosphamide in a CT26 tumor model. Sixtyfive percent of these mice rejected the rechallenge. However, with this protocol another round of Treg depletion prior to rechallenge was necessary to unravel the memory immunity³⁹. Interestingly, this group used the same type of tumor model (CT26 colon carcinoma in BALB/c mice) as Sanovic et al., whose studies showed no requirement for Treg depletion for therapeutic success. These differences might be attributed to the use of different PS (hypericin vs BPD) and/or differences in fluence and fluence rate (14 J cm^{-2} @ 27 mW cm^{-2} vs. 120 J cm^{-2} @ 100 mW cm^{-2}). Other groups assessed induction of memory immunity by resistance to rechallenge as well and reported results in line with the abovementioned findings^{46,50}.

The mediators of the adaptive immune response are antigen-specific B and T cells. Upon antigen recognition, B cells produce the antibodies necessary for eliminating extracellular pathogens. Although there are pieces of data pointing to a role for B cells in PDT-induced anti-tumor immunity^{42,48,50}, the importance of this humoral response has remained largely uninvestigated. In contrast to that, considerable efforts have been made over the past two decades to elucidate the role of the cellular immune response, i.e., the role of T lymphocytes (see below).

1.4.3.1 CD4⁺ T Helper Cells

T cells are divided into several subpopulations. When activated, CD4⁺ T helper cells differentiate into distinct lineages, a process which is dependent on the stimuli and cytokines present. Those lineages secrete defined cytokines to assist in clearance of intracellular pathogens and extracellular microorganisms. Furthermore, CD4⁺ T helper cells provide help for B cells and CD8⁺ cytotoxic T cells for their activation and the generation of memory cells. The best defined T helper cell populations are Th1, Th2, and Th17. Th2 cells and their associated cytokines—IL-4, IL-5, and IL-13—serve in the response to extracellular microorganisms and the induction of the B cell isotype switching. Th1 cells are characterized by production of IFN γ and are crucial for the eradication of intracellular pathogens. IFN γ is known to activate the bactericidal activity of macrophages and increase the expression of MHC I on normal cells and MHC II on APCs. Thereby it facilitates processing and presentation of endogenous antigens, which makes infected and aberrant cells visible to the immune system. Furthermore, IFN γ promotes activity of natural killer (NK) cells, which recognize and eliminate cells with decreased MHC I expression. Th1 cells have implications in antitumor immunity via activation and regulation of CTL, cross-priming of the immune response by APCs (this enables presentation of intracellular antigens in the context of MHC II), and direct tumor cell-killing through the release of specific cytokines⁵⁶.

The third subtype of T helper cells, that is well established by now, are Th17 cells and their signature cytokine IL-17. IL-17 leads to stimulation and de novo generation of neutrophils and is important in the response to certain extracellular bacteria and fungi⁵⁷. In cancer, Th17 cells seem to be able to have opposing roles. There are numerous reports showing eradication of tumors by Th17 cells and a beneficial effect of their abundance in the tumor microenvironment. However, an equally solid body of evidence suggests a role for this subpopulation in

tumor progression. This opposing impact of Th17 cells on tumor immunity seems to be attributable to the fact that the fine-tuning of their differentiation and function is highly dependent on a variety of factors; these include the type of tumor, the composition of stimuli leading to their activation (e.g., cytokine composition, T cell receptor signaling strength) and the therapeutic approach applied ⁵⁸. Interestingly, Th17 cells share ties with immunosuppressive Treg. In a proinflammatory environment, the decision of whether naïve T cells develop into either Treg or Th17 is dependent on the amount of available TGF- β : at low concentrations it synergizes with IL-6 and/or IL-21 and drives the induction of Th17 cells. At high TGF- β concentrations these cytokines are no longer sufficient to overcome Foxp3 (forkhead box protein 3)-mediated repression of retinoic acid receptor (RAR)-related orphan receptor (ROR)t, and the cells differentiate into Treg ⁵⁹. Additionally, Th17 cells are able to acquire a Th1-like phenotype with the ability to secrete IFN γ when they are exposed to IL-12 ⁵⁸. The role of T helper cells in PDT-mediated immunity is somewhat controversial. Experiments by Kabingu et al. showed no effect of CD4⁺ T cell depletion on PDT efficiency and induction of systemic anti-tumor immunity ⁴⁹. In contrast to that, other groups found a dependency of treatment outcome on the presence of CD4⁺ T cells. The group of Korbelik used antibodies for CD4, CD25, and a combination of both to deplete T helper cells, and saw a drop in cures by 30%–50% ^{44,54}. In line with this are results from others reporting delayed or abrogated tumor growth in naïve mice following adoptive transfer of CD4⁺ T cells from PDT-cured mice. Further analysis of this CD4⁺ population showed increased IFN γ secretion upon restimulation, which is indicative for the generation of a Th1 response ⁴⁸. However, the precise mechanisms by which CD4⁺ T cells contribute to PDT outcome remain largely elusive so far. Some light on this was shed by Brackett and coworkers, who showed an increase of Th17 cells and the corresponding signature cytokine IL-17A in the tumor-draining lymph nodes after PDT treatment ³⁷. In a very recent work Garg et al. found elevated levels of Th1 and Th17 cells in the brain immune contexture of mice treated with an immunogenic cell death (ICD)-based DC vaccine against high-grade glioma (HGG) and subsequently inoculated with the respective glioma cells. Furthermore, splenic T cells from these mice exhibited higher IFN production upon restimulation with naïve GL261 cell lysates, thus indicating expansion of localized immunostimulation in the brain to a systemic effect crucial for long-term immunity ²⁸.

1.4.3.2 CD8⁺ Cytotoxic T Lymphocytes (CTL)

CD8⁺ CTL are essential for recognition and elimination of cells that are virally infected or display aberrant self. CTL recognize intracellular peptide bound to MHC class I on the cell surface, and upon activation they exert direct cytolytic effects against the target cell accompanied by the secretion of IFN γ . First evidence for the involvement of CTL came from Korbelik et al. in 1999. This group used an EMT6 mammary carcinoma model in which depletion of CD8⁺ T cells led to a 50% decrease in cures after PDT compared to unmanipulated mice⁵⁴. Similar results were obtained by different groups using 2-iodo-5-ethylamino-9-diethylaminobenzo-phenotiazinium chloride or Photofrin® as photosensitizers, albeit Photofrin® was used in a combination approach with 5-aza-2'-deoxycytidine to induce the tumor antigen P1A^{60,61}. However, presence of P1A was not necessary to sustain long-term immunity. Likewise, adoptive transfer of CD8⁺ lymphocytes from cured animals was sufficient to protect naïve recipients from subsequent challenge with viable cancer cells from the same type^{48,61}. It should be noted that this protection did not show a requirement for additional transfer of CD4⁺ T helper cells. A study by Saji et al. further substantiates these findings with an experiment where the transfer of CD8⁺ T cell-depleted splenocytes from PDT-cured mice into naïve recipients conferred protection to rechallenge⁶². Other studies frequently found elevated levels of CD8⁺ T cells after treatment, and closer examination of those cells revealed increased lytic activity against tumor cells in an antigen-specific manner^{38,45,46}. On a clinical level, Abdel-Hady et al. were able to show that patients with vulval intraepithelial neoplasia who responded to PDT had increased levels of infiltrating CD8⁺ T cells after treatment⁶³.

1.4.3.3 Regulatory T Cells (Treg)

Regulatory T cells comprise a unique subset among the CD4⁺ T cell subpopulations. Treg cells display regulatory and suppressive activity towards other immune cells, and especially effector T cells. On the molecular level they are characterized by the constitutive expression of high levels of the transmembrane protein CD25 (IL-2R α chain)⁶⁴ and cytotoxic T lymphocyte-associated antigen 4 (CTLA-4)⁶⁵ and stable expression of the lineage-specific transcription factor Foxp3^{66,67}. By now, it is well established that Treg are required for immunological tolerance and prevention of excessive inflammatory immune responses. Neonatal

thymectomy in mice results in fatal T cell-mediated autoimmunity against various organs due to the lack of regulatory T cells ⁶⁸. Mutations in the X chromosome-encoded *Foxp3* gene, as in human IPEX patients and Scurfy mice, leads to severe immune dysregulation, polyendocrinopathy, and enteropathy related to an inability to generate Treg and establish tolerance ^{67,69}. Their origin is either in the thymus (tTreg) in response to recognition of self-antigen during negative selection or in peripheral lymphoid organs (pTreg), where naïve T cells recognize antigens in a tolerogenic environment—like that of commensal bacteria in the gut or the cancer microenvironment—and differentiate into pTreg. tTreg are considered to provide tolerance towards self-antigens that are represented in the thymus, whereas the main function of pTreg is the establishment of tolerance to antigens that are either foreign but not harmful or self-antigens not presented in the thymus during T cell development ^{70,71}. In cancer it has been shown that Treg are the predominant T cell type accumulating in tumor tissue, and low T effector/Treg ratios correlate with poor prognosis in various tumor types ^{72–74}. Regulatory T cells employ various mechanisms to suppress effector T cells. Those mechanisms include sequestration of available IL-2 via the high affinity IL-2 receptor, CTLA-4 (CD28-associated protein 4)-mediated sequestration of CD80/86 on APC surfaces, production of inhibitory cytokines like IL-10 and IL-35, production of pericellular adenosine, and direct cytotoxicity of effector T cells by granzyme B and perforin ⁷⁵. In the tumor microenvironment, Treg keep effector T cells in an intermediate state via sequestration of IL-2 and production of TGF- β . Withdrawal of IL-2 prevents full activation of effector T cells and ensures continuous availability of IL-2 produced by partially activated T cells, which Treg need for their maintenance but do not produce themselves ⁷⁶. TGF- β prevents full cytotoxic effector differentiation of tumor-specific CD8⁺ T cells and keeps memory CD8⁺ T cells in an inactive state ^{77,78}. The importance of suppression of Treg to increase PDT efficiency has recently been shown in several studies ^{39,79}. Treg depletion by cyclophosphamide followed by PDT in mice bearing CT26 colon carcinomas led to improved long-term survival and development of memory immunity ³⁹. It should be mentioned that this need for Treg depletion constitutes sort of a conundrum: lymphocytes have been shown to be especially sensitive to PDT-mediated cell death (see below). Therefore, Treg residing in the tumor microenvironment should be depleted by PDT treatment, thus abolishing the need for external depletion. However, other studies using the same tumor model did not show this requirement. Although there have been substantial differences in the treatment protocols between those studies, the reason for this partic-

ular aspect has (to the best of our knowledge) not been addressed so far and clearly needs further elucidation.

1.4.3.4 Dendritic Cells

Crucial for the induction of an adaptive immune response are dendritic cells (DCs). DCs are professional antigen-presenting cells (APC) and as such their main function is to present endogenous (e.g., viral) as well as exogenous (e.g., bacterial) antigens to lymphocytes in order to activate them and mount an appropriate immune response. They exist in two functionally distinct stages, “mature” and “immature”. Immature DCs constantly sample their environment by taking up antigens via macropinocytosis, receptor-mediated endocytosis, and phagocytosis. They are characterized by expression of CD11c and low levels of MHC I, MHC II, CD80, and CD86 and the relative absence of cytokine production. In the presence of inflammatory stimuli, those immature DCs differentiate into their mature state. This includes upregulation of processing and presentation of antigens and increased expression of MHC molecules and the costimulatory molecules CD80 and CD86. Additionally, maturation induces secretion of proinflammatory cytokines including IL-12, IL-6, and IL-1 β . Mature DCs migrate to the lymph nodes in large numbers where they present peptide–MHC complexes to lymphocytes. In combination with appropriate costimulation, this leads to activation of CD4⁺ T helper cells, CD8⁺ CTL, and B cells, and initiates the adaptive immune response^{80,81}.

Several groups have shown the importance of DCs for PDT-mediated antitumor immunity and efficiency. Jalili and coworkers were able to demonstrate that intratumoral injection of immature DCs after PDT treatment resulted in significantly delayed tumor growth of the treated tumor and of untreated tumors in the contralateral hind limb⁸². Similar outcome was reported by the group of Saji⁶². Further corroborating these findings were experiments by Preise et al.: DTR bone marrow chimera mice were inoculated with CT26 colon carcinoma cells, and subcutaneously growing tumors were subjected to PDT. Depletion of DCs by injection of diphtheria toxin (DTx) resulted in increased recurrence rates of the tumors. Mice which were systemically depleted of DCs showed 90% of disease recurrence compared to only 20% in mice which received PDT treatment only⁴⁸. Furthermore, other reports support the involvement of DCs in the response to PDT as evidenced by enhanced maturation and activation as well as increased secretion of proinflammatory cytokines after treatment^{83–86}.

2. Aim of the Study

The aim of the present study was to elucidate the possibility that PDT treatment of dendritic cells (DCs) could alter their capacity to induce regulatory T cells upon antigen exposure. In 2009, a study by Preise et al. revealed the requirement of DCs for PDT efficiency⁴⁸. Following this, work by Sanovic et al. has shown remarkable success with 100% of tumor cures using a low-dosed PDT treatment protocol with hypericin as a PS⁵⁵. Additionally, this protocol resulted in resistance to subsequent rechallenge with the same type of tumor cells, which is indicative for development of memory immunity as a consequence of the treatment. Further analysis of tumor samples from these experiments revealed an increase of IL-6 and a decrease of TGF- β on the mRNA level in response to the low-dose treatment (unpublished data). Based on these findings, we reasoned that tolerance towards the tumor must have been breached at some point. Considering the changes seen in IL-6 and TGF- β expression – two cytokines majorly involved in Treg and Th17 differentiation – and the involuntary but unavoidable treatment of DCs within the treatment field, we hypothesized that low-dosed PDT treatment might skew DC-mediated induction of Treg towards effector T cell differentiation, thus promoting recognition and elimination of the tumor rather than tolerance. However, information about the direct effects of PDT on DCs is rare to non-existent. Therefore, this study aimed at the identification of changes in murine DCs in response to hypericin-PDT and subsequent T cell activation and differentiation induced by those PDT-DCs. Specifically, this work started with the evaluation of the effect of hypericin-PDT on BMDC viability and expression of cytokines which are crucial for the subsequent differentiation of naïve T cells into effector T cells or Treg. The second part of this study was designed to determine the capacity of PDT-treated BMDCs to induce Treg and effector T cells in a co-culture system containing those two cell types. A schematic representation of the experimental design is given in figure 2.

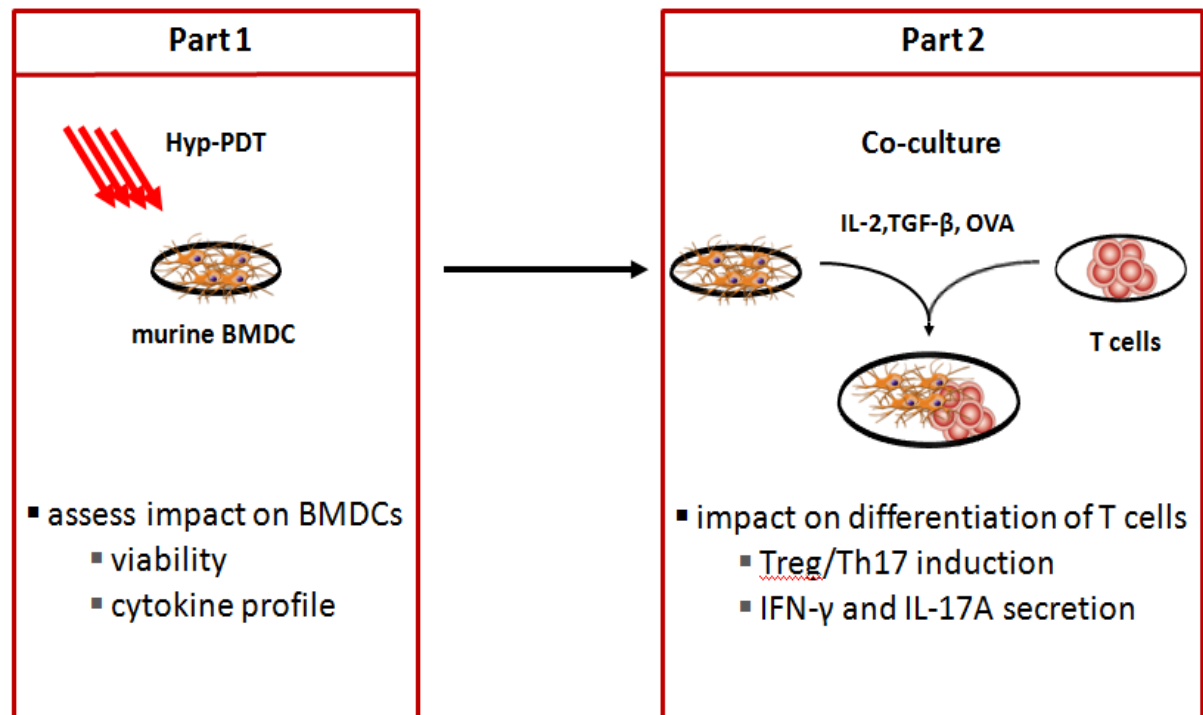


Figure 2: Schematic Representation of the Experimental Design. In the first part murine BMDCs are treated with different doses of hypericin and irradiated with a fluence of 1.1 J/cm^2 at 610 nm, followed by assessment of changes in viability and the cytokine profile. In part 2, murine PDT-BMDCs are co-cultured with naïve OVA antigen-specific T cells to determine the induction of CD4^+ T cell subtypes and the secretion of specific cytokines.

3. Materials and Methods

3.1 Cell Culture

3.1.1 Thawing and Maintenance of Cells

Cells which are stored for longer time periods are typically being kept in liquid nitrogen. Thawing and transfer of those cells into appropriate cell culture vessels should be carried out as fast as possible to protect cells from damage induced by this process. In brief, after removal of the cells from the storage, the cryo-conservation tube is shortly swirled in a 37°C water bath. This should be done to a point where only the outer layer of the frozen cone inside the tube melts to make further processing possible. Immediately afterwards, the still frozen cells are transferred into a Greiner tube containing pre-warmed complete growth medium, in which they rapidly thaw. The suspension is then centrifuged for 5 min at 1200 rpm to remove residual DMSO from the freezing medium. After aspiration the cells are resuspended in 5 mL of complete growth medium and transferred into a 25 cm² tissue culture flask for further growth and maintenance. At a density of approximately 70– 80% the cells were split at a ratio corresponding to their proliferation rate. To avoid cellular stress, the splitting frequency should not be more than every two days. In brief, the growth medium is aspirated and the cells are rinsed twice with PBS for washing. For detachment, cells are incubated with 1-fold trypsin-EDTA for 3 – 5 minutes at 37°C. After cell detachment the trypsin is inactivated by adding complete growth medium at a ratio of 1 : 4 (trypsin-EDTA : growth medium). The bottom of the flask is rinsed with the resulting suspension to detach still loosely adherent cells and the cell suspension is transferred into a Greiner tube. This is followed by centrifugation at 1200 rpm for 5 minutes. Afterwards the supernatant is aspirated and the cells are resuspended in 10 mL complete growth medium. After counting, the appropriate amount of cells to reach the desired split ratio is transferred into a new 75 cm² tissue culture flask and complete growth medium is added to a final volume of 25 mL.

3.1.2 GM-CSF Cell Culture and Generation of GM-CSF-conditioned Supernatant

Differentiation of dendritic cells from bone marrow requires GM-CSF. Instead of using recombinant GM-CSF it is possible to supplement the growth medium with GM-CSF-

conditioned supernatant (GM-CSF CSN). For this purpose a GM-CSF clone of unknown origin, kindly provided by Dr. Peter Hammerl, was used. These cells are transfected with a GM-CSF transgene, which causes them to produce GM-CSF and secrete it into the medium. Together with the GM-CSF transgene the cells carry a resistance-cassette under the control of the GM-CSF promotor that enables them to inactivate geneticin. Therefore it is possible to use geneticin as a selection marker: the cells slowly discard the GM-CSF transgene and with it the geneticin resistance gene. Since cells need the transgene to inactivate geneticin, only cells still carrying the resistance cassette will survive and expand if geneticin is added to the culture medium.

The cells themselves are suspension cells and display a homogeneous, round morphology. Parts of the culture show slight adherence which can easily be disrupted by rinsing the bottom of the cell culture flask with a pipette.

After thawing (cp. section *3.1.1 Thawing and Maintenance of Cells*), the cells were transferred into 10 mL pre-warmed R-5 (RPMI 1640, 5% FCS (heat-inactivated), 1% penicillin/streptomycin and 2 mM L-glutamine). To wash off the DMSO added for cryo-conservation the suspension was centrifuged at 1200 rpm for 7 minutes. The pellet was resuspended in 5 mL growth medium supplemented with 1 mg/mL G418 (geneticin), transferred into a 25 cm² cell culture flask and incubated at 37°C and 5% CO₂ for one day. The next day the bottom of the flask was rinsed with a pipette and the cells were resuspended. For further inoculations 0.5 mL of this suspension were again seeded in a 25 cm² cell culture flask with 5 mL growth medium plus G418 and incubated. These cells were harvested after 3 days and a fraction was stored at -80°C with 10% DMSO as 1 mL aliquots for future usage.

The rest of the obtained cells were washed 3 times to get rid of the G418 since it would remain in the conditioned supernatant and kill cells further treated with the CSN. Washing was performed by centrifuging the cells at 1200 rpm for 7 minutes, aspirating the supernatant and resuspending the cells in 10 mL growth medium. After the last washing step the cells were resuspended in 20 mL growth medium, transferred into a 75 cm² cell culture flask and incubated at 37°C and 5% CO₂ for further expansion.

When cells were dense enough, they were again harvested and washed (see above). Afterwards 4 mL of the culture were transferred into a 175 cm² flask with additional 50 mL growth medium and again objected to incubation for further expansion. The cells were allowed to grow until the first 10-20% started to undergo apoptosis (approximately 7 days).

Apoptotic cells were determined via microscopic examination. At this point the supernatant was harvested and collected in 50 mL reaction tubes. Subsequently, the supernatant was centrifuged at 2500 rpm for 15 minutes to pellet remaining cells. After centrifugation the supernatant was carefully collected, sterile filtrated and stored at 4° C. To avoid loss of biological activity of the GM-CSF, the CSN was aliquoted and stored at -20°C.

For determination of the activity of the GM-CSF CSN serial dilutions of the supernatant in medium were prepared (60/40/20/10/5/2.5/0%). 100 µL per well of each dilution were transferred into the wells of a 96-well plate. Afterwards 1×10^4 bone marrow cells (10^5 cells/mL, depleted of erythrocytes) were added to each well. This corresponds to final GM-CSF CSN concentrations of 30, 20, 10, 5 and 1.25 %. The cells were incubated for 7 days at 37°C and 5% CO₂ and analyzed for viability via MTT assay (cp. section 3.2.4 *MTT Assay*). The working dilution of the GM-CSF CSN is the percentage of CSN that gives the plateau value of viable cells (effectively 5-10%, depending on the batch). To account for loss of biological activity caused by freeze-thawing a standard percentage of 10% GM-CSF CSN was chosen.

3.1.3 Production of IL-6-conditioned Supernatant

One of the approaches used in this study is fluorescence activated cell sorting (FACS) analysis of various markers expressed by T cells and dendritic cells. Two of the antibodies used for this purpose were gained from hybridoma cells producing these antibodies (cp. section 3.1.4 *Culture of GK1.5 and N418 Cells*). These hybridoma cells require IL-6 to facilitate their growth and in some hybridoma cell lines it has been shown to increase antibody production. Similarly to GM-CSF, instead of purchasing the recombinant form, IL-6 can be added by supplementing the growth medium with IL-6-conditioned supernatant (IL-6 CSN). The IL-6-producing cells required for this are suspension cells transfected with an IL-6 transgene and an additional geneticin-resistance cassette to provide a selection marker for cells still carrying the transgene (cp. section 3.1.2 *GM-CSF Cell Culture and Generation of GM-CSF-conditioned Supernatant*).

Cells were thawed (cp. section 3.1.1 *Thawing and Maintenance of Cells*) and resuspended in 5 mL DMEM containing 1 g/l glucose with 10% FCS, 1% penicillin/streptomycin and 2 mM L-glutamine plus 1 g/l G418. Afterwards the suspension was transferred into a 25 cm² cell

culture flask and incubated at 37°C with 5% CO₂. When cells were dense the suspension was given into a 75 cm² cell culture flask and supplemented with another 5 mL of growth medium plus 1 g/l G418. The cells were kept under these conditions for one week, interrupted by splitting with a ratio of 1:5 at day 4. The surplus cells were spun down, resuspended in FCS + 15% DMSO and stored in liquid nitrogen.

After one week, IL-6 cells were washed thoroughly by centrifugation at 1200 rpm for 7 minutes, aspirating the supernatant and resuspending the pellet with growth medium without G418. This procedure was carried out three times to make sure all the G418 has been washed off. Following this, the cell suspension was transferred into a fresh 75 cm² cell culture flask and incubated at 37° C with 5% CO₂.

The supernatant containing the secreted IL-6 was harvested every 2-3 days by removing the medium from the flask, spinning the cells down at 1200 rpm for 7 minutes and collecting the supernatant. Subsequently, the supernatant was centrifuged at 2000 rpm for 15 minutes to get rid of residual cells and debris, sterile filtrated and stored at -20°C.

The remaining cells were resuspended in fresh medium and given back into the flask for another cycle of production. Since the IL-6-transfected cells discard the transgene when G418 is missing, this cycle can be repeated approximately four times before a new flask has to be inoculated.

3.1.4 Culture of GK1.5 and N418 Cells

The cell lines GK1.5 and N418 are hybridoma cell lines which produce antibodies to CD4 on T helper cells and CD11c on DCs respectively. The cells are suspension cells with a tendency to slight adherence that can easily be disrupted by rinsing the bottom of the culture vessel and they display a lymphoblast-like morphology.

Cells were cultured in hybridoma medium containing IMEM, 5% FCS, 1% penicillin/streptomycin, 2 mM L-glutamine and 5% IL-6 CSN. After reaching approximately 80% confluence in the maintenance culture (75 cm² flask), the cells were resuspended and cultures for antibody production were set up: 5 mL of the cell suspension were transferred into a 175 cm² flask containing 45 mL of hybridoma medium; for each clone three production cultures were set up. These cultures were incubated until 20 – 50% of cells were dead. At this point, the supernatant was harvested and centrifuged at 2500 rpm for 15 minutes. The resulting cell-free supernatant, which contains the secreted antibodies, was collected and

stored at 4° C. The emptied flasks were inoculated for a new cycle of production as described above. This procedure was repeated in total four times to ensure that a sufficient amount of antibodies was obtained. Starter cultures were maintained by splitting the cells at a ratio of 1:10 when the cells reached confluence.

3.1.5 Bone Marrow-Derived Dendritic Cells

3.1.5.1 Isolation of Bone Marrow Cells from Mouse Femur

To obtain bone marrow cells for generation of BMDC the femurs from Balb/c mice were dissected under sterile conditions with as little residual tissue as possible and rinsed with complete R-10. Afterwards the bones were cut open at the femoral head and flushed with R-10 using a 26G injection needle. The flowthrough containing the bone marrow was collected, resuspended to dislodge cell clusters and centrifuged at 1200 rpm for 7 minutes. After aspiration of the supernatant the remaining cells were resuspended in complete R-10 plus 10% GM-CSF CSN. If isolated bone marrow cells were subjected to freezing the cells were resuspended in FCS, adjusted to a maximum of 4×10^6 cells/mL and supplemented with 15% DMSO. Afterwards cells were stored at -80°C and, in case of long term storage, transferred into liquid nitrogen the next day.

3.1.5.2 Generation of Dendritic Cells from Bone Marrow Cells

Generation of bone marrow-derived dendritic cells (BMDCs) from bone marrow cells was carried out according to the protocol of Lutz et al.⁸⁷. Bone marrow cells obtained from Balb/c mice (see section III.1.5.1) were seeded into bacteriological 10 cm dishes at a density of $2-5 \times 10^6$ cells per dish in 10 mL complete R-10 plus 10% GM-CSF CSN and incubated at 37°C with 5% CO₂. Since bone marrow cells contain a large fraction of common myeloid progenitor cells (CMP) which give rise to dendritic cells but as well to macrophages, bacteriological culture dishes have to be used instead of tissue culture-treated dishes. If using tissue culture-treated dishes a large proportion of CMPs would adhere to the surface of the dish and give rise to macrophages in response to GM-CSF rather than to dendritic cells.

At day 3 cells were fed by adding 10 mL of fresh medium (complete R-10 plus 10% GM-CSF

CSN) per plate. At day 6 and 8 cells were fed by removing half of the medium, spinning the cells down at 800 rpm for 10 minutes, resuspending the remaining cell pellet in the same amount of fresh medium and giving it back into the plates.

BMDCs were harvested at day 9 by gently rinsing the plate with a serological pipette to detach loosely adherent cells and collected in 50 mL reaction tubes. Detachment of loosely adherent cells has to be done as gently as possible since too much mechanical stress can pose an activation signal for immature BMDCs. Subsequently, cells were centrifuged at 800 rpm for 10 minutes, resuspended in complete R-10 and either plated directly for further treatment or stored at -80°C in FCS + 15% DMSO at a maximum density of 4×10^6 cells/mL.

3.1.6 BMDC-T-cell Co-Culture

To elucidate the effect of PDT treatment on the capacity of DCs to induce regulatory T cells, BMDCs with or without treatment were co-cultured with naïve T cells. The T cells used for this purpose were obtained from DO11.RAG2^{-/-} mice. These mice on Balb/c background express a transgenic T cell receptor (TCR) that is specific for chicken ovalbumin (OVA) peptide 323-339, which is presented by the major histocompatibility complex class II (MHC II) molecule. Therefore all of the peripheral CD4⁺ T cells in those mice bear the transgenic TCR and remain naïve unless they get stimulated by OVA peptide or OVA protein. Due to the RAG2 knock out, V(D)J recombination in those mice is prevented and there is neither development of receptors of other specificity nor development of mature T and B cells. This makes it to activate T cells on demand by providing OVA peptide and any changes seen in the activation status and/or differentiation can only be attributed to applied treatments of either the APCs or the T cells themselves. Two approaches were used for the co-cultures: in the first setting unfractionated splenocytes from DO11.RAG2^{-/-} mice were co-cultured with BMDCs. In this setting endogenous APCs are present and it is not possible to add the antigen directly to the culture medium since those endogenous APCs could take up the antigen, present it to T cells and thus contribute to the changes seen in activation and differentiation of the T cells. Hence, in the second setting, fractionated T cells were used. In brief, cells were collected from spleen and lymph nodes (LN) and fractionated into lymphocytes and APCs by adherence of macrophages and DCs to tissue culture plates. By doing this it becomes possible to add the antigen directly to the culture medium and provide continuous stimulation by

exogenous APCs without endogenous APCs contributing to and skewing the obtained results.

3.1.6.1 General Co-Culture Protocol

DO11.RAG2^{-/-} cells were cultured in C-10 medium (RPMI 1640, 10% FCS, 1% penicillin / streptomycin, 2 mM L-glutamine, 1% HEPES, 1% sodium pyruvate, 1% non-essential amino acids, 50 μ M β -ME). The cell suspension was supplemented with 4 ng/mL recombinant murine TGF- β 1 and 200 U/mL of recombinant murine IL-2; this equals a final concentration in the co-culture of 2 ng/mL TGF- β 1 and 100 U/mL IL-2. While IL-2 is necessary for general proliferation and differentiation of naïve T lymphocytes into mature T lymphocytes of the effector and suppressor type, the presence of TGF- β 1 is a specific requirement to skew differentiation towards regulatory T cells. For co-culturing, the cells were seeded with into 96-well U-bottom plates (5-8 wells constituting one sample) at a density which would result in a T cell : DC ratio of 5 to 1 (see below) and allowed to rest for about one hour in the incubator. After incubation, 1×10^4 BMDCs in 100 μ L C-10 were added gently on top of the DO11.RAG2^{-/-} cells. These BMDCs had been matured with LPS and pre-loaded with different concentrations of OVA peptide previously (0.01, 0.03 and 0.1 μ g/mL; cp. section 3.2.3 *Treatment, Maturation and Antigen Loading of BMDCs for Co-Culture* and 4.6 *Titration of OVA Peptide Dose*), since only mature, antigen-presenting DCs are capable of inducing T cell proliferation and differentiation (cp. section 1.4.3.4 *Dendritic Cells*). The resulting co-cultures were left for incubation for 5 days (37°C with 5% CO₂) to allow differentiation and proliferation of the lymphocytes before further analysis.

3.1.6.2 BMDC – Splenocyte Co-Culture

The co-culture was carried out under the conditions described in section 3.1.5.1. DO11.RAG2^{-/-} splenocytes were diluted to a concentration of 3.33×10^6 cells/mL since naïve CD4⁺ T cells account for approximately 12% of total splenocytes in DO11.RAG2^{-/-} mice. Thus, 1 mL of cell suspension would contain about 4×10^5 lymphocytes. 1×10^4 PDT-treated BMDCs (cp. 3.2.3 *PDT Treatment, Maturation and Antigen Loading of BMDCs for Co-Culture*) were added to the splenocytes.

3.1.6.3 BMDC – T Lymphocyte Co-Culture

Naïve DO11.RAG2^{-/-} lymphocytes and PDT-treated BMDCs were generally co-cultured as described in section III.1.6.1. Since fractionated T cells were used in this setting (cp. *section 3.1.6 BMDC-T-cell Co-Culture*), total lymphocytes were diluted to 4x10⁵ cells/mL before seeding into 96-well plates. Furthermore, in addition to pre-loading the BMDCs with OVA peptide, the corresponding concentrations of OVA (0.01, 0.03 and 0.1 µg/mL) were added directly into the culture medium to enable continuous antigen supply. This was done in order to account for loss of presented antigen by the BMDCs due to the natural membrane turnover of MHC II: continuous availability of OVA peptide within the culture medium allows for uptake, processing and presentation of the antigen beyond the initial pre-loading throughout the co-culture duration.

3.2 Assays and Treatments

3.2.1 Dark Cytotoxicity

In order to assess the effect of the PS without excitation by light on immature BMDCs, cells were treated with hypericin and kept dark for 24 h afterwards. 20.000 cells per well (2 x10⁵ cells/mL) were seeded into a 96-well cell culture plate with R-10 plus 2% GM-CSF CSN and incubated o.n. at 37°C and 5% CO₂. The next day the medium was aspirated and replaced by 100 µL SFM containing increasing concentrations of hypericin, followed by 3 hours of incubation in the dark at 37°C. Afterwards the hypericin-containing medium was replaced by 100 µL/well of R-10. For the following 24 h cells were kept dark in the incubator. To evaluate the effect of this treatment on cell viability cells were objected to MTT assay after 24 h (cp. *section 3.2.4 MTT Assay*).

3.2.2 Phototoxicity Assay

To evaluate the phototoxic effect of hypericin on the cells a dose-dependent PDT protocol was used: 20.000 cells per well (2x10⁵ cells/mL) in their respective growth medium were seeded into a 96-well cell culture plate and incubated for 24 hours at 37°C and 5% CO₂. The next day

the medium was aspirated and replaced by 100 μ L serum-free medium containing increasing concentrations of hypericin (40 nM, 60 nM, 80 nM, 100 nM, 150 nM, 200 nM, 300 nM, 400 nM, 500 nM, 600 nM, 700 nM, 800 nM), followed by 3 hours of incubation in the dark at 37°C. Afterwards the hypericin-containing medium was replaced by 100 μ L of normal growth medium.

Immediately after changing the medium the cells were irradiated for 10 minutes at 610 nm using a LED array which corresponds to a fluence of 1.1 J/cm². Subsequently, cells were incubated in the dark for another 24 hours and viability was assessed the next day by performing a MTT assay (cp. section 3.2.4 *MTT Assay*).

To assess the dose-dependency of the phototoxic effect of hypericin the following concentrations were used: 40 nM, 60 nM, 80 nM, 100 nM, 150 nM, 200 nM, 300 nM, 400 nM, 500 nM, 600 nM, 700 nM and 800 nM. Additionally, one group of cells was treated with serum-free medium without hypericin to serve as control.

To verify induction of cell death in tumor cells at the given dose range, the same protocol was carried out using the tumor cell lines A431 (human epidermoid carcinoma; https://www.lgcstandards-atcc.org/Products/All/CRL-1555.aspx?geo_country=at) and CT26 (murine colon carcinoma; https://www.lgcstandards-atcc.org/products/all/CRL-2638.aspx?geo_country=at).

3.2.3 PDT Treatment, Maturation and Antigen Loading of BMDCs for Co-Culture

BMDCs intended for co-culture were seeded in bacteriological plates and PDT-treated with 80 nM and 300 nM of hypericin plus light according to the protocol described in section 3.2.2. These two doses had been defined previously as low-dose (80 nM) and high-dose (300 nM) based on the results from the phototoxicity assay (cp. section 4.2 *Light-dependent Cytotoxicity*). After irradiation (1.1 J/cm² at 610 nm) cells were allowed to rest for 6 hours (37°C, 5% CO₂, dark). For maturation, the treated BMDCs were stimulated for 12 hours with 100 ng/mL lipopolysaccharide (LPS). Since maturation of BMDCs is accompanied by a decrease in phagocytic capacity and an increase in antigen processing and presentation, loading of the cells with OVA antigen is done simultaneously by adding the antigen to the culture medium. The antigen doses tested with untreated BMDCs were 0.01, 0.03 and 0.1 μ g/mL based on work published by Yamazaki et al ⁸⁸. For further assays, the most and the least permissive dose for Treg induction was used (cp. section 4.6 *Titration of OVA Peptide*

Dose). Following stimulation and antigen loading, the cells were harvested: the culture medium was collected in 50 mL reaction tubes and replaced with 3 – 8 mL of 3 mM EDTA solution. After 5 min of incubation the plates were rinsed and the EDTA solution containing the remaining PDT-treated BMDCs was added to the respective reaction tube. Subsequently, the cells were washed twice by centrifugation at 800 rpm for 10 min, aspiration of the supernatant and resuspension with growth medium. Afterwards, the cells were resuspended in 5 mL of C-10, counted and subjected to further use.

BMDCs which were intended for RNA isolation and subsequent qRT-PCR were seeded into tissue culture treated plates. This difference was made to avoid loss of cells by making use of the BMDCs tendency to firmly adhere to tissue culture treated vessels. Furthermore, these cells were only PDT-treated and stimulated but not loaded with antigen. Since these cells were used to compare the ability to mature of PDT-treated vs. untreated BMDCs, antigen loading was not required. After LPS stimulation the culture medium was aspirated and the cells were subjected to RNA isolation (cp. section 3.2.5 *RNA Isolation*). Additionally, unstimulated samples were carried along as controls.

3.2.4 MTT Assay

In order to determine the viability of cells after treatment the MTT assay was employed. This assay is based upon the fact that metabolically active cells are able to convert MTT [3-[4,5-dimethylthiazolyl]-2,5-diphenyltetrazolium bromide) into formazan whereas dead or dying cells are not. Formazan is an insoluble, blue-colored product generated by enzymes using reducing equivalents like NADH. The exact mechanism by which MTT is reduced into formazan still has to be fully elucidated but it is assumed that mitochondrial enzymes are responsible. Therefore mitochondrial activity of the cells is determined. Since formazan is insoluble it has to be set free from the cells and solubilized, which is typically done with DMSO. Afterwards the absorbance of formazan can be measured at 550 nm.

After photodynamic treatment the cells were incubated for 24 hours at 37°C and 5% CO₂. The next day 10 µL MTT solution was added to each well and the cells were incubated at the same conditions for another 4 hours. Afterwards the medium was exchanged with 100 µL DMSO per well to solubilize the generated formazan. Subsequently, absorbance was assessed at 550 nm with a microplate reader.

To determine the relative viability of the hypericin-treated cells compared to an untreated control the absorbance values were compared to each other (hypericin-treated / untreated). The resulting value shows whether a given concentration of hypericin has a proliferative, cytostatic or cytotoxic effect on the treated cells compared to the untreated control.

3.2.5 RNA-Isolation

For subsequent gene expression studies, RNA was isolated using self-made TRI reagent. All steps were performed under nuclease-free conditions and at 4°C. At least 5×10^5 cells were lysed with the appropriate amount of TRI reagent (1 mL / 10 cm² culture vessel area) and transferred into sterile, nuclease-free 1.5 mL reaction tubes. For RNA separation, 200 µL chloroform per 1 mL of TRI reagent were added. The mix was thoroughly mixed, incubated for 3 min on ice and centrifuged for 15 min at 15.000 rpm. After centrifugation the aqueous upper phase containing the RNA was transferred into a new reaction tube containing 5µg glycogen (to improve precipitation) and mixed with 500 µL of isopropanol per 1 mL TRI reagent for RNA precipitation. The samples were incubated 15 min at RT and centrifuged at 15.000 rpm for 10 min afterwards. The supernatant was carefully removed and the remaining RNA pellet was washed by adding 180 µL ethanol and a last centrifugation step at 15.000 rpm for 5 min. The ethanol was removed and the pellet was dried by air to let residual ethanol evaporate. Finally, the RNA was redissolved by adding 25 µL of nuclease-free water and leaving it on 4°C for 90 min. To determine concentration and purity of the RNA sample an Implen NanoPhotometer® P330 was used. Only samples with A260/280 and A260/230 ratios of ≥ 2.0 were chosen for further use (absorption at 280 nm hints to contamination of the sample by proteins while absorption at 230 nm reflects the presence of TRIzol, phenols or peptides). Isolated RNA samples were stored at -20°C or objected to further usage immediately.

3.2.6 cDNA Generation

cDNA was generated using RevertAid H Reverse Transcriptase. Previously isolated RNA samples were incubated for 5 min on 65°C to remove potential loops. Afterwards 2-4 µg RNA per sample were mixed with 1 µL Oligo-d(T)-primer and incubated at 65°C for 7 min to

facilitate annealing of the primer to the RNA. Since this primer only anneals to poly(A) sequences which are typically present at the 3' end of intact mRNAs, using this primer avoids the risk of transcribing degraded mRNA or genomic DNA into cDNA. Next, 9 μ L master mix (6 μ L 5x RT buffer, 2 μ L dNTPs, 1 μ L reverse transcriptase) was added to each sample, followed by 80 min at 42°C for reverse transcription of the samples. To hydrolyze the remaining RNA within the samples, 10 μ L NaOH (0.1M) was added to each one, incubated at 70°C for 10 min and neutralized with the same amount of HCl per sample. Finally, the cDNA was diluted with another 160 μ L of DEPC-treated water (total ratio of 1:10) and stored at -20°C.

3.2.7 Quantitative Real-Time PCR

3.2.7.1 Primer Design

The primers needed for the gene expression analyses conducted in this study were designed using NCBI PrimerBlast [<https://www.ncbi.nlm.nih.gov/tools/primer-blast/>], primer3 [<http://primer3.ut.ee/>] and OligoAnalyzer 3.1 from Integrated DNA Technologies [<https://eu.idtdna.com/calc/analyzer>]. Annealing temperatures as well as primer efficiencies were determined by gradient PCR runs. The specificity of the primers was checked by objecting the PCR products to gelelectrophoresis and examining the appearing bands. Primers used in this study are listed in Table 2.

Table 2: Primers used for Gene Expression Studies

Target Gene	Primer Sequence	Annealing Temp.
β-Actin	fwd: ACAGCTTCTTTGCAGCTCCTTCG rev: ATCGTCATCCATGGCGAACTGGTG	70°C
GAPDH	fwd: ACCCAGAAGACTGTGGATGG rev: ACACATTGGGGGTAGGAACA	57°C
HPRT 1	fwd: GTTGGGCTTACCTCACTGCTTTC rev: CCTGGTTTCATCATCGCTAATCAC	62°C
IL-1β	fwd: TGCCACCTTTTGACAGTGATG rev: AAGGTCCACGGGAAAGACAC	56°C

IL-6	fwd: TCCTCTCTGCAAGAGACTTCCATC rev: TGGTTGTCACCAGCATCAGTCC	62°C
IL-12 (p35)	fwd: GATGACATGGTGAAGACGGC rev: AAGGCACAGGGTCATCATCA	65°C
TGF-β (transforming growth factor β)	fwd: TCAGACATTCGGGAAGCAGT rev: TCGAAAGCCCTGTATTCCGT	65°C

3.2.7.2 *qRT-PCR*

qRT-PCR was carried out using the GoTaq®qPCR Master Mix kit from Promega. Briefly, 4 μ L sample cDNA were mixed with 10 μ L GoTag®qPCR Master Mix 2X, 2 μ L nuclease-free water and 4 μ L of a primer mix containing 1 μ M forward primer and 1 μ M reverse primer, leading to a final concentration of 0.1 μ M of each primer in the 20 μ L reaction volume. Depending on the expected abundancy of the respective target the cDNA was used at a ratio of 1:10 (cp. section 3.2.6 *cDNA Generation*) or further diluted with DEPC-treated water to a ratio of 1:250.

PCR cycles were performed with a CFXConnect™ Real-Time System and analysis was conducted with the associated software CFX Manager 3.1. The thermal program applied followed the recommendations of the kits manufacturer Promega and took into account the previously determined annealing temperature for the respective primers. Table 3 shows the exact cycling parameters applied for qRT-PCR. The dissociation (“melt curve”) step at end of the program was included to be able to check whether only one product has been amplified or not.

To be able to adequately analyze the obtained gene expression data, gene expression profiles of the house keeping genes β -actin, glyceraldehyde-3-phosphate dehydrogenase (GAPDH) and hypoxanthine-guanine phosphoribosyltransferase 1 (HPRT 1) was assessed as well and the gene expression levels, represented by the C_q (cycle of quantification) values, of the targets in question were normalized against the ones of the house keeping genes. Finally the fold-change of the expression level relative to an untreated control was calculated.

Table 3: Cycling Parameters applied for qRT-PCR

	# Cycles	Time (s)	Temperature
Hot-Start	1	120	95°C
Activation			
Denaturation		15	95°C
Annealing /	40	60	depending on the
Extension			primer
Dissociation	1		60 – 95°C

3.2.8 FACS Analysis

Flow cytometry is a method used to characterize cells depending on their morphology but as well on cellular content when fluorescent dyes or fluorochrome-coupled antibodies are used to specifically tag cells. Very basically, this method makes use of optical and fluorescence characteristic of cells which are passed by a monochromatic light source, usually a laser beam. For this, cells in suspension are drawn into a stream which generates a laminar flow. This allows for passing of cells through the beam of the light source one by one. The emitted light, which is given off by each cell, gets directed to a series of dichroic mirrors, filters and detectors to collect the light signal(s). Subsequently, these signals are digitalized for computational analysis. The morphology of cells is distinguished by their ability to scatter light when passing the laser beam: the size of cells is represented by their ability to scatter light in forward angle direction (FSC). Additionally, cells scatter light in sideways angle direction (SSC) depending on their intracellular complexity. This makes it possible to analyze cells for relative size and internal structure.

Fluorescent dyes, which intercalate with or bind to DNA and/or RNA, can be used to evaluate the nucleic acid content within cells. This approach allows for cell cycle studies or the identification of tumor cells since the fluorescent signal is directly proportional to the cellular DNA content. Furthermore, some of these dyes (i.e. propidium iodide) can be used to discriminate between living and dead cells due to the circumstance that they can only permeate cells with disrupted membrane integrity.

Monoclonal antibodies can be used to label cells by binding to the corresponding antigen,

which can either be on the cell surface or intracellular. Although those antibodies do not emit fluorescence themselves, they can be coupled to fluorochromes which emit fluorescent light when they are excited by a laser of appropriate wavelength. By using this method it is possible to analyze cells with respect to phenotypic and functional characteristics.


For staining with fluorochrome-conjugated antibodies, $0.5 - 10 \times 10^6$ cells are used in 100 μL staining solution. After collection of the samples, they are centrifuged at 1500 rpm and 4°C for 5 min. The supernatant is discarded and the cells are being washed twice. This is done by resuspending the pelleted cells in 1 mL PBS, followed by centrifugation at 1500 rpm and 4°C for 5 min and aspiration of the supernatant. For staining of targets on the surface, the cells are resuspended in 100 μL of a staining solution containing the antibodies of interest in a suitable dilution (this dilution has to be titrated for each antibody since it may vary depending on the antibody itself and the specific lot). Subsequently, the cells are incubated for 30 min at 4°C in the dark. After incubation, unbound antibodies are removed by washing the cells twice as described above. If the targets of interest are exclusively extracellular, the cells are resuspended in 200 μL of PBS (or FACS buffer containing 10% FCS to protect the still viable cells) and analyzed on the flow cytometer. In case of additional intracellular targets (in this work namely Foxp3), the cells are fixated and permeabilized using the Nuclear Factor Fixation and Permeabilization Buffer Set according to the manufacturer's instructions (BioLegend Inc., San Diego, USA). Afterwards, cells are stained with 100 μL permeabilization buffer containing the appropriate amount of antibody for 35 min at RT in the dark. For assessment on the flow cytometer the samples are again washed twice and resuspended in 200 μL of PBS or FACS buffer. The flow cytometer used in this work is a FACSCanto™ II from Becton Dickinson and the analysis of the obtained data was conducted using the Kaluza Flow Cytometry Analysis Software 1.5a from Beckman Coulter. A list of fluorochrome-conjugated antibodies used for this work is given in Table 4.

Table 4: Antibodies used for FACS Analysis

Antibody	Clone	Conjugated	
		Fluorochrome	Manufacturer
CD4	GK1.5	FITC	self-generated
CD11c	N418	FITC	self-generated
CD25	PC61	PE	BioLegend Inc., San Diego, USA
CD40	HM40-3	Alexa Fluor® 647	BioLegend Inc., San Diego, USA
CD86	GL-1	PE	BioLegend Inc., San Diego, USA
FoxP3	MF-14	Alexa Fluor® 647	BioLegend Inc., San Diego, USA
MHC II	M5/114.15.2	Pacific Blue™	BioLegend Inc., San Diego, USA

3.2.9 Sandwich ELISA

The sandwich ELISA (enzyme-linked immunosorbent assay) is typically used to analyse complex, unpurified samples for antigens of interest. The principle of this assay is based on the binding of specific antibodies to their cognate antigen and the fact that antibodies can have the same specificity while recognizing the antigen via different epitopes. This enables the use of more than one antibody to detect a certain antigen which increases assay accuracy and sensitivity. For the sandwich ELISA a microtiter plate is coated with a so-called capture antibody. This antibody is intended to pull as much antigen as possible from the sample therefore polyclonal antibodies are frequently used as capture antibodies. After washing off unbound sample the second antibody is applied (so-called detection antibody). As a monoclonal antibody it binds to a single epitope of the cognate antigen and allows for highly sensitive detection and quantification of small differences in antigen concentration. Besides being specific for the antigen of interest the detection antibody has to be biotinylated to enable enzymatic coupling: the enzyme (typically horseradish peroxidase) needed for conversion of a substrate to yield a colored product is covalently linked to avidin or streptavidin. Streptavidin is a protein isolated from *Streptomyces avidinii* and possesses a remarkable affinity towards biotin and biotin conjugates with almost no nonspecific binding. Therefore, the amount of



bound horseradish peroxidase directly depends on the amount of detection antibody which is bound to the antigen. This is reflected by the amount of substrate which can be converted by the enzyme in a given time and can be measured as absorbance of the product.

For detection of cytokines secreted by mature PDT-BMDCs (i.e. IL-6) the cells were treated according to the treatment protocol, seeded into bacteriological 100 mm dishes at a density of 2×10^5 cells/ml (24.5 mL / dish), stimulated with 100 ng/mL LPS for 13 h, washed, counted and reseeded into 96-well tissue culture plates at a density of 2×10^5 cells/ml (100 μ L/well). After 48 h the supernatant was harvested (6 wells constituting one sample) and analyzed for IL-6 content. For cytokines secreted by T lymphocytes (i.e. IFN γ and IL-17A) or PDT-BMDCs (i.e. IL-6) in the context of the co-culture, the supernatants from the co-cultures were collected after the culture duration (5 d) and analyzed for the cytokines of interest. All ELISA assays used in this work were purchased from BioLegend and carried out according to the manufacturer's instructions.

3.3 List of Chemicals, Reagents and Technical Equipment

Table 5: Technical Equipment

Technical Equipment	Manufacturer
Petri dishes, 100 mm	Greiner Bio-One International AG, Kremsmünster, Austria
Cell culture flasks	Sarstedt AG & Co., Nümbrecht Germany Greiner Bio-One International AG, Kremsmünster, Austria
Cell culture plate, 96 well, clear	Greiner Bio-One International AG, Kremsmünster, Austria
Cell culture plate, 96 well, clear, U-bottom	Greiner Bio-One International AG, Kremsmünster, Austria
CFX Connect™ Real-Time System	Bio-Rad Laboratories Inc., Hercules, USA
CFX Manager 3.1	Bio-Rad Laboratories Inc., Hercules, USA
CO ₂ Incubator Steri-Cycle	Thermo Electron Corporation (Thermo Fisher Scientific), Waltham, USA
FACSCanto™ II	Becton, Dickinson and Company, New Jersey, USA
Hard-Shell PCR Plates 96-well	Bio-Rad Laboratories Inc., Hercules, USA
Infinite M200 Pro	Tecan, Groedig/Salzburg, Austria
Centrifuge Megafuge 1.0R Sorvall	Heraeus Sepatech, Hanau, Germany
Microseal® 'B' Film	Bio-Rad Laboratories Inc., Hercules, USA
Nanophotometer™ P-Class P330	Implen GmbH, Munich, Germany
RoboCycler gradient 40	Stratagene, La Jolla, USA
ZelluTrans Dialysis Membrane TX	Carl Roth GmbH & Co. KG, Karlsruhe, Germany

Table 6: Chemicals and Reagents

Chemicals and Reagents	Manufacturer
Ammonium thiocyanate	Sigma-Aldrich Co., St. Louis, USA
β -Mercaptoethanol	Sigma-Aldrich Co., St. Louis, USA
Chloroform	VWR International LLC, West Chester, USA
dATP, dCTP, dGTP, dTTP 100 mM	Fermentas (Thermo Fisher Scientific), Waltham, USA
DEPC	AppliChem GmbH, Darmstadt, Germany
DMSO	FlukaChemie GmbH (Sigma-Aldrich Co.), St. Louis, USA
DMEM – high glucose (D6429 Sigma)	Sigma-Aldrich Co., St. Louis, USA
EDTA 50 mM	Fermentas (Thermo Fisher Scientific), Waltham, USA
Ethanol (purity > 99,9%)	Merck KGaA, Darmstadt, Germany
Ethidiumbromide (0,5 mg/mL EtBr in 2500 mL 1x TAE)	Carl Roth GmbH & Co. KG, Karlsruhe, Germany
Fetal bovine serum	Sigma-Aldrich Co., St. Louis, USA
Fixable Viability Dye eFluor® 780	eBioscience Inc., San Diego, USA
GeneRuler™ 100bp DNA ladder	Fermentas (Thermo Fisher Scientific), Waltham, USA
Geneticin 418 (G418)	Sigma-Aldrich Co., St. Louis, USA
Glacial acetic acid	Carl Roth GmbH & Co. KG, Karlsruhe, Germany
Glycerol anhydrous (purity > 99,9%)	FlukaChemie GmbH (Sigma-Aldrich Co.), St. Louis, USA
GoTaq®qPCR Master Mix, 2x	Promega, Madison, USA
Guanidine thiocyanate	FlukaChemie GmbH (Sigma-Aldrich Co.), St. Louis, USA
HEPES Buffer 1M	Lonza Group Ltd., Basel, Switzerland
Hypericin	Planta Naturstoffe Vertriebs Ges.m.b.H., Vienna, Austria
IL-2, recombinant mouse	ImmunoTools GmbH, Friesoythe, Germany

IL-6, recombinant mouse	PeproTech, New Jersey, USA
KHCO ₃	Sigma-Aldrich Co., St. Louis, USA
L-Glutamine (200 mM)	Sigma-Aldrich Co., St. Louis, USA
MEM Non-Essential Amino Acid Solution 100x	Sigma-Aldrich Co., St. Louis, USA
NH ₄ Cl	Sigma-Aldrich Co., St. Louis, USA
Nuclear Factor Fixation and Permeabilization Buffer Set	BioLegend Inc., San Diego, USA
Oligo (dT) ₁₈ Primer 100 µM	Fermentas (Thermo Fisher Scientific), Waltham, USA
Gibco®Opti-MEM® I (1X) + GlutaMax™ - I	Lifetechnologies (Thermo Fisher Scientific), Waltham, USA
PBS	Sigma-Aldrich Co., St. Louis, USA
Penicillin-Streptomycin (10000 units penicillin, 10 mg streptomycin per mL in 0,9% NaCl)	Sigma-Aldrich Co., St. Louis, USA
peqGOLD Universal Agarose	Peqlab Biotechnologie GmbH, Erlangen, Germany
Primer for real-time PCR	Sigma-Aldrich Co., St. Louis, USA
Propan-2-ol	VWR International LLC, West Chester, USA
5x Reaction Buffer for RT	Fermentas (Thermo Fisher Scientific), Waltham, USA
RevertAid™H Minus Reverse Transcriptase 200 U/µL	Fermentas (Thermo Fisher Scientific), Waltham, USA
RiboLock™RNase Inhibitor 40 U/µL	Fermentas (Thermo Fisher Scientific), Waltham, USA
Sodium acetate trihydrate	Merck KGaA, Darmstadt, Germany
Sodium citrate	VWR International LLC, West Chester, USA
Sodium-Pyruvate Solution 100 mM	PAA Laboratories GmbH, Pasching, Austria
Spectra/Gel Absorbent	Spectrum Laboratories Incorporated, Houston, USA

TGF- β , recombinant mouse	New England BioLabs Inc., Massachusetts
Thiazolyl Blue Tetrazolium Bromide	Sigma-Aldrich Co., St. Louis, USA

Table 7: Media, Buffers and Solutions

Media, Buffers and Solutions	Mixture
ACK lysis buffer	8.29 g NH_4Cl (0.15 M) 1 g KHCO_3 (10 mM) 0.1 mM EDTA adjusted to pH 7.4 ddH ₂ O ad 1000 mL autoclaved
C-10	RPMI 1640 10% FBS (heat-inactivated) 1% L-Glutamine 1% Penicillin/Streptomycin 1% sodium pyruvate 1% HEPES 1% non-essential aa 50 μM β -ME
DEPC water	50 μL DEPC in 50 mL ddH ₂ O stir o.n. inactivation of DEPC by autoclaving
D-10	DMEM 10% FBS (heat-inactivated) 1% L-Glutamine 1% Penicillin/Streptomycin
dPBS	9.6 g/l in ddH ₂ O
Ethanol 75%	75% ethanol 25% ddH ₂ O
FACS staining buffer	PBS 10% FBS
Freezing medium	FBS

	15% DMSO
GM-CSF CSN	RPMI 1640 5% FBS (heat-inactivated) 1% L-Glutamine 1% Penicillin/Streptomycin secreted GM-CSF used at 5-10% depending on the batch
Hybridoma medium	Opti-MEM® I (1X) + GlutaMax™-I 5% FBS (heat-inactivated) 1% Penicillin/Streptomycin 100 U/mL rmIL-6
Hypericin (stock 2 mM)	MW _{Hyp} = 504.4 g/mol diluted in DMSO
MTT solution	5 mg/mL thiazolyl blue tetrazolium bromide dPBS
R-5	RPMI 1640 5% FBS (heat-inactivated) 1% L-Glutamine 1% Penicillin/Streptomycin 50 µM β-ME
R-10	RPMI 1640 10% FBS (heat-inactivated) 1% L-Glutamine 1% Penicillin/Streptomycin 50 µM β-ME
SFM	RPMI 1640 1% L-Glutamine 1% Penicillin/Streptomycin
TAE buffer 1x	1% TAE 10x 90% ddH ₂ O
TAE buffer 10x	48.4 g Tris base 11.42 mL glacial acetic acid 20 mL 500 mM EDTA (pH 8.0)

	ddH ₂ O ad 1000 mL
TRI reagent	15.2 mL phenol (equilibrated in 0.1 M NaAc), c = 38% 4.72 g guanidine thiocyanate (0,8 M) 3.04 g ammonium thiocyanate (0,4 M) 1.34 mL sodium acetate pH 5,0 (0,1 M) 2.3 mL glycerol 87%, c = 5% DEPC water ad 40 mL

4. Results

The present study was designed to evaluate the effects of hypericin-PDT on murine BMDCs with respect to changes in viability and the expression of specific cytokines in response to an inflammatory stimulus. Additionally, this study aimed at exploring the capacity of PDT-treated BMDCs to induce regulatory T cell in response to antigen exposure.

4.1 Dark Cytotoxicity on BMDCs

In order to assess a possible cytotoxic effect of non-excited hypericin on immature BMDCs, cells were treated for 3 h with increasing concentrations of hypericin without irradiation. Evaluation of cell viability by MTT 24 h post treatment is shown in Fig. 3. Treatment with hypericin without irradiation shows a stimulating effect on cell viability in the range of 20 – 100 nM as reflected by relative viability higher than that of the untreated control immediately after treatment (C0). Starting at 150 nM, unexcited hypericin exerts a cytotoxic effect on the BMDCs, which reaches statistical significance at 300 nM.

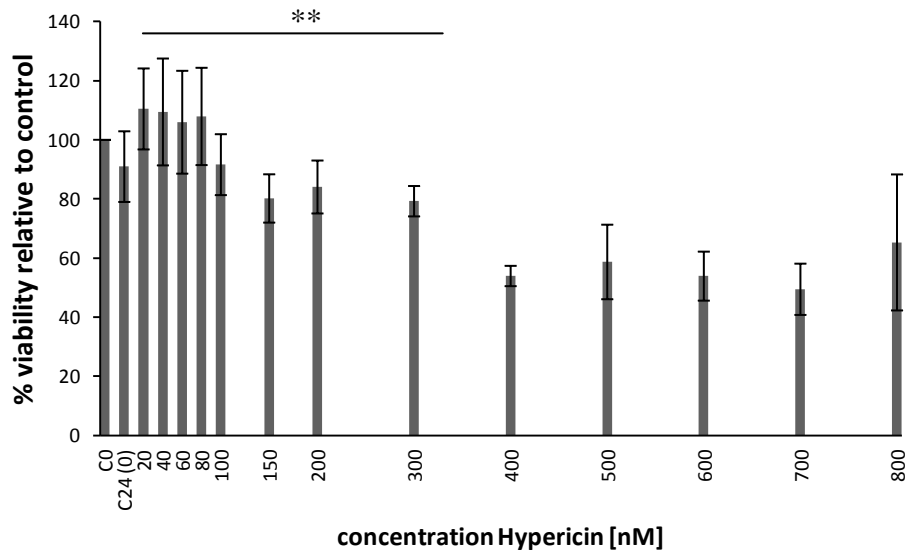


Figure 3: Effect of Unexcited Hypericin on BMDC viability. BMDCs were treated with increasing concentrations of hypericin in serum-free medium for 3 h. Viability was assessed 24 h post treatment using MTT assay.

4.2 Light-dependent Cytotoxicity on BMDCs

To determine the cytotoxic effect of photodynamic treatment on immature BMDCs, cells were subjected to treatment with increasing concentrations of hypericin in the range of 0 nM to 800 nM for 3 h, followed by red light irradiation (610 nm) with a fluence of 1.1 J/cm². Evaluation of the obtained data shows that immature BMDCs display a statistically significant increase in viability relative to the untreated control up to 124% ± 9% at a hypericin concentration of 80 nM, which is indicative for ongoing proliferation in response to the treatment. In contrast, at 300 nM cells show a profound and statistically significant decrease in viability to 62% ± 7%, indicating a cytotoxic effect of the treatment on BMDCs with higher concentrations of the PS (Fig. 4). The effect of photodynamic treatment with hypericin on immature BMDCs shows a clear dose-dependency with positive effects on viability and proliferation at very low PS concentrations and increasing cytotoxicity with concentrations above 200 nM.

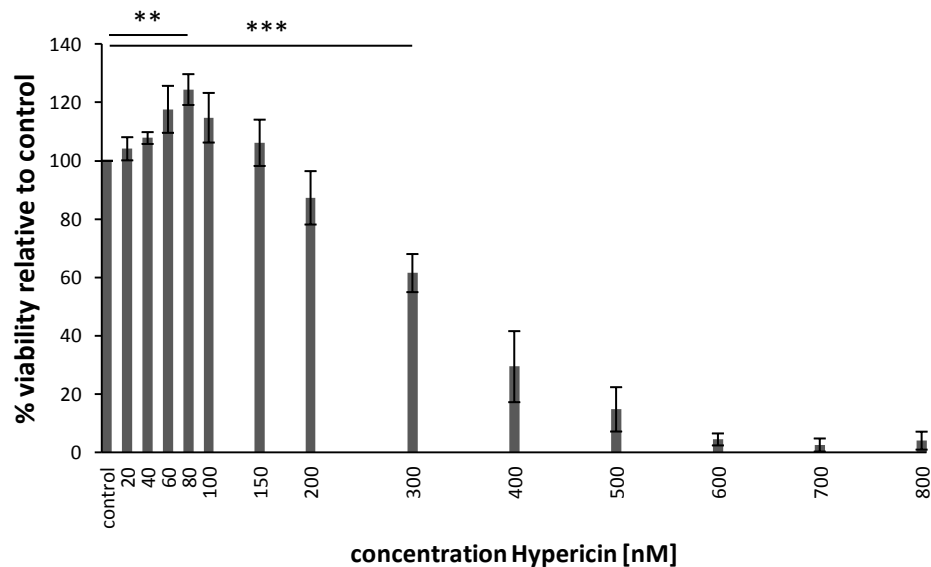


Figure 4: Light-dependent Cytotoxicity of Hypericin on BMDCs. BMDCs were treated with increasing concentrations of hypericin in serum-free medium for 3 h and irradiated with a fluence of 1.1 J/cm². Viability was assessed 24 h post treatment using MTT assay.

Based on the data from the light-dependent cytotoxicity assays, two hypericin concentrations were chosen for subsequent experiments: first, low-dosed hypericin at 80 nM, since the cells showed the most profound positive reaction in viability at this concentration. The second dose was chosen as control with 40% of cells not surviving the treatment (LD₄₀). LD₄₀ was reached at 300 nM of hypericin at the given fluence and fluence rate.

4.3 Induction of Cell Death in Tumor Cell Lines with Low-Dose Treatment

Induction of an adaptive immune response is crucially dependent on the presence of a respective antigen. Therefore, any treatment aiming at inducing such an immune response against a tumor has to induce cancer cell death as well to make tumor-derived antigens available to APCs. To verify that the low-dosed treatment protocol applied on the BMDCs would be sufficient to affect tumor cells as well, light dependent cytotoxicity of the same hypericin concentration range was tested on tumor cell lines. For this, two different tumor cell lines were used: A431 cells, a human epidermoid carcinoma cell line, and CT26 cells, a murine colon carcinoma cell line. Both cell lines show a reduction in viability of about 20% at 80 nM (A431: 83% \pm 10%; CT26: 78% \pm 13%) and about 73% at 300 nM (A431: 29% \pm 7%; CT26: 26% \pm 12%) compared to the untreated control 24 h post treatment (Fig. 5 and 6). Contrasting this and in line with previous reports, hypericin shows no dark cytotoxicity in these cell lines with any of the tested concentrations (Fig. 7).

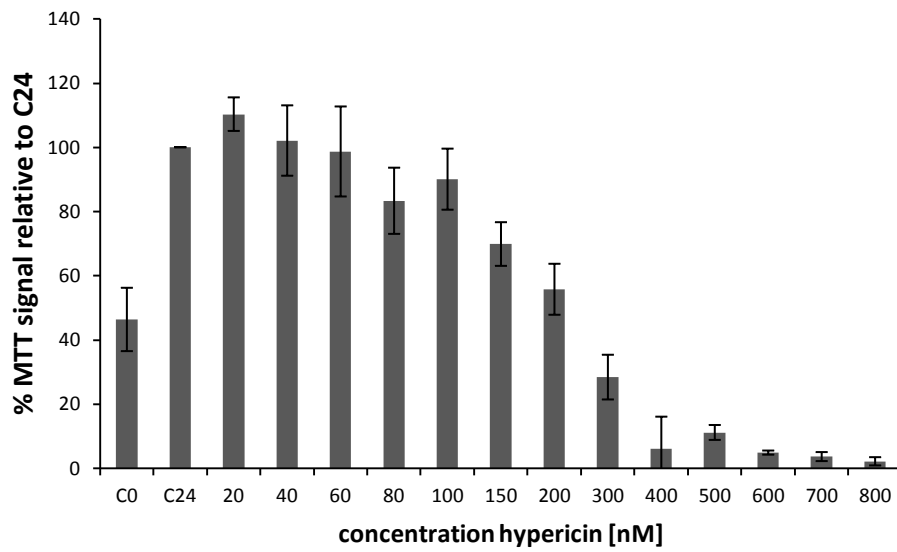


Figure 5: Light-dependent Cytotoxicity of Hypericin on A431 Cells. A431 cells were treated with increasing concentrations of hypericin in serum-free medium for 3 h and irradiated with a fluence of 1.1 J/cm². Viability was assessed 24 h post treatment using MTT assay.

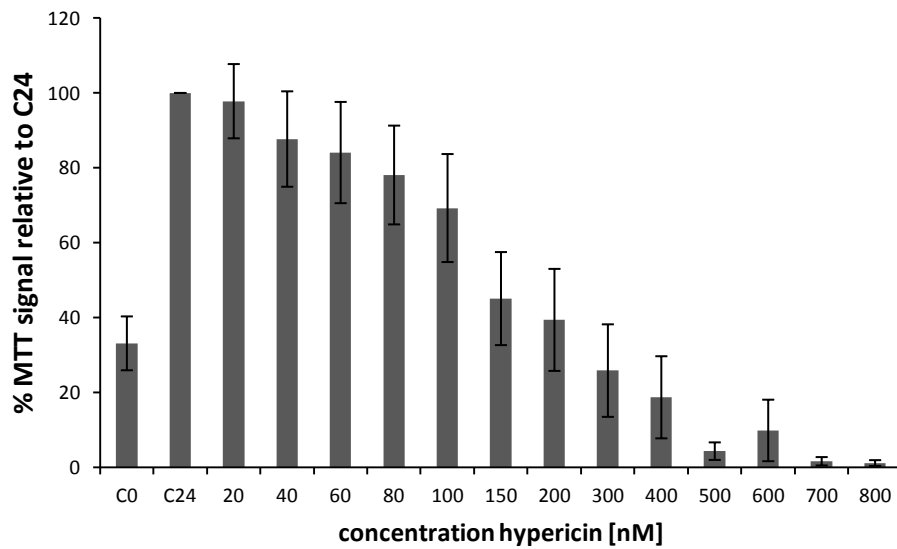


Figure 6: Light-dependent Cytotoxicity of Hypericin on CT26 Cells. CT26 cells were treated with increasing concentrations of hypericin in serum-free medium for 3 h and irradiated with a fluence of 1.1 J/cm². Viability was assessed 24 h post treatment using MTT assay.

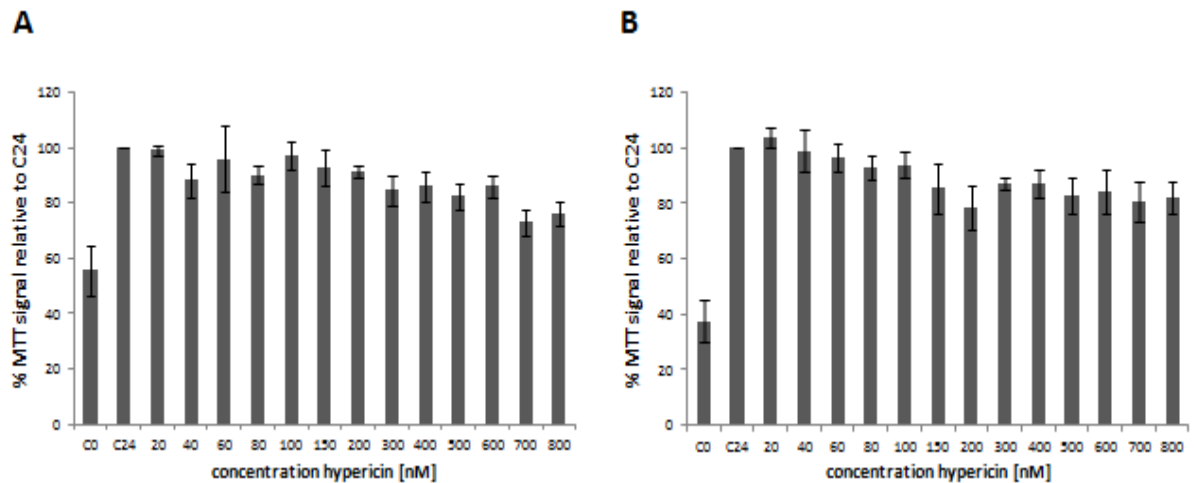


Figure 7: Effect of Unexcited Hypericin on A431 and CT26 Cells. Cells were treated with increasing concentrations of hypericin in serum-free medium for 3 h. Viability was assessed 24 h post treatment using MTT assay. (A) A431 cells (B) CT26 cells

4.4 Expression of Cytokine mRNA in BMDCs in Response to PDT

To assess the induction of cytokine expression in BMDCs after PDT treatment, LPS-stimulated and unstimulated BMDCs treated with 0, 80 and 300 nM hypericin-PDT were subjected to qRT-PCR. To evaluate the capacity of these cells to induce cytokine expression the obtained values from LPS-stimulated PDT-DCs were set relative to unstimulated controls. The cytokines analyzed were IL-1 β , IL-6, IL-12 and TGF- β due to their role as proinflammatory signature cytokines of mature DCs and their requirement for subsequent induction of Th17 cells and Treg.

4.4.1 Expression of IL-1 β and IL-6

As to be expected in response to an inflammatory stimulus like LPS, untreated mature BMDCs showed highly elevated levels of IL-1 β relative to the unstimulated control (596-fold increase; Fig. 8). BMDCs treated with 80 nM hypericin-PDT exhibited a reduced capacity to induce IL-1 β mRNA expression upon LPS stimulation. The mRNA levels in these samples reached only 66% of those found in untreated samples. Treatment with 300 nM hypericin-PDT caused a reduction in IL-1 β mRNA expression as well in response to LPS. However, this reduction is less than that seen for 80 nM hypericin-PDT with only 17% difference between

treated and untreated cells.

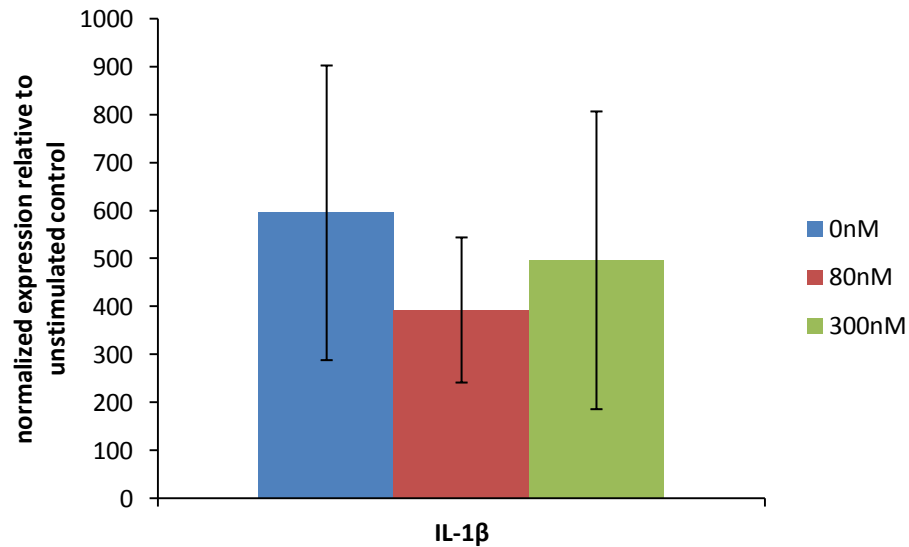


Figure 8: IL-1 β Expression in PDT-treated BMDCs. BMDCs were treated with indicated concentrations of hypericin in serum-free medium for 3 h and irradiated with a fluence of 1.1 J/cm². mRNA was isolated 24 h post treatment and the respective expression levels were analyzed stimulated / unstimulated. Expression level of the unstimulated control was set to 1.

IL-6 is another proinflammatory cytokine which is typically strongly induced in mature DCs. IL-6 mRNA was highly upregulated in untreated mature BMDCs compared to the unstimulated control (571-fold increase; Fig. 9). Treatment of BMDCs with 80 nM hypericin-PDT did not result in any changes in their capacity to induce IL-6 mRNA expression upon LPS stimulation. Treatment with 300 nM hypericin-PDT led to a downregulation of mRNA expression of 27% in comparison to the untreated control.

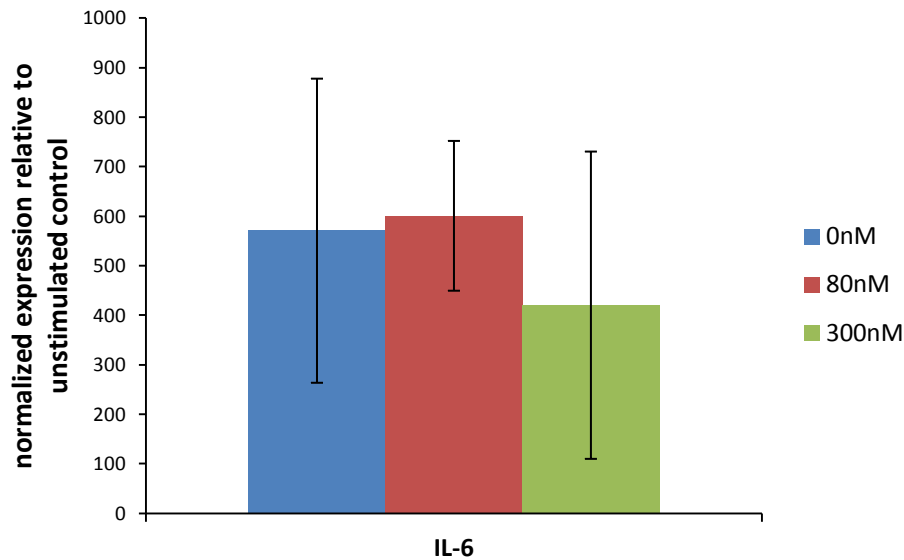


Figure 9: IL-6 Expression in PDT-treated BMDCs. BMDCs were treated with indicated concentrations of hypericin in serum-free medium for 3 h and irradiated with a fluence of 1.1 J/cm². mRNA was isolated 24 h post treatment and the respective expression levels were analyzed stimulated / unstimulated. Expression level of the unstimulated control was set to 1.

Of note, the induction of mRNA expression of both cytokines regarding the individual samples for each treatment condition showed a marked heterogeneity as can be seen from the high standard deviation.

4.4.2 Expression of IL-12 and TGF- β

Another proinflammatory cytokine which is characteristic for mature DCs with a medium to high expression in immunogenic DCs is IL-12. Hence, as to be expected, untreated LPS-stimulated BMDCs showed increased IL-12 mRNA expression with an average of 6.5-fold higher mRNA levels than the unstimulated control (Fig. 10). Upon treatment with 80 nM hypericin-PDT BMDCs exhibited an enhanced capacity to induce IL-12 expression, reaching a 20-fold increase compared to the unstimulated control (300% of the stimulated control). In contrast, treatment with 300 nM hypericin-PDT resulted in only 37% of IL-12 mRNA levels in comparison to the stimulated control (2.4-fold increase relative to the unstimulated control).

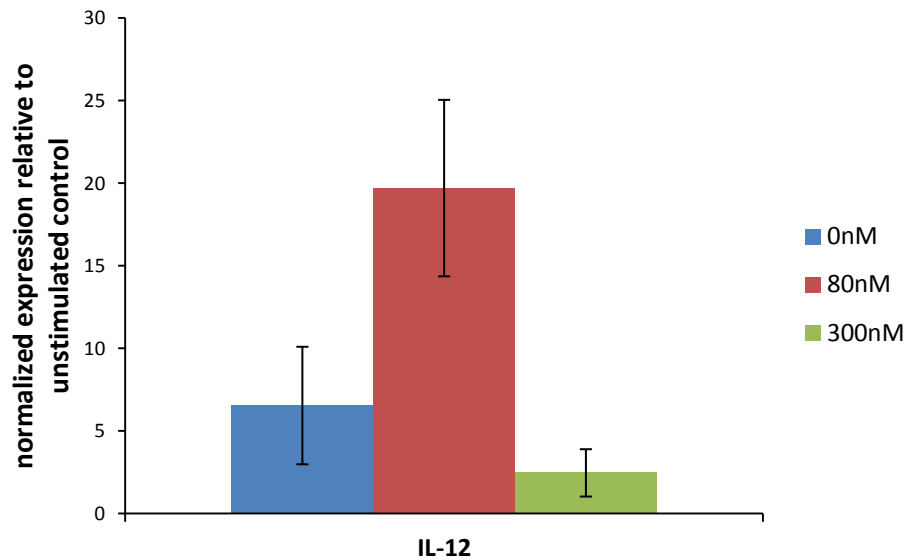


Figure 10: IL-12 Expression in PDT-treated BMDCs. BMDCs were treated with indicated concentrations of hypericin in serum-free medium for 3 h and irradiated with a fluence of 1.1 J/cm². mRNA was isolated 24 h post treatment and the respective expression levels were analyzed stimulated / unstimulated. Expression level of the unstimulated control was set to 1.

TGF- β is a pleiotropic cytokine which is crucial for Treg differentiation and highly abundant in a variety of cancers. Mature untreated BMDCs showed a minor increase in TGF- β expression of 1.8-fold relative to the unstimulated control (Fig. 11). Treatment with hypericin-PDT resulted in a diminished capacity of BMDCs to induce TGF- β expression: BMDCs treated with 80 nM hypericin-PDT exhibited a decreased capacity to induce TGF- β mRNA expression with levels reaching only 0.78-fold of those found in unstimulated controls (42% of the stimulated control). Upon treatment with 300 nM hypericin-PDT BMDCs displayed a reduction in TGF- β mRNA levels as well, albeit to a lesser extent: mRNA levels reached 69% of those seen in the stimulated control (1.3-fold relative to the unstimulated control).

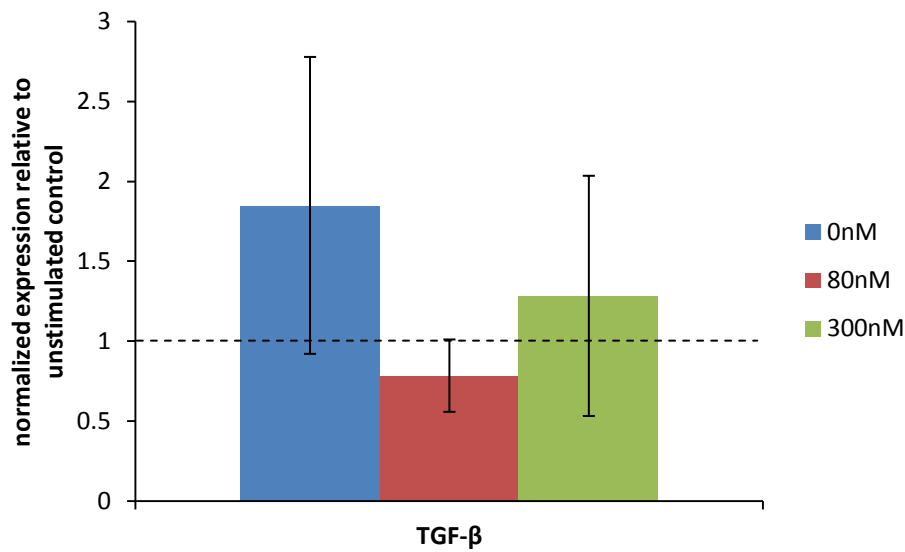


Figure 11: TGF- β Expression in PDT-treated BMDCs. BMDCs were treated with indicated concentrations of hypericin in serum-free medium for 3 h and irradiated with a fluence of 1.1 J/cm². mRNA was isolated 24 h post treatment and the respective expression levels were analyzed stimulated / unstimulated. Expression level of the unstimulated control was set to 1.

4.5 Secretion of IL-6 by BMDCs in Response to PDT

ELISA assay was carried out to measure the secretion of IL-6 by mature PDT-treated BMDCs since the degree between transcription (mRNA expression) and translation with subsequent secretion can differ due to posttranscriptional events. There was no difference in IL-6 secretion detectable between mature untreated BMDCs and mature BMDCs, which had received treatment with 80 nM hypericin-PDT. In contrast, BMDCs treated with 300 nM hypericin-PDT showed significantly decreased levels of IL-6 with only 46% \pm 11% of the cytokine content found in the supernatants from untreated control and low-dose treated cells (Fig. 12).

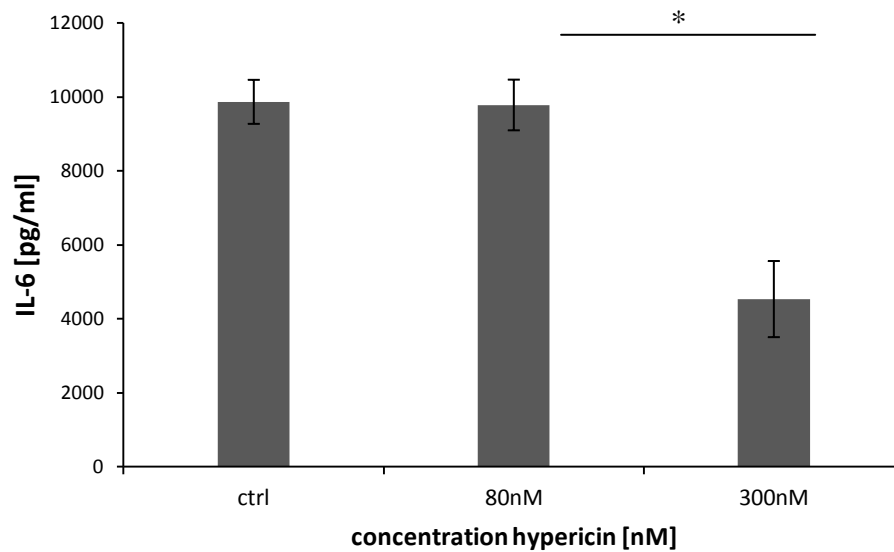


Figure 12: IL-6 Secretion by PDT-treated BMDCs. BMDCs were treated with indicated concentrations of hypericin in serum-free medium for 3 h and irradiated with a fluence of 1.1 J/cm². Cells were stimulated with LPS for 13 h and seeded with 2x10⁵ cells/mL. After 48 h the supernatant was collected and analyzed for IL-6 content.

Analysis of the IL-6 content in the co-culture medium largely showed the same distribution as for the PDT-treated BMDCs only (Fig. 12) when the samples containing 0.03 µg/mL OVA peptide were concerned: Supernatants from co-cultures with untreated or 80 nM hypericin-PDT treated BMDCs display the same level of IL-6 content (Fig. 13). Contrasting this, in co-culture supernatants, where 300 nM hypericin-PDT treated BMDCs were used a decrease in IL-6 secretion was observed. Only 60% ± 37% of the IL-6 content found in the former groups were detectable. An increase of the antigen dose led to increased IL-6 levels under all conditions (Fig.13). Significantly elevated levels of IL-6 were found in co-cultures containing untreated BMDCs (Fig. 13, blue columns, p = 0.03). In supernatants from cultures containing either 80 nM or 300 nM hypericin-PDT treated BMDCs decreased IL-6 levels compared to the control were observed. Supernatants from co-cultures with 80 nM-treated BMDCs contained only 72% ± 20% of the IL-6 content detected in the control group; however, this difference did not reach significance. Under 300nM conditions the supernatant displayed 49% ± 10% of IL-6 levels (relative to the control); this difference was significant with p = 0.02.

In summary, co-culture supernatants exhibit an antigen-dose dependent increase in IL-6 levels. 300 nM hypericin-PDT of BMDCs results in a decrease of secreted IL-6 for both antigen concentrations while 80 nM hypericin-PDT only does so to a lesser extent and in the presence of higher antigen doses.

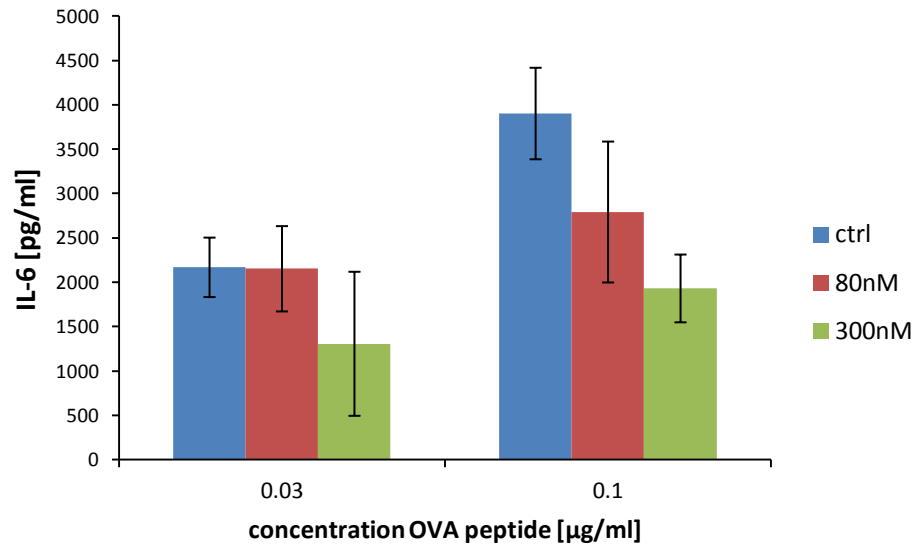


Figure 13: IL-6 Content in Co-Culture Supernatants. Supernatants from PDT-BMDC – T-cell co-cultures were collected after 5 days and analyzed for IL-6 content.

4.6 Titration of OVA Peptide Dose

The extent of Treg induction is dependent on TCR signaling strength and antigen dose (cp. section 1.4.3.3 *Regulatory T Cells (Treg)*). To establish the OVA dose to be used to achieve most effective induction of Treg by BMDCs, co-culture experiments were conducted with non-treated BMDCs. The antigen doses to be evaluated were chosen based on the work published by Yamazaki et al ⁸⁸, who had shown the antigen-dose dependency of Treg induction by BMDCs. However, co-cultures without addition of antigen already revealed the existence of a small population of Treg in both approaches (Fig. 14; average value of 0.015% and 1.24% Treg of alive KJ⁺ lymphocytes respectively). This can be attributed to the presence

of naturally occurring Treg, which had been isolated with the rest of the lymphocytes. Co-cultures of BMDCs and splenocytes showed only miniscule levels of detectable Treg (Fig. 14A). The reason for this is most likely the disappearance of available antigen due to the membrane turnover of MHC II, which presents the antigen. Prolonged antigen processing and presentation is not possible since the culture medium cannot be supplemented with additional antigen due to the presence of endogenous APCs as part of the unfractionated splenocytes. Unfortunately, this could obscure the obtained results and make small changes in Treg induction by BMDCs undetectable. Therefore, only fractionated lymphocytes were cultured with BMDCs for further assays and the culture medium was supplemented with the corresponding OVA antigen concentration for prolonged antigen supply. 0.03 $\mu\text{g/mL}$ OVA peptide was shown to be the most permissive antigen dose for Treg induction in this system with an average of 10.23% detectable Treg after co-culture (Fig. 14B). An increase of the antigen dose to 0.1 $\mu\text{g/mL}$ resulted in only 3.25% of $\text{CD4}^+\text{CD25}^+\text{Foxp3}^+$ cells. Therefore, these two doses were chosen to be used for further co-culture experiments to analyze treatment-induced alterations in Treg induction.

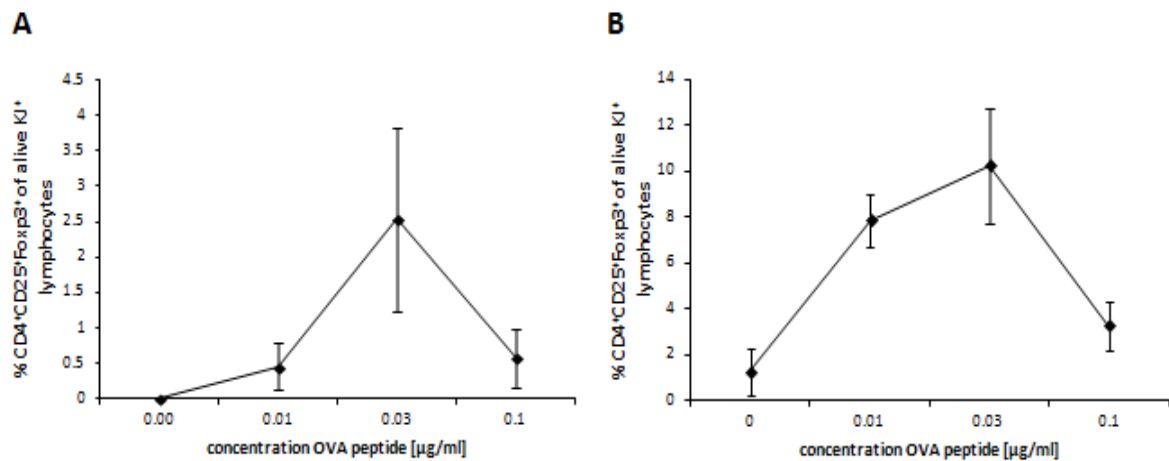


Figure 14: Antigen-dose dependent Treg Induction by BMDCs. Co-cultures from BMDCs and DO11.RAG2^{-/-} splenocytes (A) and T lymphocytes (B) were incubated in the presence of increasing concentrations of OVA antigen, IL-2 and TGF- β for 5 days. After 5 days the cells were collected and analyzed for abundance of $\text{CD4}^+\text{CD25}^+\text{Foxp3}^+$ cells (Treg).

4.7 Induction of Regulatory T Cells by PDT-treated BMDCs in Response to OVA

To evaluate the possibility that PDT treatment of BMDCs could change their ability to induce Treg in response to antigen, mature PDT-treated DCs were co-cultured with naïve DO11.RAG2^{-/-} T lymphocytes in the presence of OVA peptide. As to be expected from the experiments for the antigen dose titration (cp. section 4.6 *Titration of OVA Peptide Dose*) administration of 0.03 µg/mL OVA led to induction of substantially higher levels of Treg than administration of 0.1 µg/mL OVA (Fig. 15). This was true for all PS concentration applied (0, 80 and 300 nM). Treatment of BMDCs with low-dose hypericin-PDT resulted in diminished induction of Treg in the presence of 0.03 µg/mL as well as 0.1 µg/mL OVA compared to the untreated control (10.2% ± 2.5 vs. 7.8% ± 1.8 and 3.2% ± 1.0 vs. 1.6% ± 0.5 respectively). Nevertheless, this reduction in generation of Treg did not reach significance. Treatment of BMDCs with hypericin-PDT at a concentration of 300 nM did not reveal any changes in subsequent Treg induction for both antigen concentrations (10.2% ± 2.5 vs. 9.4% ± 2.5 and 3.2% ± 1.0 vs. 4.0% ± 2.0 respectively).

Taken together, these results show a tendency towards a decrease in Treg induction by BMDCs treated with low-dose hypericin-PDT.

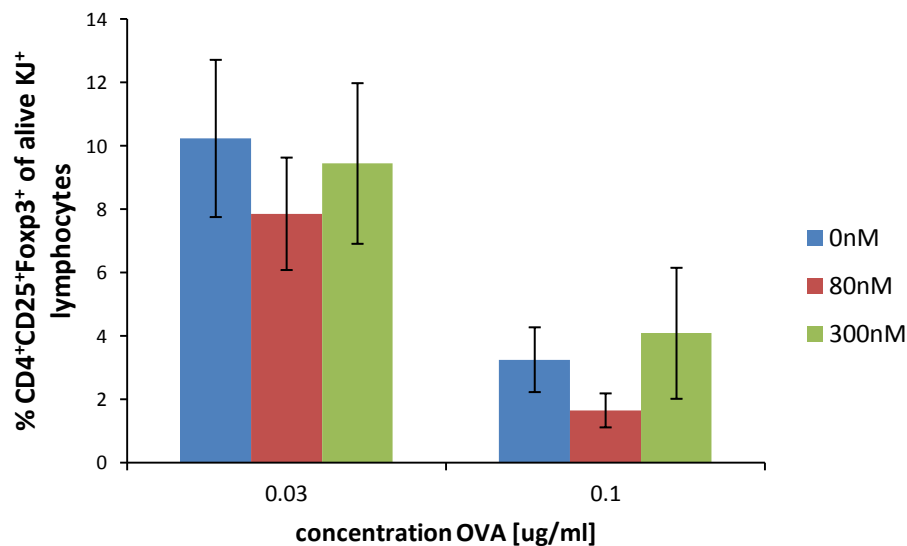


Figure 15: Treg Induction by PDT-treated BMDCs in Response to OVA.

DO11.RAG2^{-/-} T lymphocytes were co-cultured with PDT-treated BMDCs in the presence of the indicated concentrations of OVA antigen, IL-2 and TGF-β for 5 days. After 5 days the cells were collected and analyzed for abundance of CD4⁺CD25⁺Foxp3⁺ cells (Treg).

4.8 Cytokine Secretion by T Cells in the Co-Culture

T lymphocytes produce subtype-specific cytokines. Analysis of these cytokines can be used to determine the presence of certain T cell subtypes; in the present study this applies for Th1 and Th17 cells with their signature cytokines IFN γ and IL-17A.

4.8.1 IFN γ in the Co-Culture Supernatant

ELISA analysis of the co-culture supernatant for IFN γ content shows no significant changes in IFN γ levels within the supernatant independently of the PDT dose applied. Furthermore, the analysis reveals the same degree of IFN γ secretion with 0.03 $\mu\text{g/mL}$ antigen as well as with 0.1 $\mu\text{g/mL}$ (Fig. 16).

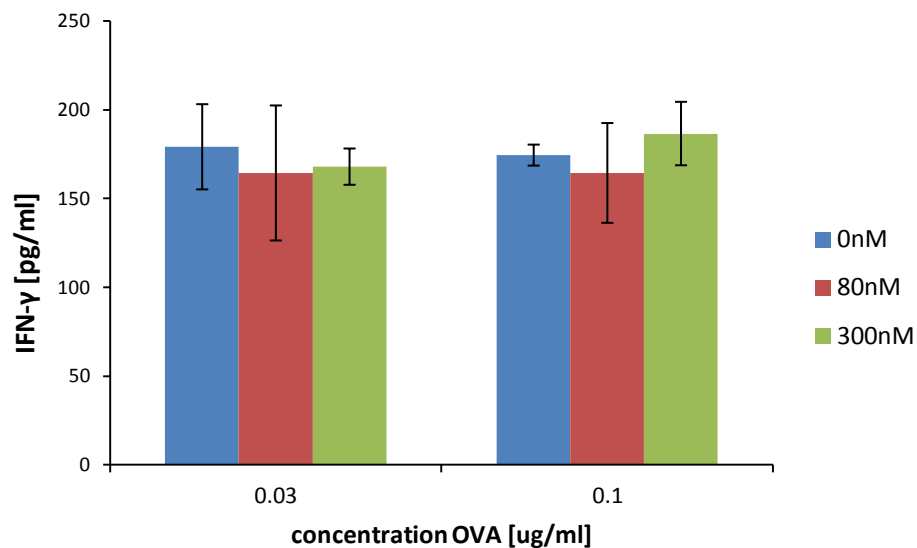


Figure 16: IFN- γ Content in Co-Culture Supernatants. Supernatants from PDT-BMDC – T-cell co-cultures were collected after 5 days and analyzed for IFN- γ content.

4.8.2 IL-17A in the Co-Culture Supernatant

Analysis of IL-17A levels in the supernatants of co-cultures with 0.03 $\mu\text{g/ml}$ OVA peptide showed an induction of IL-17A secretion by T lymphocytes induced by BMDCs treated with

80 nM as well as 300 nM of hypericin-PDT. On average the levels of IL-17A were 132% higher as those found in the control (Fig. 17). However, evaluation of the single values revealed that this increase was mainly caused by one high outlier for each treatment condition (Fig. 18, open diamonds). After exclusion of these outliers, IL-17A showed no increased secretion at 80 nM and only a moderate increase at 300 nM (1.7 ± 0.13 fold change relative to control).

In the co-culture supernatants containing 0.1 µg/ml OVA antigen a slight decrease in cytokine secretion was visible at 80 nM. In contrast, at 300 nM the supernatant displayed a marked increase in IL-17A levels (Fig. 17). In general, these cultures exhibited an increase in IL-17A secretion to levels comparable to (0 nM, 80 nM) or higher than (300 nM) those found in cultures containing 0.03 µg/ml antigen and BMDCs treated with 300 nM hypericin PDT. Similar to supernatants from 0.03 µg/ml OVA antigen cultures, detailed review of the single values showed the existence of one outlier per PDT treatment condition (Fig. 19, open diamonds). Dismissal of these values results in an equal degree of cytokine secretion between lymphocytes from control and 80 nM co-cultures. Lymphocytes from co-cultures with 300 nM hypericin-PDT treated BMDCs exhibit a significant increase in IL-17A secretion (1.8 ± 0.03 fold increase relative to control; p-value = 0.004).

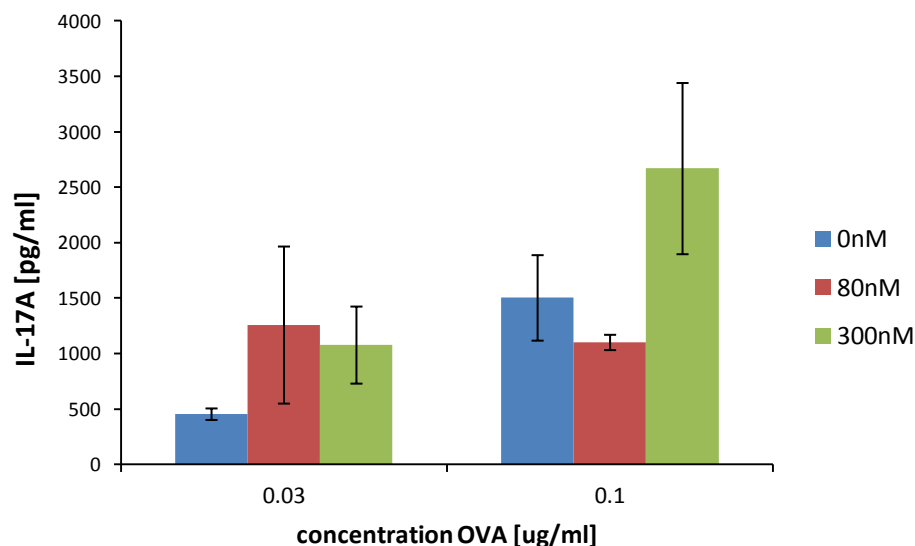


Figure 17: IL-17A Content in Co-Culture Supernatants. Supernatants from PDT-BMDC – T-cell co-cultures were collected after 5 days and analyzed for IL-17A content.

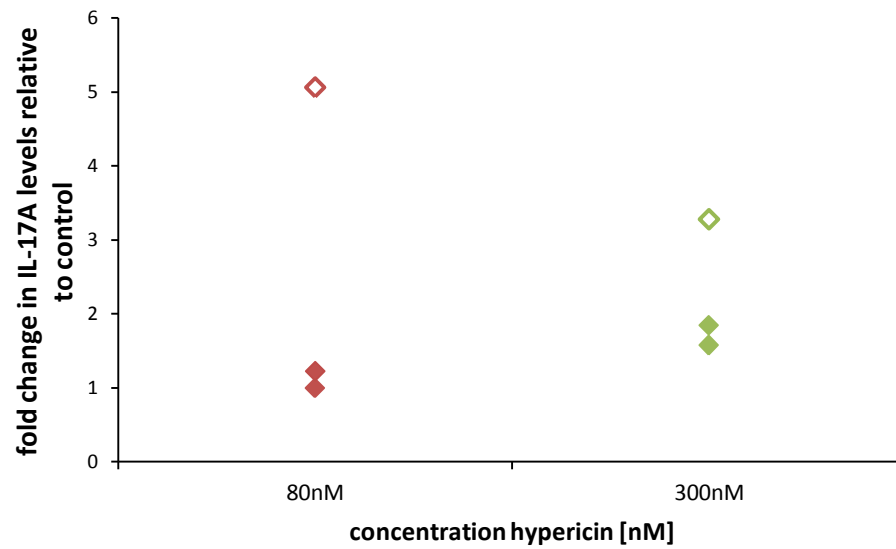


Figure 18: Single Values of Fold Change in IL-17A Content relative to Controls in Supernatants from Co-Cultures containing 0.03 µg/ml OVA Peptide. Supernatants from PDT-BMDC – T-cell co-cultures were collected after 5 days and analyzed for IL-17A content. The obtained cytokine levels were set relative to the levels found in corresponding controls.

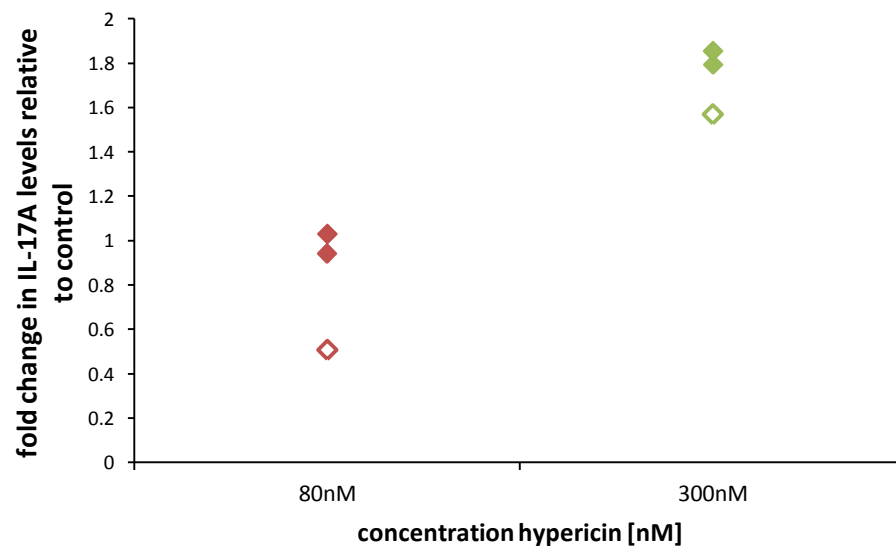


Figure 19: Single Values of Fold Change in IL-17A Content relative to Controls in Supernatants from Co-Cultures containing 0.1 µg/ml OVA Peptide. Supernatants from PDT-BMDC – T-cell co-cultures were collected after 5 days and analyzed for IL-17A content. The obtained cytokine levels were set relative to the levels found in corresponding controls.

Calculation of the ratio between IL-17A and IFN γ (as a surrogate for the ratio between Th1 and Th17 cells) in the culture supernatants confirmed these results: lymphocytes from co-cultures with 0.03 $\mu\text{g/mL}$ antigen show a slight but not significant increase in the IL-17A/IFN γ ratio with increasing PDT dose (Fig. 20). In cultures with 0.1 $\mu\text{g/mL}$ OVA this ratio is similar for the control and the 80 nM fraction. In contrast, the 300 nM fraction displays a significantly higher IL-17A/IFN γ ratio than the control (10.74 ± 1.33 vs. 5.41 ± 0.76 ; p-value = 0.039).

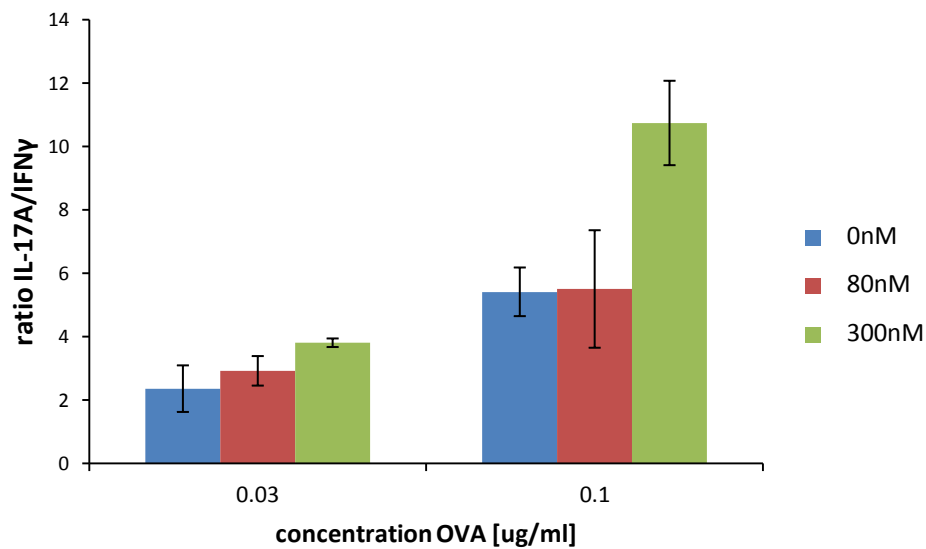


Figure 20: Ratio of IL-17A / IFN- γ Content in Co-Culture Supernatants. Supernatants from PDT-BMDC – T-cell co-cultures were collected after 5 days and analyzed for cytokine content. The cytokine levels within each sample were set relative to each other and the average was calculated based on the resulting single values for each treatment condition.

5. Discussion

The present study was designed to investigate the influences of hypericin-PDT on DCs and subsequent T cell activation and differentiation with special emphasis on the induction of Treg and / or Th17 cells. In 2009, a study by Preise et al. had shown the requirement of DCs for PDT efficiency. In this study, local as well as systemic depletion of DCs accompanying treatment led to significantly increased tumor recurrence rates compared to those observed in unmanipulated mice receiving the treatment (Fig. 21) ⁴⁸.

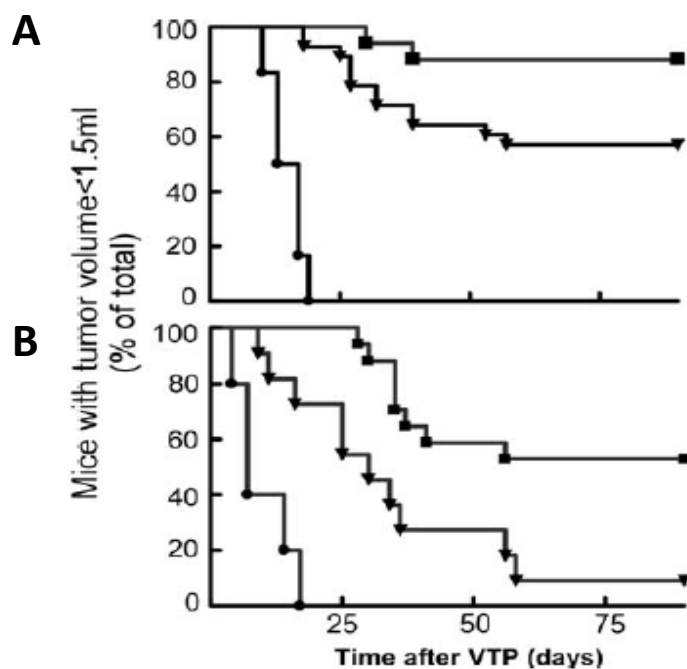


Figure 21: Requirement of DCs for PDT Efficiency. Effect of (A) local depletion and (B) systemic depletion of DCs on PDT efficiency using diphtheria toxin (DTx)-sensitive bone marrow chimeras. Mice bearing s.c. CT26 tumors were either subjected to vascular-targeted therapy (VTP) only (squares), VTP with depletion (triangles) or DTx only (circles) ⁴⁸.

Additionally, Sanovic et al. achieved a striking success with a low-dose hypericin-PDT treatment protocol: mice receiving this type of treatment (2.5 mg/kg hypericin, incubation time 0.5 h, light dose 14 J/cm², fluence rate 27 mW/cm²) showed a 100% cure rate and resistance to subsequent rechallenge with tumor cells of the same type (CT26 colon carcinoma cells). In contrast, mice treated with a standard protocol (10 mg/kg hypericin, incubation time 4 h, light dose 60 J/cm², fluence rate 50 mW/cm²) only showed delayed tumor growth (Fig. 22) ⁵⁵.

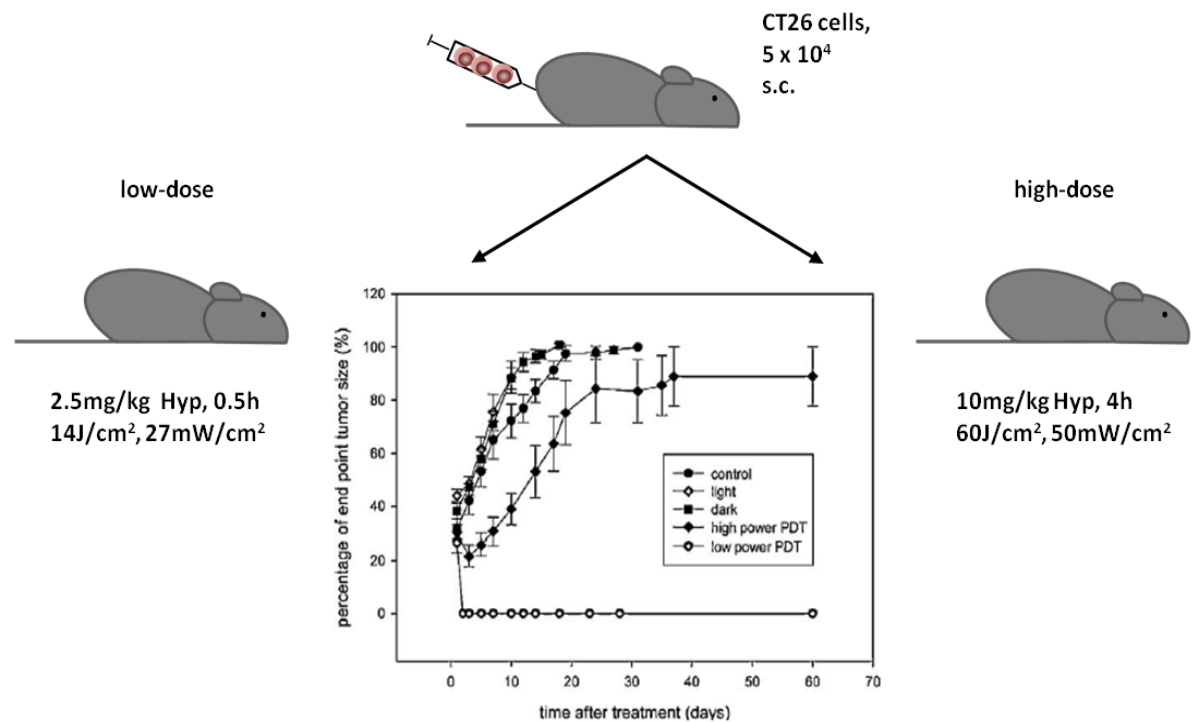


Figure 22: Schematic Representation of the Low-Dose Hypericin-PDT Treatment Protocol and Subsequent Tumor Response. Mice were inoculated with CT26 colon carcinoma cells and treated with the indicated protocols (as described above) when the tumors were established. Tumor response was assessed for 60 days or until they reached the end point size of 10 mm. Modified from Sanovic et al., 2011.

These findings prompted the hypothesis that low-dose PDT treatment of the DCs in the treatment area could influence these DCs in a way which would affect subsequent T cell activation and differentiation. Since the immunological tolerance towards the tumor must have been breached at some point to generate memory immunity (as evidenced by resistance to rechallenge), it was reasoned that this break might have occurred on the level of Treg induction by DCs upon antigen exposure. However, information about the direct effects of PDT on DCs is rare to non-existent. Therefore, this work started with the evaluation of the effect of hypericin-PDT on DC viability and expression of cytokines which are crucial for the subsequent differentiation of naïve T cells into effector T cells or Treg. The second part of this study was dedicated to the determination of the capacity of those PDT-treated DCs to induce Treg and effector T cells.

PDT treatment of immature BMDCs with hypericin showed a dose-dependent bidirectional

effect on cell viability: hypericin doses up to 100 nM followed by red light irradiation (610 nm) with a fluence of 1.1 J/cm² resulted in a proliferative effect which was most pronounced at a hypericin concentration of 80 nM (Fig. 4). Concentrations higher than 150 nM exerted a cytotoxic effect which reached significance at 300 nM. This raises the possibility that the dose applied for PDT treatment – if not chosen carefully – could not only kill the tumor cells but DCs residing in the treatment area as well. This would be detrimental for uptake of antigen from dying/dead tumor cells and subsequent presentation to T lymphocytes, which is needed for the initiation of an adaptive immune response against the tumor. Hypericin doses in preclinical *in vivo* studies typically range between 1 and 5 mg/kg (2 – 10 μM)⁸⁹. In a study on biodistribution and photodynamic effects of hypericin in PDT, Chen et al. showed that 5 μg hypericin / g wet tissue (10 μM) accumulated in the tumor within 3 h after i.v. injection of 5 mg/kg hypericin. In contrast, after 0.5 h most of the PS was located within the tumor blood vessels⁹⁰. Immature DCs possess a high phagocytic/endocytic activity, which they need to screen their environment for potentially harmful antigens. Therefore, it seems likely that prolonged incubation times and high doses of hypericin would result in increased accumulation of the PS within DCs, leading to cell death upon irradiation. A similar phenomenon was found for tumor-associated macrophages by several groups⁹¹. Interestingly, macrophages which resided close to blood vessels generally displayed a higher PS content⁹². Of note, in the study by Sanovic et al., which resulted in 100% tumor cures, 2.5 mg/kg (5 μM) of hypericin with an incubation time of 0.5 h were used⁵⁵. The present study demonstrates that most of the DCs already succumbed to light-dependent cytotoxicity at a concentration of 800 nM hypericin. However, in an *in vivo* setting it seems likely that the DCs in the vicinity of the tumor would effectively take up an amount of PS which resembles the doses shown to have a beneficial effect on DC viability more closely. This could be due to two particular reasons: first, most of the PS would be located within the tumor vessels at an incubation time of 0.5 h; thus, only a fraction of the PS would reach the DCs which are closer to the tumor mass. Second, tumor cells keep DCs in a semi-mature state which includes a decreased phagocytic/endocytic capacity. Therefore, these educated DCs might not be able to take up as much PS as the immature BMDCs used in this study. Nevertheless, the hypericin uptake and content of tumor-educated DCs at different doses and incubation times should be investigated further to improve treatment protocols which are designed to stimulate the host's tumor-specific immune response.

Importantly, cancer cells actively induce apoptosis of DCs via tumor-derived factors (e.g.

gangliosides, neuropeptides, HMGB-1). This includes the death of precursors, early apoptosis of DCs and acceleration of the turn-over rate thus leading to decreased numbers of DCs in the vicinity of the tumor^{80,93}. The proliferative effect of low-dose PDT on DCs could improve the number of available DCs in the tumor microenvironment (TME), which could result in increased antigen uptake and presentation and a more efficient induction of anti-tumor immunity.

Interestingly, even without irradiation hypericin exerted proliferative as well as cytotoxic effects on BMDCs (Fig. 3). At 80 nM the BMDCs displayed an increase in viability of about 19% and became increasingly cytotoxic at concentrations of 150 nM and higher. Therefore, it is possible that the response of DCs to hypericin-PDT treatment is a result of increased accumulation of and a high sensitivity against the PS. Furthermore, application of hypericin might pose a serious threat to the induction of an adaptive immune response by diminishing DCs numbers when improper doses are used.

For further investigations two hypericin doses were chosen: 80 nM for its pronounced beneficial effect on BMDC viability and 300 nM as a control with LD₄₀. This was based on the assumption that DCs had a benefit from the low-dose treatment protocol in the *in vivo* study from Sanovic et al. that facilitated the induction of an adaptive anti-tumor response.

To verify that cancer cells respond to the low hypericin-PDT doses utilized for the BMDCs A431 and CT26 cells were analyzed for light-dependent cytotoxicity when the same dose range was used. At 80 nM both cell types showed a marked decrease in viability compared to the untreated control (Fig. 5 and 6). However, whether this decrease in viability was caused by diminished proliferation or induction of cell death remains to be determined. Nevertheless – based on the results from Sanovic et al. - it is likely that low-dose hypericin-PDT is sufficient to provide tumor-derived antigens necessary for the induction of an adaptive immune response by inducing cancer cell death. Of note, at lower concentrations A431 cells displayed no change or a slight increase in viability in comparison to the control. This implies that in the context of hypericin-PDT as tumor therapy the type of tumor has to be taken into consideration when choosing the dose: doses below the cell type specific susceptibility could hamper PDT efficiency by stimulating cancer cell proliferation instead of cancer cell death. This is further supported by the notion that MCF-7 cells exhibit a lesser sensitivity to hypericin-PDT than other cell lines^{19,94}.

Upon maturation induced by an inflammatory stimulus, DCs increase the expression of (proinflammatory) cytokines which are essential for subsequent differentiation of naïve T lymphocytes into mature effector T cells. Therefore, LPS-stimulated PDT-BMDCs were analyzed for mRNA expression of cytokines which are known to be upregulated upon DC maturation and/or are necessary for the differentiation of T cell subtypes involved in tumor immunity (Fig. 23). The cytokines analyzed were IL-1 β , IL-6, IL-12 and TGF- β .

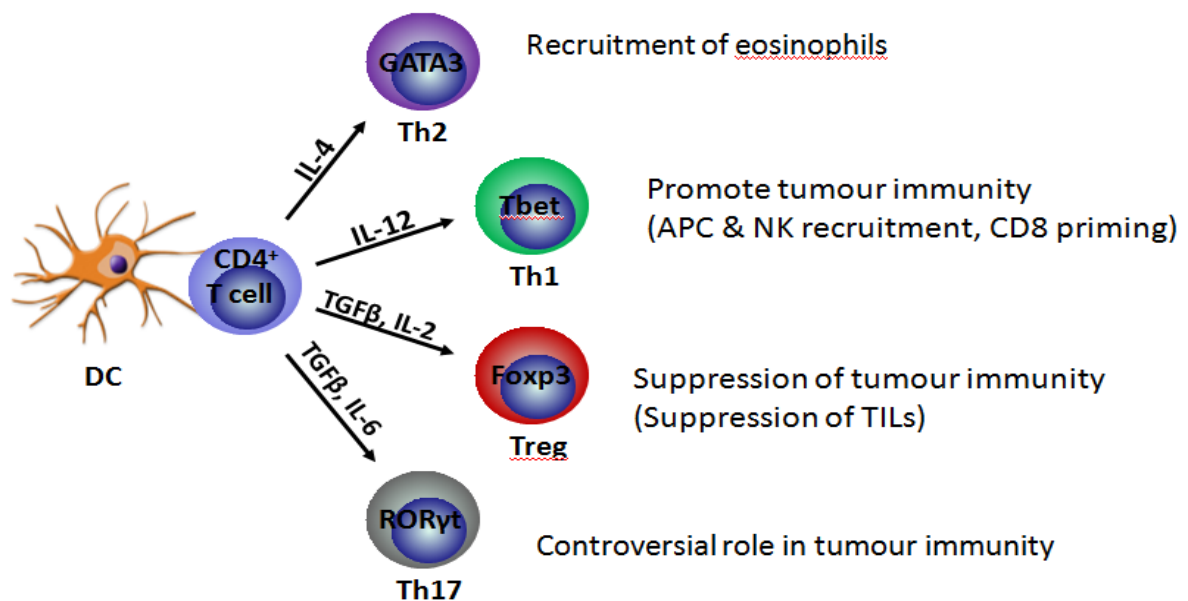


Figure 23: Schematic Representation of the Involvement of T Helper Cells in Tumor Immunity and the Cytokines Needed for Their Induction

IL-1 β is a proinflammatory cytokine, which is typically produced by epithelial cells, macrophages and mature DCs. Functionally, it is involved in a variety of biological processes including the induction of acute phase protein synthesis, attraction of neutrophils by induction of CXCL2 and T cell differentiation, i.e. the differentiation of Th17 cells albeit only in an accessory fashion ⁹⁵.

In the present study, PDT-BMDCs showed a 34% decrease of IL-1 β expression in low-dose treated cells and a minor decrease of 17% in 300 nM hypericin-PDT treated cells. Contrasting this result, IL-1 β has been found to be upregulated after PDT in *in vivo* settings by several groups ^{35–37}. Additionally, it was shown that IL-1 β is crucial for PDT outcome

since it mediates treatment-induced neutrophilia which is necessary for PDT efficiency and blocking of this cytokine results in decreased tumor cures and neutrophils in the TDLNs. Moreover, Gollnick et al. found that in their hands the most efficient protocol (with respect to fluence and fluence rate) induced only moderate neutrophil infiltration whereas the highest degree of neutrophil influx was found with a far less efficient protocol ³³. Therefore, a moderate increase in IL-1 β after treatment might be more useful than a higher one. Mechanistically, Brackett et al. were able to show that IL-1 β governs the expression of CXCL2 which is necessary for neutrophil migration into the tumor ³⁷. However, none of these studies elaborated which cell types were the producers of IL-1 β in the respective systems. Interestingly, Brackett et al. additionally found that the expression of IL-1 β was regulated by IL-17A which was upregulated after treatment as well. Thus, it seems unlikely that the source of IL-1 β in these studies were DCs. However, diminished IL-1 β secretion by PDT-treated DCs might still influence DC-induced Th17 differentiation and/or the functional phenotype of these cells.

IL-6 is a pleiotropic cytokine with pro- and anti-inflammatory functions and a signature cytokine of functionally mature DCs. In the context of cancer, IL-6 is functionally involved in proliferation, angiogenesis, inhibition of apoptosis and promotion of survival, invasiveness and metastasis ⁹⁶. It is found in high levels in the serum and tumor tissues of a variety of cancers and the main source of IL-6 in the TME are the tumor cells themselves as well as fibroblasts, myeloid-derived suppressor cells, tumor-associated macrophages and CD4⁺ T cells. A recent meta-analysis of the clinical literature on the relation between IL-6 serum levels and the prognosis of cancer patients by Lippitz and Harris found an inverse correlation between IL-6 levels and median survival ⁹⁷. Proinflammatory signaling by IL-6 (trans-signaling via the soluble IL-6 receptor sIL-6R) leads to upregulation of the proinflammatory cytokines TNF- α and IL-1 β . Additionally, this form of IL-6 signaling facilitates the recruitment of T lymphocytes to the site of inflammation by inducing the expression of chemoattractants like CCL4, CCL5, CCL17 and CXCL10. Moreover, STAT3-dependent upregulation of anti-apoptotic proteins including Bcl-2 and Bcl-xL is induced by proinflammatory IL-6 signaling and contributes to cell survival and proliferation in the TME. Anti-inflammatory IL-6 signaling (classical signaling via membrane-bound IL-6 receptor mbIL-6R) promotes proliferation and regeneration, partially by downregulating TNF- α and IL-1 β expression and upregulation of anti-inflammatory molecules such as IL-1 receptor

antagonist protein, TNF soluble receptor and extrahepatic protease inhibitors. Moreover, this type of signaling by IL-6 is responsible for its role in the activation of the acute phase response. The proinflammatory actions of IL-6 in the TME are thought to be required to exert its tumor promoting effects. On the other hand, the TME is characterized by a state of chronic inflammation rather than an acute inflammatory response. Therefore, within the TME the balance of pro- and anti-inflammatory actions of IL-6 is crucial for initiation of this chronic state and maintenance of the host-tumor homeostasis.

Upregulation of IL-6 after PDT treatment has been shown in numerous reports^{29,30,44,98}. This upregulation is the result of an insult leading to an acute inflammatory response within the treatment area. Hence, the TME would be shifted from a state of tumor-promoting chronic inflammation to a state of acute inflammation which can trigger an immune response directed against the tumor. Induction of IL-6 expression in the treatment area may result in the activation of two important functions of IL-6 in the context of (PDT-mediated) anti-tumor response: firstly, IL-6 is involved in the recruitment of neutrophils to sites of infection and inflammation. Treatment-induced neutrophilia has been shown to be important for PDT efficiency and blocking of IL-6 (and IL-1 β) resulted in reduced neutrophilia after PDT^{34,36,37,44,45}. Secondly, IL-6 in concert with TGF- β is responsible for the differentiation of naïve T lymphocytes into Th17 cells. Although the role of Th17 cells in anti-tumor immunity remains controversial, there exists a body of evidence suggesting that Th17 cells assist in the eradication of tumor cells^{99–101}. In the context of PDT, Brackett et al. have shown an increase of Th17 cells and IL-17 post-treatment which regulated accumulation of neutrophils in the tumor draining lymph nodes³⁷. Interestingly, differentiation of Th17 cells appears to be mediated by IL-6 signaling via mbIL-6R while activated Th17 cells seem to be maintained by IL-6 signaling via sIL-6R¹⁰².

In the present study, mature PDT-treated BMDCs showed no change in IL-6 mRNA expression and IL-6 secretion upon low-dose treatment (Fig. 9 and 12). In contrast, PDT treatment with 300 nM hypericin resulted in diminished expression of IL-6 and significantly lower levels of secreted IL-6 by BMDCs (Fig. 9 and 12). However, with higher antigen doses all treatment conditions displayed an increase of secreted IL-6 (Fig. 13). This increase was significant for the untreated control group and less pronounced for co-cultures containing 80 nM or 300 nM hypericin-PDT treated BMDCs. Nevertheless, the higher treatment dose again resulted in significantly lower levels of IL-6 compared to the control (1930.87 ± 382.03 pg/mL vs. 3902.48 ± 515.69 pg/mL). Taken together, these data indicate that higher doses of

PDT downregulate the expression and secretion of IL-6 by BMDCs. This could negatively affect the induction of the acute phase response, neutrophil recruitment and Th17 differentiation in response to the treatment when high doses of hypericin are used in PDT. A scenario like this would clearly hamper the induction of an effective tumor-specific immune response.

IL-12 is a hallmark cytokine of DC maturation. It is a proinflammatory cytokine with a pivotal role in the differentiation of Th1 cells from naïve T lymphocytes and thereby crucial for the induction of the adaptive immune response against viruses, intracellular bacteria and as well tumor antigens. Furthermore, it supports recognition and elimination of aberrant cells by enhancing the cytotoxic activity exerted by natural killer (NK) cells and CTLs. In this work, BMDCs reacted differentially to low- and high-dose treatment with hypericin-PDT: treatment with 80 nM hypericin-PDT led to an increased capacity of about 300% to induce IL-12 mRNA expression compared to the untreated control (Fig. 10). On the other hand, treatment with 300 nM hypericin-PDT resulted in diminished IL-12 expression with only 37% of the mRNA levels seen in the untreated control. This raises the possibility that higher doses of hypericin-PDT would diminish the differentiation of Th1 cells in response to antigen which is taken up and presented by DCs from the treatment field. As a consequence, the lack of IFN- γ -producing Th1 cells could lead to decreased activation of macrophages and CTLs, which are necessary for the elimination of tumor cells.

TGF- β is an immunosuppressive cytokine which is highly abundant in the TME and is associated with tumor progression by facilitating tumor cell invasion and the functional inhibition of immune cells¹⁰³. TGF- β is able to suppress or alter the function of nearly all immune cells; thereby it inhibits the innate as well as the adaptive arm of the immune response which results in immune evasion of the tumor¹⁰⁴. In NK cells, which are responsible for the recognition and elimination of aberrant cells with decreased MHC I expression, TGF- β has been shown to impair their cytolytic activity and the production of IFN- γ . Additionally, expression of NKG2D, the activating receptor for NK cell activity was found to be downregulated in response to TGF- β . For neutrophils an inhibition of their cytotoxic activity was observed. Additionally, characterization of tumor-associated neutrophils revealed an expression profile which facilitates angiogenesis and metastasis. In support of the involvement of TGF- β in controlling this phenotype, a number of studies found conversion of

these neutrophils towards an anti-tumor phenotype under conditions inhibiting TGF- β ^{105–109}. Regarding DCs, TGF- β shows a variety of effects on their biology and function: Tumor-infiltrating DCs display dysfunctional APC capabilities, decreased phagocytic/endocytic capacity and abnormal motility ^{80,110–112}. Furthermore, their number is decreased due death of precursors, early apoptosis and an accelerated turn-over rate ^{93,113}. Additionally, these DCs are being kept in a semi-mature state characterized by downregulation of MHC II, co-stimulatory molecules and impaired secretion of TNF, IFN- α and IL-12 ^{93,104}. These DCs promote anergy, exhaustion and pro-tumorigenic activity. Importantly, cancer cells can turn DCs into TGF- β secreting cells which facilitate Treg induction and thereby tolerogenicity towards the tumor ¹¹³. T helper cells are affected by TGF- β as well: tumor-infiltrating lymphocytes are shifted from a Th1 phenotype to a Th2 phenotype, thereby inhibiting an effective anti-tumor response ¹¹⁴. A more complex picture emerges for Th17 cells and Treg: the differentiation of Treg is crucially dependent on TGF- β and Treg have been shown to be the predominant T lymphocytes subtype to accumulate in the tumor tissue ^{72–74}. TGF- β is as well needed for differentiation of Th17 cells. The differentiation and proliferation of this subtype also requires IL-6 and can be modulated by IL-1 β . All three cytokines are known to be expressed by tumor cells and cells from the TME and accumulation of Th17 cells was found in a number of different cancers ^{115,116}. However – as mentioned above – promising studies reported eradication of established tumors by Th17 either upon adoptive transfer or as a result of Th17 induction using tumor cells which had been transduced to secrete IL-6 ^{99–101}. Of note, these Th17 cells had been induced by the combination of IL-6 and TGF- β with no apparent involvement of IL-1 β . Therefore, the balance between the cytokines involved in Th17 differentiation and maintenance might be crucial for the effect which these cells exert on the tumor cells.

The present study showed that hypericin-PDT can modulate the TGF- β expression by BMDCs (Fig. 11): 80 nM hypericin-PDT resulted in decreased TGF- β mRNA expression with levels reaching only 42% of the stimulated control (0.78-fold of the unstimulated control). Upon treatment with 300 nM hypericin-PDT BMDCs displayed a reduction in TGF- β mRNA levels as well, albeit to a lesser extent: mRNA levels reached 69% of those seen in the stimulated control (1.28-fold relative to the unstimulated control). Therefore, it seems possible that low-dose hypericin-PDT can diminish the secretion of TGF- β by DCs from the TME. This could lead to impaired induction of immunosuppressive Treg, which assist the tumor in immune evasion. In combination with the results obtained for IL-6 this could

furthermore indicate a skewing of T helper cell differentiation towards induction of Th17 cells: differentiation of Th17 cells requires both cytokines, IL-6 and TGF- β . However, it has been shown that the ratio of IL-6 and TGF- β is crucial to abolish Treg induction and facilitate development of Th17 cells. At low concentrations TGF- β synergizes with IL-6 and drives the induction of Th17 cells. At high TGF- β concentrations IL-6 is no longer sufficient to overcome Foxp3-mediated repression of ROR γ t and the cells differentiate into Treg⁵⁹. Since low-dose treated PDT-BMDCs displayed no change in IL-6 expression and secretion compared to the untreated control while exhibiting reduced TGF- β expression, it seems feasible that this could result in a shift in the cytokine composition favoring DC-mediated Th17 induction.

Evaluation of Treg induction by PDT-BMDCs in this study did not reveal significant changes in Treg levels in co-cultures containing PDT-BMDCs compared to those with untreated BMDCs. However, in co-cultures with low-dose hypericin-PDT treated BMDCs a trend towards a reduced induction of Treg was visible (Fig. 15). Additionally, it could be possible that the Treg induced by PDT-BMDCs did not retain their suppressive capacity and would therefore not be able to exert their inhibitory effects on effector T cells and other immune cells. This scenario is supported by a report from Reginato et al.; in their study Treg cells from patients with esophageal squamous cell carcinoma receiving PDT treatment lost their suppressive capacity while maintaining the same levels as those seen in the control group¹¹⁷. However, this option could not be tested in this study and should be subject to further investigations.

To gain further insight into the composition of the effector T cell population (CD4⁺CD25⁺Foxp3⁻ T cells) supernatants from the co-cultures were analyzed for the Th1 and Th17 signature cytokines IFN- γ and IL-17A. For IFN- γ no change in cytokine levels was observed independently of antigen dose and PDT treatment conditions (Fig. 16). In cancer (and the general adaptive immune response as well) IFN- γ has a multitude of functions: it increases the expression of MHC I and II on normal cells and APCs, thereby promoting endogenous antigen processing and presentation to make infected and aberrant cells visible to the immune system. Furthermore, it enhances the activity of NK cells, which recognize and kill cells with decreased MHC I expression. Additionally, it is involved in the activation and regulation of CTLs, the cross-priming of the immune system by APCs and direct elimination of tumor cells via the release of specific cytokines⁵⁶. Increased IFN- γ levels are often

considered as a sign of an ongoing Th1 response and have been found after PDT treatment by several groups ^{28,38,48}. Interestingly, the results observed for IFN- γ in this study indicate that the same levels of Th1 cells were induced by BMDCs independently of antigen doses and treatment conditions. Nevertheless, this conclusion has some caveats: T lymphocytes proliferate substantially more in response to the higher antigen dose, therefore the induced Th1 cells could have secreted less IFN- γ per cell which would result in equal IFN- γ levels despite an increase in the Th1 population. Additionally, Th17 cells have been shown to be capable of co-producing IL-17A and IFN- γ ⁵⁸. Thus, there is a possibility that the detected IFN- γ – or some of it – might not have been produced by Th1 cells at all.


In contrast to IFN- γ , IL-17A levels differed in an antigen as well as in a PDT dose-dependent manner: firstly, IL-17A levels were generally increased in co-cultures with 0.1 $\mu\text{g/ml}$ OVA compared to those seen in co-cultures receiving 0.03 $\mu\text{g/ml}$ OVA. Secondly, co-cultures with 300 nM hypericin-PDT treated BMDCs contained significantly higher amounts of IL-17A at high antigen concentrations (and moderately elevated levels with low antigen dose) while there was no difference in cytokine levels detectable between co-cultures with untreated or low-dose hypericin-PDT treated BMDCs (Fig. 17, 18 and 19). These results were confirmed by the IL-17A/IFN γ ratio from the single experiments (Fig. 20). Th17 cells are the main – and in this system the only – producers of IL-17A. Hence, secretion of IL-17A is directly associated with the induction of Th17 cells from naïve T lymphocytes initially present in the co-culture. Therefore, it can be concluded that Th17 cells were induced to the same degree by untreated and low-dose hypericin-PDT treated BMDCs at both antigen doses. The significantly increased levels of IL-17A in co-cultures with 300 nM hypericin-PDT treated BMDCs at high antigen doses seem to reflect an increased induction of Th17 cells under these conditions. However, due to the increased proliferation of T lymphocytes in response to higher doses of antigen a definite statement about the size of this population cannot be made. To do so, a more detailed analysis of these cells would be necessary, e.g. using FACS staining for specific transcription factors and intracellular cytokines to detect CD4⁺CD25⁺ROR γ t⁺IL17⁺ cells; these would be activated IL-17-secreting Th17 cells. The same approach could be used to identify Th17 cells producing IL-17A and IFN- γ (CD4⁺CD25⁺ROR γ t⁺IL17⁺ cells) and Th1 cells (CD4⁺CD25⁺Tbet⁺IFN- γ ⁺ cells).

6. Conclusion

The present study shows that low-dose hypericin-PDT seems to maintain the expression of proinflammatory cytokines by DCs in response to an inflammatory stimulus, while higher PDT doses hamper their proinflammatory capacity of DCs. Therefore, low-dose hypericin-PDT might rescue or re-induce their proinflammatory phenotype which is actively repressed by tumor cells. This would lead to increased antigen uptake and presentation with subsequent activation and differentiation of tumor-specific effector T cells and thus aid in the induction of an effective adaptive immune response against the tumor. However, as mentioned above, DCs in the TME are educated by the tumor cells and being kept in a semi-mature state with dysfunctional and even suppressive properties. Since PDT treatment in the course of tumor therapy would target these cells (as opposed to conventional DC with normal functional properties) it would be necessary to evaluate how those tumor-educated DCs respond to the same type of treatment.

Regarding the induction of Treg and effector T cells by low-dose hypericin-PDT treated BMDCs this study did not reveal significant changes for both subtypes in comparison to induction by untreated BMDCs. However, the beneficial effect of low-dose hypericin-PDT with respect to the induction of the adaptive immune response might be the functional restoration of the immune response in the TME: T lymphocytes are highly sensitive to PDT-mediated cell death and it has been shown that CD3⁺ lymphocytes (with CD3 as part of the T cell receptor being expressed by all T cells) disappear from the treatment area shortly after PDT and repopulate it about 24 h later with levels exceeding those prior to treatment^{48,50,118,119}. Thus, it seems intriguing to speculate that with the PDT treatment the TME would be depleted of Treg supporting the tumor while at the same time DCs could efficiently take up tumor-derived antigen, present it to T lymphocytes and initiate a tumor-specific immune response which is not skewed by the TME. However, the phenotype of the T cells repopulating the treatment area as not been elucidated in detail so far and clearly needs further investigation.

Taken together, low-dose hypericin-PDT shows promising beneficial effects on BMDCs with respect to viability and proinflammatory capacity. Furthermore, it maintains their ability to induce differentiation of T lymphocytes upon antigen uptake. Therefore, detailed studies



should be conducted to determine the effects of this treatment regimen on tumor-educated DCs and further analyze the phenotype and functionality of the induced T cells. Additionally, *in vivo* studies should be employed to evaluate the effect of low-dose PDT on DC numbers and functionality in the TME and to assess the composition of the T cell population in the TME and the tumor-draining lymph nodes after treatment.

7. References

1. Agostinis, P. *et al.* Photodynamic therapy of cancer: an update. *CA. Cancer J. Clin.* **61**, 250–281 (2011).
2. Dougherty, T. J. An update on photodynamic therapy applications. *J. Clin. Laser Med. Surg.* **20**, 3–7 (2002).
3. Allison, R. R. & Sibata, C. H. Oncologic photodynamic therapy photosensitizers: a clinical review. *Photodiagnosis Photodyn. Ther.* **7**, 61–75 (2010).
4. Plaetzer, K., Krammer, B., Berlanda, J., Berr, F. & Kiesslich, T. Photophysics and photochemistry of photodynamic therapy: fundamental aspects. *Lasers Med. Sci.* **24**, 259–268 (2009).
5. Brackett, C. M. & Gollnick, S. O. Photodynamic therapy enhancement of anti-tumor immunity. *Photochem. Photobiol. Sci. Off. J. Eur. Photochem. Assoc. Eur. Soc. Photobiol.* **10**, 649–652 (2011).
6. Huygens, A. *et al.* Permeation of hypericin in spheroids composed of different grade transitional cell carcinoma cell lines and normal human urothelial cells. *J. Urol.* **174**, 69–72 (2005).
7. Hamblin, M. R. & Newman, E. L. On the mechanism of the tumour-localising effect in photodynamic therapy. *J. Photochem. Photobiol. B* **23**, 3–8 (1994).
8. Sibani, S. A., McCarron, P. A., Woolfson, A. D. & Donnelly, R. F. Photosensitiser delivery for photodynamic therapy. Part 2: systemic carrier platforms. *Expert Opin. Drug Deliv.* **5**, 1241–1254 (2008).
9. Kim, G. & Gaitas, A. Extracorporeal photo-immunotherapy for circulating tumor cells. *PloS One* **10**, e0127219 (2015).
10. Vogl, T. J. *et al.* Interstitial photodynamic laser therapy in interventional oncology. *Eur. Radiol.* **14**, 1063–1073 (2004).
11. Bechet, D., Mordon, S. R., Guillemain, F. & Barberi-Heyob, M. A. Photodynamic therapy of malignant brain tumours: a complementary approach to conventional therapies. *Cancer Treat. Rev.* **40**, 229–241 (2014).
12. Hsu, C.-Y., Chen, C.-W., Yu, H.-P., Lin, Y.-F. & Lai, P.-S. Bioluminescence resonance energy transfer using luciferase-immobilized quantum dots for self-illuminated photodynamic therapy. *Biomaterials* **34**, 1204–1212 (2013).
13. Kim, Y. R. *et al.* Bioluminescence-activated deep-tissue photodynamic therapy of cancer. *Theranostics* **5**, 805–817 (2015).
14. Ascencio, M., Collinet, P., Farine, M. O. & Mordon, S. Protoporphyrin IX fluorescence photobleaching is a useful tool to predict the response of rat ovarian cancer following hexaminolevulinate photodynamic therapy. *Lasers Surg. Med.* **40**, 332–341 (2008).

15. Gamrekelashvili, J., Greten, T. F. & Korangy, F. Immunogenicity of necrotic cell death. *Cell. Mol. Life Sci. CMLS* **72**, 273–283 (2015).
16. Adkins, I., Fucikova, J., Garg, A. D., Agostinis, P. & Špišek, R. Physical modalities inducing immunogenic tumor cell death for cancer immunotherapy. *Oncoimmunology* **3**, e968434 (2014).
17. Akilov, O. E. *et al.* Vaccination with photodynamic therapy-treated macrophages induces highly suppressive T-regulatory cells. *Photodermatol. Photoimmunol. Photomed.* **27**, 97–107 (2011).
18. Kang, B. Y., Chung, S. W. & Kim, T. S. Inhibition of interleukin-12 production in lipopolysaccharide-activated mouse macrophages by hypericin, an active component of *Hypericum perforatum*. *Planta Med.* **67**, 364–366 (2001).
19. Kimáková, P. *et al.* Photoactivated hypericin increases the expression of SOD-2 and makes MCF-7 cells resistant to photodynamic therapy. *Biomed. Pharmacother. Biomedecine Pharmacother.* **85**, 749–755 (2017).
20. Maeding, N., Verwanger, T. & Krammer, B. Boosting Tumor-Specific Immunity Using PDT. *Cancers* **8**, (2016).
21. Schnurr, M. *et al.* Apoptotic pancreatic tumor cells are superior to cell lysates in promoting cross-priming of cytotoxic T cells and activate NK and gammadelta T cells. *Cancer Res.* **62**, 2347–2352 (2002).
22. Scheffer, S. R. *et al.* Apoptotic, but not necrotic, tumor cell vaccines induce a potent immune response in vivo. *Int. J. Cancer* **103**, 205–211 (2003).
23. Goldszmid, R. S. *et al.* Dendritic cells charged with apoptotic tumor cells induce long-lived protective CD4⁺ and CD8⁺ T cell immunity against B16 melanoma. *J. Immunol. Baltim. Md 1950* **171**, 5940–5947 (2003).
24. Bartholomae, W. C. *et al.* T cell immunity induced by live, necrotic, and apoptotic tumor cells. *J. Immunol. Baltim. Md 1950* **173**, 1012–1022 (2004).
25. Gamrekelashvili, J. *et al.* Primary sterile necrotic cells fail to cross-prime CD8(+) T cells. *Oncoimmunology* **1**, 1017–1026 (2012).
26. Gamrekelashvili, J. *et al.* Peptidases released by necrotic cells control CD8⁺ T cell cross-priming. *J. Clin. Invest.* **123**, 4755–4768 (2013).
27. Mroz, P., Hashmi, J. T., Huang, Y.-Y., Lange, N. & Hamblin, M. R. Stimulation of anti-tumor immunity by photodynamic therapy. *Expert Rev. Clin. Immunol.* **7**, 75–91 (2011).
28. Garg, A. D. *et al.* Dendritic cell vaccines based on immunogenic cell death elicit danger signals and T cell-driven rejection of high-grade glioma. *Sci. Transl. Med.* **8**, 328ra27 (2016).
29. Kick, G., Messer, G., Goetz, A., Plewig, G. & Kind, P. Photodynamic therapy induces expression of interleukin 6 by activation of AP-1 but not NF-kappa B DNA binding.

- Cancer Res.* **55**, 2373–2379 (1995).
30. Gollnick, S. O. *et al.* Role of cytokines in photodynamic therapy-induced local and systemic inflammation. *Br. J. Cancer* **88**, 1772–1779 (2003).
 31. Du, H., Bay, B.-H., Mahendran, R. & Olivo, M. Hypericin-mediated photodynamic therapy elicits differential interleukin-6 response in nasopharyngeal cancer. *Cancer Lett.* **235**, 202–208 (2006).
 32. Wei, L.-H. *et al.* Interleukin-6 trans signalling enhances photodynamic therapy by modulating cell cycling. *Br. J. Cancer* **97**, 1513–1522 (2007).
 33. Henderson, B. W. *et al.* Choice of oxygen-conserving treatment regimen determines the inflammatory response and outcome of photodynamic therapy of tumors. *Cancer Res.* **64**, 2120–2126 (2004).
 34. Cecic, I. & Korbelik, M. Mediators of peripheral blood neutrophilia induced by photodynamic therapy of solid tumors. *Cancer Lett.* **183**, 43–51 (2002).
 35. de Vree, W. J., Essers, M. C., Koster, J. F. & Sluiter, W. Role of interleukin 1 and granulocyte colony-stimulating factor in photofrin-based photodynamic therapy of rat rhabdomyosarcoma tumors. *Cancer Res.* **57**, 2555–2558 (1997).
 36. Sun, J., Cecic, I., Parkins, C. S. & Korbelik, M. Neutrophils as inflammatory and immune effectors in photodynamic therapy-treated mouse SCCVII tumours. *Photochem. Photobiol. Sci. Off. J. Eur. Photochem. Assoc. Eur. Soc. Photobiol.* **1**, 690–695 (2002).
 37. Brackett, C. M., Muhitch, J. B., Evans, S. S. & Gollnick, S. O. IL-17 promotes neutrophil entry into tumor-draining lymph nodes following induction of sterile inflammation. *J. Immunol. Baltim. Md 1950* **191**, 4348–4357 (2013).
 38. Mroz, P., Szokalska, A., Wu, M. X. & Hamblin, M. R. Photodynamic therapy of tumors can lead to development of systemic antigen-specific immune response. *PloS One* **5**, e15194 (2010).
 39. Reginato, E. *et al.* Photodynamic therapy plus regulatory T-cell depletion produces immunity against a mouse tumour that expresses a self-antigen. *Br. J. Cancer* **109**, 2167–2174 (2013).
 40. Korbelik, M. PDT-associated host response and its role in the therapy outcome. *Lasers Surg. Med.* **38**, 500–508 (2006).
 41. de Vree, W. J. *et al.* Evidence for an important role of neutrophils in the efficacy of photodynamic therapy in vivo. *Cancer Res.* **56**, 2908–2911 (1996).
 42. Korbelik, M., Kros, G., Kros, J. & Dougherty, G. J. The role of host lymphoid populations in the response of mouse EMT6 tumor to photodynamic therapy. *Cancer Res.* **56**, 5647–5652 (1996).
 43. Gollnick, S. O., Liu, X., Owczarczak, B., Musser, D. A. & Henderson, B. W. Altered expression of interleukin 6 and interleukin 10 as a result of photodynamic therapy in vivo. *Cancer Res.* **57**, 3904–3909 (1997).


44. Korbelik, M. & Cecic, I. Contribution of myeloid and lymphoid host cells to the curative outcome of mouse sarcoma treatment by photodynamic therapy. *Cancer Lett.* **137**, 91–98 (1999).
45. Kousis, P. C., Henderson, B. W., Maier, P. G. & Gollnick, S. O. Photodynamic therapy enhancement of antitumor immunity is regulated by neutrophils. *Cancer Res.* **67**, 10501–10510 (2007).
46. Shams, M., Owczarczak, B., Manderscheid-Kern, P., Bellnier, D. A. & Gollnick, S. O. Development of photodynamic therapy regimens that control primary tumor growth and inhibit secondary disease. *Cancer Immunol. Immunother. CII* **64**, 287–297 (2015).
47. Canti, G. *et al.* Antitumor immunity induced by photodynamic therapy with aluminum disulfonated phthalocyanines and laser light. *Anticancer. Drugs* **5**, 443–447 (1994).
48. Preise, D. *et al.* Systemic antitumor protection by vascular-targeted photodynamic therapy involves cellular and humoral immunity. *Cancer Immunol. Immunother. CII* **58**, 71–84 (2009).
49. Kabingu, E., Vaughan, L., Owczarczak, B., Ramsey, K. D. & Gollnick, S. O. CD8+ T cell-mediated control of distant tumours following local photodynamic therapy is independent of CD4+ T cells and dependent on natural killer cells. *Br. J. Cancer* **96**, 1839–1848 (2007).
50. Rocha, L. B., Gomes-da-Silva, L. C., Dąbrowski, J. M. & Arnaut, L. G. Elimination of primary tumours and control of metastasis with rationally designed bacteriochlorin photodynamic therapy regimens. *Eur. J. Cancer Oxf. Engl. 1990* **51**, 1822–1830 (2015).
51. Thong, P. S.-P. *et al.* Photodynamic-therapy-activated immune response against distant untreated tumours in recurrent angiosarcoma. *Lancet Oncol.* **8**, 950–952 (2007).
52. Kabingu, E., Oseroff, A. R., Wilding, G. E. & Gollnick, S. O. Enhanced systemic immune reactivity to a Basal cell carcinoma associated antigen following photodynamic therapy. *Clin. Cancer Res. Off. J. Am. Assoc. Cancer Res.* **15**, 4460–4466 (2009).
53. Morrison, S. A., Hill, S. L., Rogers, G. S. & Graham, R. A. Efficacy and safety of continuous low-irradiance photodynamic therapy in the treatment of chest wall progression of breast cancer. *J. Surg. Res.* **192**, 235–241 (2014).
54. Korbelik, M. & Dougherty, G. J. Photodynamic therapy-mediated immune response against subcutaneous mouse tumors. *Cancer Res.* **59**, 1941–1946 (1999).
55. Sanovic, R., Verwanger, T., Hartl, A. & Krammer, B. Low dose hypericin-PDT induces complete tumor regression in BALB/c mice bearing CT26 colon carcinoma. *Photodiagnosis Photodyn. Ther.* **8**, 291–296 (2011).
56. Knutson, K. L. & Disis, M. L. Tumor antigen-specific T helper cells in cancer immunity and immunotherapy. *Cancer Immunol. Immunother. CII* **54**, 721–728 (2005).
57. Stockinger, B. & Veldhoen, M. Differentiation and function of Th17 T cells. *Curr. Opin. Immunol.* **19**, 281–286 (2007).

58. Bailey, S. R. *et al.* Th17 cells in cancer: the ultimate identity crisis. *Front. Immunol.* **5**, 276 (2014).
59. Zhou, L. *et al.* TGF-beta-induced Foxp3 inhibits T(H)17 cell differentiation by antagonizing RORgammat function. *Nature* **453**, 236–240 (2008).
60. Hendrzak-Henion, J. A., Knisely, T. L., Cincotta, L., Cincotta, E. & Cincotta, A. H. Role of the immune system in mediating the antitumor effect of benzophenothiazine photodynamic therapy. *Photochem. Photobiol.* **69**, 575–581 (1999).
61. Wachowska, M. *et al.* 5-Aza-2'-deoxycytidine potentiates antitumour immune response induced by photodynamic therapy. *Eur. J. Cancer Oxf. Engl. 1990* **50**, 1370–1381 (2014).
62. Saji, H., Song, W., Furumoto, K., Kato, H. & Engleman, E. G. Systemic antitumor effect of intratumoral injection of dendritic cells in combination with local photodynamic therapy. *Clin. Cancer Res. Off. J. Am. Assoc. Cancer Res.* **12**, 2568–2574 (2006).
63. Abdel-Hady, E. S. *et al.* Immunological and viral factors associated with the response of vulval intraepithelial neoplasia to photodynamic therapy. *Cancer Res.* **61**, 192–196 (2001).
64. Sakaguchi, S., Sakaguchi, N., Asano, M., Itoh, M. & Toda, M. Immunologic self-tolerance maintained by activated T cells expressing IL-2 receptor alpha-chains (CD25). Breakdown of a single mechanism of self-tolerance causes various autoimmune diseases. *J. Immunol. Baltim. Md 1950* **155**, 1151–1164 (1995).
65. Takahashi, T. *et al.* Immunologic self-tolerance maintained by CD25(+)CD4(+) regulatory T cells constitutively expressing cytotoxic T lymphocyte-associated antigen 4. *J. Exp. Med.* **192**, 303–310 (2000).
66. Fontenot, J. D., Gavin, M. A. & Rudensky, A. Y. Foxp3 programs the development and function of CD4+CD25+ regulatory T cells. *Nat. Immunol.* **4**, 330–336 (2003).
67. Khattri, R., Cox, T., Yasayko, S.-A. & Ramsdell, F. An essential role for Scurfin in CD4+CD25+ T regulatory cells. *Nat. Immunol.* **4**, 337–342 (2003).
68. Sakaguchi, S., Wing, K. & Miyara, M. Regulatory T cells - a brief history and perspective. *Eur. J. Immunol.* **37 Suppl 1**, S116-123 (2007).
69. Bennett, C. L. *et al.* The immune dysregulation, polyendocrinopathy, enteropathy, X-linked syndrome (IPEX) is caused by mutations of FOXP3. *Nat. Genet.* **27**, 20–21 (2001).
70. Sakaguchi, S., Yamaguchi, T., Nomura, T. & Ono, M. Regulatory T cells and immune tolerance. *Cell* **133**, 775–787 (2008).
71. Schmitt, E. G. & Williams, C. B. Generation and function of induced regulatory T cells. *Front. Immunol.* **4**, 152 (2013).
72. Beyer, M. & Schultze, J. L. Regulatory T cells in cancer. *Blood* **108**, 804–811 (2006).
73. Nishikawa, H. & Sakaguchi, S. Regulatory T cells in tumor immunity. *Int. J. Cancer J. Int. Cancer* **127**, 759–767 (2010).

74. Darrasse-Jèze, G. & Podsypanina, K. How numbers, nature, and immune status of foxp3(+) regulatory T-cells shape the early immunological events in tumor development. *Front. Immunol.* **4**, 292 (2013).
75. Vignali, D. A. A., Collison, L. W. & Workman, C. J. How regulatory T cells work. *Nat. Rev. Immunol.* **8**, 523–532 (2008).
76. Roychoudhuri, R., Eil, R. L. & Restifo, N. P. The interplay of effector and regulatory T cells in cancer. *Curr. Opin. Immunol.* **33**, 101–111 (2015).
77. Chen, M.-L. *et al.* Regulatory T cells suppress tumor-specific CD8 T cell cytotoxicity through TGF-beta signals in vivo. *Proc. Natl. Acad. Sci. U. S. A.* **102**, 419–424 (2005).
78. Kalia, V., Penny, L. A., Yuzefpolskiy, Y., Baumann, F. M. & Sarkar, S. Quiescence of Memory CD8(+) T Cells Is Mediated by Regulatory T Cells through Inhibitory Receptor CTLA-4. *Immunity* **42**, 1116–1129 (2015).
79. Castano, A. P., Mroz, P., Wu, M. X. & Hamblin, M. R. Photodynamic therapy plus low-dose cyclophosphamide generates antitumor immunity in a mouse model. *Proc. Natl. Acad. Sci. U. S. A.* **105**, 5495–5500 (2008).
80. Dudek, A. M., Martin, S., Garg, A. D. & Agostinis, P. Immature, Semi-Mature, and Fully Mature Dendritic Cells: Toward a DC-Cancer Cells Interface That Augments Anticancer Immunity. *Front. Immunol.* **4**, 438 (2013).
81. Strioga, M. *et al.* Dendritic cells and their role in tumor immunosurveillance. *Innate Immun.* **19**, 98–111 (2013).
82. Jalili, A. *et al.* Effective photoimmunotherapy of murine colon carcinoma induced by the combination of photodynamic therapy and dendritic cells. *Clin. Cancer Res. Off. J. Am. Assoc. Cancer Res.* **10**, 4498–4508 (2004).
83. Gollnick, S. O. & Brackett, C. M. Enhancement of anti-tumor immunity by photodynamic therapy. *Immunol. Res.* **46**, 216–226 (2010).
84. Gollnick, S. O., Owczarczak, B. & Maier, P. Photodynamic therapy and anti-tumor immunity. *Lasers Surg. Med.* **38**, 509–515 (2006).
85. Kushibiki, T., Tajiri, T., Tomioka, Y. & Awazu, K. Photodynamic therapy induces interleukin secretion from dendritic cells. *Int. J. Clin. Exp. Med.* **3**, 110–114 (2010).
86. Zheng, Y. *et al.* Photodynamic-therapy Activates Immune Response by disrupting Immunity Homeostasis of Tumor Cells, which Generates Vaccine for Cancer Therapy. *Int. J. Biol. Sci.* **12**, 120–132 (2016).
87. Lutz, M. B. *et al.* An advanced culture method for generating large quantities of highly pure dendritic cells from mouse bone marrow. *J. Immunol. Methods* **223**, 77–92 (1999).
88. Yamazaki, S. *et al.* Dendritic cells are specialized accessory cells along with TGF- for the differentiation of Foxp3+ CD4+ regulatory T cells from peripheral Foxp3 precursors. *Blood* **110**, 4293–4302 (2007).
89. Jendželovská, Z., Jendželovský, R., Kuchárová, B. & Fedoročko, P. Hypericin in the

- Light and in the Dark: Two Sides of the Same Coin. *Front. Plant Sci.* **7**, (2016).
90. Chen, B. *et al.* Efficacy of antitumoral photodynamic therapy with hypericin: relationship between biodistribution and photodynamic effects in the RIF-1 mouse tumor model. *Int. J. Cancer J. Int. Cancer* **93**, 275–282 (2001).
 91. Korbelik, M. & Hamblin, M. R. The impact of macrophage-cancer cell interaction on the efficacy of photodynamic therapy. *Photochem. Photobiol. Sci. Off. J. Eur. Photochem. Assoc. Eur. Soc. Photobiol.* **14**, 1403–1409 (2015).
 92. Korbelik, M. & Kros, G. Cellular levels of photosensitisers in tumours: the role of proximity to the blood supply. *Br. J. Cancer* **70**, 604–610 (1994).
 93. Ma, Y., Shurin, G. V., Peiyuan, Z. & Shurin, M. R. Dendritic cells in the cancer microenvironment. *J. Cancer* **4**, 36–44 (2013).
 94. Vandenberghe, A. L. *et al.* Differential cytotoxic effects induced after photosensitization by hypericin. *J. Photochem. Photobiol. B* **38**, 136–142 (1997).
 95. Veldhoen, M., Hocking, R. J., Atkins, C. J., Locksley, R. M. & Stockinger, B. TGFβ in the context of an inflammatory cytokine milieu supports de novo differentiation of IL-17-producing T cells. *Immunity* **24**, 179–189 (2006).
 96. Kumari, N., Dwarkanath, B. S., Das, A. & Bhatt, A. N. Role of interleukin-6 in cancer progression and therapeutic resistance. *Tumour Biol. J. Int. Soc. Oncodevelopmental Biol. Med.* **37**, 11553–11572 (2016).
 97. Lippitz, B. E. & Harris, R. A. Cytokine patterns in cancer patients: A review of the correlation between interleukin 6 and prognosis. *Oncoimmunology* **5**, (2016).
 98. Yom, S. S. *et al.* Elevated serum cytokine levels in mesothelioma patients who have undergone pleurectomy or extrapleural pneumonectomy and adjuvant intraoperative photodynamic therapy. *Photochem. Photobiol.* **78**, 75–81 (2003).
 99. Muranski, P. *et al.* Tumor-specific Th17-polarized cells eradicate large established melanoma. *Blood* **112**, 362–373 (2008).
 100. Martin-Orozco, N. *et al.* T helper 17 cells promote cytotoxic T cell activation in tumor immunity. *Immunity* **31**, 787–798 (2009).
 101. Gnerlich, J. L. *et al.* Induction of Th17 cells in the tumor microenvironment improves survival in a murine model of pancreatic cancer. *J. Immunol. Baltim. Md 1950* **185**, 4063–4071 (2010).
 102. Scheller, J., Chalaris, A., Schmidt-Arras, D. & Rose-John, S. The pro- and anti-inflammatory properties of the cytokine interleukin-6. *Biochim. Biophys. Acta* **1813**, 878–888 (2011).
 103. Massagué, J. TGFβ in Cancer. *Cell* **134**, 215–230 (2008).
 104. Flavell, R. A., Sanjabi, S., Wrzesinski, S. H. & Licona-Limón, P. The polarization of immune cells in the tumour environment by TGFβ. *Nat. Rev. Immunol.* **10**, 554–567 (2010).

105. Fridlender, Z. G. *et al.* Polarization of tumor-associated neutrophil phenotype by TGF-beta: 'N1' versus 'N2' TAN. *Cancer Cell* **16**, 183–194 (2009).
106. Nozawa, H., Chiu, C. & Hanahan, D. Infiltrating neutrophils mediate the initial angiogenic switch in a mouse model of multistage carcinogenesis. *Proc. Natl. Acad. Sci. U. S. A.* **103**, 12493–12498 (2006).
107. Pekarek, L. A., Starr, B. A., Toledano, A. Y. & Schreiber, H. Inhibition of tumor growth by elimination of granulocytes. *J. Exp. Med.* **181**, 435–440 (1995).
108. Tazawa, H. *et al.* Infiltration of neutrophils is required for acquisition of metastatic phenotype of benign murine fibrosarcoma cells: implication of inflammation-associated carcinogenesis and tumor progression. *Am. J. Pathol.* **163**, 2221–2232 (2003).
109. Hicks, A. M. *et al.* Transferable anticancer innate immunity in spontaneous regression/complete resistance mice. *Proc. Natl. Acad. Sci. U. S. A.* **103**, 7753–7758 (2006).
110. Ito, M. *et al.* Tumor-derived TGFbeta-1 induces dendritic cell apoptosis in the sentinel lymph node. *J. Immunol. Baltim. Md 1950* **176**, 5637–5643 (2006).
111. Weber, F. *et al.* Transforming growth factor-beta1 immobilises dendritic cells within skin tumours and facilitates tumour escape from the immune system. *Cancer Immunol. Immunother. CII* **54**, 898–906 (2005).
112. Halliday, G. M. & Le, S. Transforming growth factor-beta produced by progressor tumors inhibits, while IL-10 produced by regressor tumors enhances, Langerhans cell migration from skin. *Int. Immunol.* **13**, 1147–1154 (2001).
113. Shurin, G. V., Ma, Y. & Shurin, M. R. Immunosuppressive mechanisms of regulatory dendritic cells in cancer. *Cancer Microenviron. Off. J. Int. Cancer Microenviron. Soc.* **6**, 159–167 (2013).
114. Maeda, H. & Shiraishi, A. TGF-beta contributes to the shift toward Th2-type responses through direct and IL-10-mediated pathways in tumor-bearing mice. *J. Immunol. Baltim. Md 1950* **156**, 73–78 (1996).
115. Miyahara, Y. *et al.* Generation and regulation of human CD4+ IL-17-producing T cells in ovarian cancer. *Proc. Natl. Acad. Sci. U. S. A.* **105**, 15505–15510 (2008).
116. Su, X. *et al.* Tumor microenvironments direct the recruitment and expansion of human Th17 cells. *J. Immunol. Baltim. Md 1950* **184**, 1630–1641 (2010).
117. Reginato, E. *et al.* Photodynamic therapy downregulates the function of regulatory T cells in patients with esophageal squamous cell carcinoma. *Photochem. Photobiol. Sci. Off. J. Eur. Photochem. Assoc. Eur. Soc. Photobiol.* **13**, 1281–1289 (2014).
118. Hunt, D. W. *et al.* Consequences of the photodynamic treatment of resting and activated peripheral T lymphocytes. *Immunopharmacology* **41**, 31–44 (1999).
119. Fox, F. E., Niu, Z., Tobia, A. & Rook, A. H. Photoactivated hypericin is an anti-proliferative agent that induces a high rate of apoptotic death of normal, transformed, and malignant T lymphocytes: implications for the treatment of cutaneous lymphoproliferative



and inflammatory disorders. *J. Invest. Dermatol.* **111**, 327–332 (1998).

Appendix I: Summary

Photodynamic therapy (PDT) is a cancer treatment modality which is based on three components: a non-toxic photosensitizer (PS), visible light and molecular oxygen. Briefly, the PS is applied systemically or locally and after accumulation of the PS at the tumor site the PS is photoactivated with light of appropriate wavelength. This leads to generation of reactive oxygen species as the excited PS reacts with molecular oxygen. As a consequence, tumor cells are eliminated by direct and indirect effects. Indirectly, PDT facilitates the induction of an inflammatory response and tumor-specific immune reactions. In this context, generation of memory immunity *in vivo* and a requirement for dendritic cells (DC) for PDT efficiency has been shown. However, tumors are known to generate a tolerogenic environment to evade immune recognition, including the induction of regulatory T cells (Treg). In order to enable a tumor-specific immune response and generate memory immunity, tolerance towards the tumor must have been breached at some point due to the treatment. We hypothesized that PDT treatment might skew DC-mediated induction of Treg in the tumor microenvironment towards effector T cell differentiation, thereby promoting recognition and elimination of the tumor. Since information about the direct effects of PDT on DCs is rare, this study was split in two parts: Part 1 was designed to assess direct effects of PDT using hypericin as PS on DCs, while the second part evaluated the capacity of treated DCs to induce Treg and effector T cells in a co-culture system of PDT-DCs and naive OVA antigen specific T lymphocytes. DCs showed increased proliferation at concentrations up to 100 nM hypericin and a cytotoxic effect at concentrations higher than 200 nM in response to PDT (irradiation with a fluence of 1.1 J/cm² at 610 nm). Additionally, expression of proinflammatory IL-12 was upregulated and anti-inflammatory TGF- β was downregulated with low-dose treatment (80 nM). In contrast, at 300 nM expression of IL-12 and IL-6 was downregulated while TGF- β was similar to untreated controls. Induction of Treg by PDT-DCs displayed a tendency towards reduced Treg levels in response to low-dose treatment. Secretion of T helper cell type 1 and 17 signature cytokines IFN- γ and IL-17 showed similar IFN- γ levels across all treatment conditions and increased IL-17 levels in co-cultures with 300 nM hypericin-PDT treated DCs and high doses of antigen. In summary, this study shows a beneficial effect of low-dose hypericin-PDT on DC viability and proinflammatory capacity. Furthermore, it points to diminished induction of Treg by PDT-DCs and maintenance of normal effector T cell induction comparable to that seen with untreated DCs. These effects could partially explain the anti-tumor immunity triggered by PDT.

Appendix II: Zusammenfassung

Die photodynamische Therapie (PDT) ist eine Krebstherapie, die auf einem nicht-toxischen Photosensitizer (PS), sichtbarem Licht und molekularem Sauerstoff basiert. Der PS wird lokal oder systemisch verabreicht, reichert sich im Tumorgewebe an und wird mittels Licht einer geeigneten Wellenlänge angeregt. Durch Reaktion des angeregten PS mit molekularem Sauerstoff führt dies zur Entstehung von sog. ‚reactive oxygen species‘. Hierdurch werden Tumorzellen durch direkte und indirekte Effekte zerstört. Indirekt unterstützt PDT die Einleitung einer entzündlichen Immunantwort und tumorspezifischer Immunreaktionen. Diesbezüglich wurde die Entstehung eines immunologischen Gedächtnisses *in vivo* nach PDT ebenso gezeigt wie die Erfordernis dendritischer Zellen (DC) für die therapeutische Effizienz von PDT. Es ist jedoch bekannt, dass Tumorzellen eine tolerogene Umgebung erschaffen, um ihre Erkennung durch das Immunsystem zu verhindern; dies beinhaltet unter anderem die Induktion regulatorischer T Zellen (Treg). Um eine tumorspezifische Immunantwort und die Ausbildung einer Gedächtnisimmunität zu ermöglichen, muss die Toleranz gegenüber dem Tumor gebrochen werden. Nach unserer Hypothese verschiebt PDT-Behandlung die DC-vermittelte Induktion von Treg im Mikromilieu des Tumors in Richtung der Differenzierung von Effektor-T-Zellen und fördert so die Erkennung und Eliminierung von Tumorzellen. Da kaum Informationen zu den Effekten von PDT auf DCs existieren, wurden in dieser Studie sowohl direkte Effekte von PDT mit Hypericin als PS auf DCs als auch die Kapazität behandelter DCs, Treg und Effektor-T-Zellen zu induzieren, evaluiert. DCs zeigten gesteigerte Proliferation nach PDT-Behandlung (Bestrahlung mit einem Fluss von $1,1 \text{ J/cm}^2$ bei 610 nm) mit bis zu 100 nM Hypericin als PS und zytotoxische Effekte ab einer Konzentration von mehr als 200 nM. Bei niedriger Konzentration (80 nM) war die Expression von proinflammatorischem IL-12 gesteigert und die von anti-inflammatorischem TGF- β vermindert. Bei einer Konzentration von 300 nM war die Expression von IL-12 und IL-6 vermindert. Die Induktion von Treg durch PDT-DCs war bei niedriger Konzentration tendenziell verringert. Die Th1 und Th17 spezifischen Zytokine IFN- γ und IL-17A zeigten gleichbleibende IFN- γ Niveaus unter allen Bedingungen und gesteigerte IL-17A Sekretion in Ko-Kulturen, die mit 300 nM Hypericin-PDT behandelte DCs enthielten. Der exakte Phänotyp der Zytokin-produzierenden T Zellen konnte hier jedoch nicht näher bestimmt werden.

Zusammenfassend zeigt diese Studie einen vorteilhaften Effekt von niedrig dosierter Hypericin-PDT auf die Lebensfähigkeit von DCs und deren proinflammatorische Kapazität, eine verringerte Induktion von Treg und die Erhaltung der normalen Differenzierung von Effektor-T-Zellen durch PDT-DCs. Diese Effekte könnten die Antitumor-Immunität nach PDT teilweise erklären.

Appendix III: List of Figures

Figure 1 Photochemical Reactions upon Excitation of a PS with Light.....	3
Figure 2 Schematic Representation of the Experimental Design.....	18
Figure 3 Effect of Unexcited Hypericin on BMDC Viability.....	42
Figure 4 Light-dependent Cytotoxicity of Hypericin on BMDCs.....	43
Figure 5 Light-dependent Cytotoxicity of Hypericin on A431 Cells.....	45
Figure 6 Light-dependent Cytotoxicity of Hypericin on CT26 Cells.....	45
Figure 7 Effect of Unexcited Hypericin on A431 and CT26 Cells.....	46
Figure 8 IL-1 β Expression in PDT-treated BMDCs.....	47
Figure 9 IL-6 Expression in PDT-treated BMDCs.....	48
Figure 10 IL-12 Expression in PDT-treated BMDCs.....	49
Figure 11 TGF- β Expression in PDT-treated BMDCs.....	50
Figure 12 IL-6 Secretion by PDT-treated BMDCs.....	51
Figure 13 IL-6 Content in Co-Culture Supernatants.....	52
Figure 14 Antigen-dose dependent Treg Induction by BMDCs.....	53
Figure 15 Treg Induction by PDT-treated BMDCs in Response to OVA.....	54
Figure 16 IFN- γ Content in Co-Culture Supernatants.....	55
Figure 17 IL-17A Content in Co-Culture Supernatants.....	56
Figure 18 Single Values of Fold Change in IL-17A Content relative to Controls in Supernatants from Co-Culture containing 0.03 μ g/mL OVA Peptide.....	57
Figure 19 Single Values of Fold Change in IL-17A Content relative to Controls in Supernatants from Co-Culture containing 0.1 μ g/mL OVA Peptide.....	57
Figure 20 Ratio of IL-17A/IFN- γ Content in Co-Culture Supernatants.....	58
Figure 21 Requirement of DCs for PDT Efficiency (Preise et al. 2009 ⁴⁸).....	59
Figure 22 Schematic Representation of the Low-Dose Hypericin-PDT Treatment Protocol and subsequent Tumor Response.....	60

Figure 23 Schematic Representation of the Involvement of T Helper Cells in Tumor Immunity and the Cytokines Needed for Their Induction.....	63
--	-----------

Appendix IV: List of Tables

Table 1 Clinically Approved Photosensitizers and Their Indications.....	5
Table 2 Primers used for Gene Expression Studies.....	30
Table 3 Cycling Parameters applied for qRT-PCR.....	32
Table 4 Antibodies used for FACS Analysis.....	34
Table 5 Technical Equipment.....	36
Table 6 Chemicals and Reagents.....	37
Table 7 Media, Buffers and Solutions.....	39



Appendix V: Published Review²⁰

‘Boosting Tumor-Specific Immunity Using PDT’

Review

Boosting Tumor-Specific Immunity Using PDT

Nicole Maeding, Thomas Verwanger and Barbara Krammer *

Division of Molecular Tumor Biology, Department of Molecular Biology, University of Salzburg,
Hellbrunnerstrasse 34, 5020 Salzburg, Austria; nicole.maeding.hh@gmail.com (N.M.);
thomas.verwanger@sbg.ac.at (T.V.)

* Correspondence: barbara.krammer@sbg.ac.at; Tel.: +43-662-8044-5703

Academic Editor: Michael R. Hamblin

Received: 8 August 2016; Accepted: 4 October 2016; Published: 6 October 2016

Abstract: Photodynamic therapy (PDT) is a cancer treatment with a long-standing history. It employs the application of nontoxic components, namely a light-sensitive photosensitizer and visible light, to generate reactive oxygen species (ROS). These ROS lead to tumor cell destruction, which is accompanied by the induction of an acute inflammatory response. This inflammatory process sends a danger signal to the innate immune system, which results in activation of specific cell types and release of additional inflammatory mediators. Activation of the innate immune response is necessary for subsequent induction of the adaptive arm of the immune system. This includes the priming of tumor-specific cytotoxic T lymphocytes (CTL) that have the capability to directly recognize and kill cells which display an altered self. The past decades have brought increasing appreciation for the importance of the generation of an adaptive immune response for long-term tumor control and induction of immune memory to combat recurrent disease. This has led to considerable effort to elucidate the immune effects PDT treatment elicits. In this review we deal with the progress which has been made during the past 20 years in uncovering the role of PDT in the induction of the tumor-specific immune response, with special emphasis on adaptive immunity.

Keywords: photodynamic tumor therapy; tumor-specific immunity; antitumor immunity, regulatory T cells; dendritic cells; memory

1. Introduction

Photodynamic therapy (PDT) is a cancer treatment modality, for which the principle had already been proposed over a century ago [1]. It is an alternative treatment among the currently available therapies that offers minimal side effects for the patient while maintaining high efficiency [2]. As a clinically approved therapy it is used for the treatment of early staged disease and superficial cancer types, and as palliative easement in terminal/late staged cancers [3,4]. PDT utilizes a light-sensitive photosensitizer (PS), which is applied systemically or locally, and visible light of appropriate wavelengths to excite the PS. After tumor-selective accumulation, the photosensitizer is locally photoactivated by nonthermal light irradiation; subsequently it either emits fluorescence light (diagnostic use), or reacts with surrounding molecules. In the presence of molecular oxygen, reactive oxygen species (ROS) are formed, which oxidize proteins and lipids in the target cells. This leads to stimulation of signaling processes as well as target destruction by apoptotic and necrotic cell death (therapeutic use) [3,5]. Indirect effects leading to tumor cell destruction include vascular shutdown by damaging endothelial cells and the vascular basement membrane. This results in blood flow stasis, tissue hemorrhages, and oxygen deprivation. Furthermore, induction of an inflammatory response and immune reactions directed against the tumor contribute to fighting off primary as well as secondary disease manifestations [6]. However, PDT still constitutes more of a fringe option than a regular treatment for cancer patients. This might be attributed to several limitations PDT faces:

obviously, applicability is restricted by tumor site accessibility and penetration depth of light needed to excite the photosensitizer. This limits therapeutic success, mainly to outer and inner body surfaces and flat tumors. In addition, classical PDT is only suited for solid tumors. Tumor cells circulating in the vasculature cannot be treated using traditional PDT protocols. During the past years, efforts have been made to develop advanced protocols that overcome these disadvantages. Interstitial PDT using optical fibers as light source and self-illuminated PDT show promising results for the treatment of solid tumors of larger size (as compared to flat tumors) and for solid lesions in parenchymal organs. For eradication of circulating tumor cells, efforts are being made to develop extracorporeal PDT protocols which employ an antibody-conjugated PS to target specific cells, and illumination of the blood is conducted afterwards [7–9]. Most advantageous—and currently under extensive research—is the induction of antitumor immune reactions by PDT. These reactions serve to support primary tumor elimination and to extend the local antitumor response to systemic surveillance to combat disease recurrence, metastases, or circulating tumor cells [10]. This has even led to several approaches to use PDT as vaccine [11,12]. In this review we focus on a collection of findings related to PDT-mediated tumor-specific immunity and their implications for future directions in the field of photodynamic tumor therapy.

2. PDT and Innate Immunity

The local trauma inflicted by PDT treatment on the tumor cells, the vasculature, and the surrounding tissue causes induction and release of various mediators leading to an inflammatory reaction to initiate an immune response. The oxidative stress due to the excessive generation of ROS results in surface expression and secretion of damage-associated molecular patterns (DAMPs) as well as inflammatory mediators which are released from dying and damaged cells. DAMPs are molecules derived from host cells to signal cell injury or death. They predominantly comprise nuclear or cytosolic proteins which become released from the cell or exposed on its surface and serve in the initiation of a noninfectious immune response. Recognition of DAMPs via engagement with their respective receptors on infiltrating immune cells (so-called pattern recognition receptors, PRRs) aids in signaling the nature of the underlying threat to the immune system and enabling the appropriate immune response. DAMPs reported to be necessary for the generation of antitumor immunity and induced upon PDT include surface calreticulin (CRT), heat shock protein (HSP) 70, HSP90, ATP, and high-mobility group box 1 protein (HMGB1) [13,14]. Inflammatory mediators include cytokines and chemokines. Cytokines are small, secreted proteins produced mostly by immune cells, but also by endothelial and stromal cells as well as fibroblasts. Their main function is to promote or inhibit proliferation, activation, and differentiation of immune cells, thus they are commonly divided into proinflammatory and anti-inflammatory or immunosuppressive cytokines. Prominent examples for proinflammatory cytokines are interleukin (IL)-12 and IL-4, which are necessary for the differentiation of T helper cells type 1 (Th1) and type 2 (Th2), respectively. Classical anti-inflammatory or immunosuppressive cytokines include IL-10 and transforming growth factor (TGF)- β . IL-10 effectively inhibits expression of Th1 cytokines and major histocompatibility complex (MHC) II and macrophage activation. TGF- β inhibits cell proliferation and induces differentiation of regulatory T cells (Treg), an immunosuppressive subtype of T helper cells. Chemokines are small cytokines which build up gradients in the affected area and serve as chemoattractants. They are essential for directing the migration and activation of phagocytes and lymphocytes in the course of an inflammatory reaction. Guided by chemotactic gradients, inflammatory immune cells enter the affected region to launch an immune reaction and remove the source of the threat.

2.1. Cytokine Release

Elevated levels of a variety of cytokines have been shown in animal as well as human studies. Increased production of IL-6 appears to be a frequent event after PDT [15–19]. IL-6 is considered to be a proinflammatory cytokine which stimulates the immune response, the induction of fever,

and acute-phase proteins. However, results on the impact or function of IL-6 in PDT outcome differ. In a system of EMT6 tumors treated with Photofrin[®]-PDT, blocking of IL-6 with respective antibodies significantly reduced PDT-induced neutrophilia at 2 hours and 8 hours post-treatment [20]. Contrasting this, another study found no effect of anti-IL-6 treatment on intratumoral neutrophil levels after PDT [16]. Those contradictory findings may be attributed to the different photosensitizers used, evaluation of blood neutrophil levels vs intratumoral neutrophil numbers, and different treatment protocols and evaluation time points. Another prominent cytokine elevated after PDT is IL-1 β . In a model of rat rhabdomyosarcoma it was shown that increased IL-1 β preceded PDT-induced neutrophilia [21]. In subsequent studies, other groups were able to demonstrate that IL-1 β is indeed a crucial mediator in PDT outcome and neutrophilia since blocking of this cytokine led to a significantly decreased rate of tumor cures and neutrophils in the tumor-draining lymph nodes (TDLN) in response to treatment [22,23]. Other cytokines that have been reported to be elevated post PDT include tumor necrosis factor (TNF)- α and interferon (IFN) γ [10]. The chemokines CXCL1 (chemokine (C-X-C) ligand 1 or keratinocyte chemoattractant, KC) and CXCL2 (macrophage inflammatory protein-2, MIP-2) were also shown to be increased after PDT treatment in a murine model of EMT6 carcinoma. These two chemokines are known for possessing neutrophil chemoattractant activity. However, only CXCL2 was shown to be necessary for neutrophil migration into the tumors in this setting [16]. In a rather recent report, Brackett et al. found induction of the cytokine IL-17 after treatment. This cytokine proved its importance by acting upstream of IL-1 β to regulate its expression levels. Thereby, it indirectly controlled the expression of CXCL2 which was dependent on IL-1 β . Diminished levels were found for TGF- β in the sera of CT26 colon carcinoma-bearing mice after PDT treatment with benzoporphyrin derivative (BPD) [24]. Additionally, blockade of immunosuppressive cytokines TGF- β and IL-10 has been shown to greatly enhance PDT-mediated tumor cure rates in C3H/HeN mice with subcutaneous FsaR fibrosarcomas [25].

2.2. Neutrophils

The importance of neutrophils in PDT efficiency has been proven in numerous studies. Neutrophils pose the first line of defense against pathogens and inflammatory insults to the host. In order to do so they secrete leukotrienes, prostaglandins, and cytokines to initiate the development of the inflammatory response. Furthermore, they are able to directly kill pathogens and they have been reported to be able to present antigens via MHC class II under certain circumstances. This raises the possibility that neutrophils could aid in the activation of CD4⁺ T helper cells. Increased levels of neutrophils following PDT have been reported frequently [22,23,26–28]. Moreover, Korbelik et al. showed that depletion of neutrophils led to a drop in mice cured from EMT6 tumors to 30%, with tumors recurring after 2–3 weeks [29]. In line with this are findings from Kousis and coworkers demonstrating that neutrophil depletion resulted in diminished numbers of activated cytotoxic T lymphocytes (CTL) in the TDLN and the tumor tissue [30]. In a different approach using blockade of neutrophil migration by administering anti-ICAM1 (intercellular adhesion molecule 1) the group of Sun demonstrated complete abrogation of the curative outcome of their treatment regimen. Additionally, this work showed an impairment of the curative effect following administration of anti-IL-1 β [22]. This finding was further highlighted by studies from Brackett et al. [23]. In their setting, neutrophil entry into TDLN post-PDT was mediated by CXCR2–CXCL2 interaction, with CXCL2 induction being dependent on IL-17A and IL-1 β . Interestingly, the degree of neutrophil infiltration appears to be governed by the treatment regimen applied. Work from Shams et al. revealed that the highest degree of neutrophil influx into tumor tissue and TDLN was achieved with a treatment regimen delivering a low fluence at a low fluence rate. This was further accompanied by a substantial increase in activated CTL [31]. A previous study already demonstrated the highest degree of induction of proinflammatory cytokines IL-6, MIP-1, and MIP-2 under these treatment conditions compared to regimens delivered at higher fluence and/or higher fluence rate [19].

2.3. Dendritic Cells

Crucial for the induction of an adaptive immune response are dendritic cells (DCs). DCs are professional antigen-presenting cells (APC) and as such their main function is to present endogenous (e.g., viral) as well as exogenous (e.g., bacterial) antigens to lymphocytes in order to activate them and mount an appropriate immune response. They exist in two functionally distinct stages, “mature” and “immature”. Immature DCs constantly sample their environment by taking up antigens via macropinocytosis, receptor-mediated endocytosis, and phagocytosis. They are characterized by expression of CD11c and low levels of MHC I, MHC II, CD80, and CD86 and the relative absence of cytokine production. In the presence of inflammatory stimuli, those immature DCs differentiate into their mature state. This includes upregulation of processing and presentation of antigens and increased expression of MHC molecules and the costimulatory molecules CD80 and CD86. Additionally, maturation induces secretion of proinflammatory cytokines including IL-12, IL-6, and IL-1 β . Mature DCs migrate to the lymph nodes in large numbers where they present peptide–MHC complexes to lymphocytes. In combination with appropriate costimulation, this leads to activation of CD4⁺ T helper cells, CD8⁺ CTL, and B cells, and initiates the adaptive immune response [32,33].

Several groups have shown the importance of DCs for PDT-mediated antitumor immunity and efficiency. Jalili and coworkers were able to demonstrate that intratumoral injection of immature DCs after PDT treatment resulted in significantly delayed tumor growth of the treated tumor and of untreated tumors in the contralateral hind limb [34]. Similar outcome was reported by the group of Saji [35]. Further corroborating these findings were experiments by Preise et al.: DTR bone marrow chimera mice were inoculated with CT26 colon carcinoma cells, and subcutaneously growing tumors were subjected to PDT. Depletion of DCs by injection of diphtheria toxin (DTx) resulted in increased recurrence rates of the tumors. Mice which were systemically depleted of DCs showed 90% of disease recurrence compared to only 20% in mice which received PDT treatment only [36]. Furthermore, other reports support the involvement of DCs in the response to PDT as evidenced by enhanced maturation and activation as well as increased secretion of proinflammatory cytokines after treatment [37–40].

3. PDT and Adaptive Immunity

The first evidence for induction of a tumor-specific immune response following PDT came from Canti et al. in 1994. This group demonstrated that normal mice cured from MS-2 fibrosarcoma by PDT were able to resist a rechallenge with tumor cells in a tumor-specific manner. In contrast to this, immunosuppressed counterparts were not able to resist the rechallenge [41]. Since then, several studies have shown that an intact immune system—specifically the adaptive arm of the immune response—is crucial for PDT outcome. Korbelik et al. demonstrated that treatment of BALB/c mice bearing EMT6 mammary carcinomas with PDT resulted in complete cures, whereas SCID mice did not elicit the same antitumor response with the identical PDT regimen [27]. Since SCID mice lack mature T lymphocytes, they are not able to mount a cellular adaptive immune response. Likewise, the group of Preise successfully treated BALB/c mice with a vascular-targeted PDT approach from CT26 tumors with cure rates of more than 70%. When the same experiments were carried out in BALB/nude or SCID mice, cure rates dropped to 18% and 11%, respectively [36]. Similar findings were repeatedly reported from other groups as well over the years [10,42,43].

Induction of systemic and memory immunity following PDT treatment has also been verified in numerous studies. Systemic immunity is reflected by the extension of the locally induced immune response to distant nontreated areas. A study by Kabingu and coworkers demonstrated the destruction of lung metastases indicative of an ongoing systemic immune response: mice were inoculated subcutaneously (s.c.) and intravenously (i.v.) with EMT6 tumor cells to generate a primary tumor (s.c.) and lung tumors mimicking metastases (i.v.). Treatment of the primary tumor with Photofrin®–PDT led to 90%–100% of tumor ablation, and analysis of lung metastases 10 days after PDT revealed a significant reduction of lung tumors compared to nontreated controls [42]. Likewise, Mroz et al.

reported regression of distant untreated tumors. In their model, mice bearing bilateral s.c. CT26.CL25 tumors were treated with BPD-PDT on one side while the contralateral tumor was left untreated. In a total of seven out of nine mice, this approach led to complete and permanent regression of the contralateral tumor [10]. Recent publications by other groups further support those findings [31,43]. Additionally, clinical observations report the regression of lesions outside the treatment field after PDT-treatment as well, thus indicating the generation of systemic immunity in human patients [44–46].

Recurring disease can only be prevented when memory immunity is successfully generated. In experimental models of cancer, generation of such a memory immunity can be evaluated by resistance of previously cured subjects to rechallenge with the same type of cancer cells. The first study indicating the induction of tumor-specific immune memory was published by Korbelik et al. in 1999: this work showed the ability of SCID mice to resist tumor cell rechallenge after they were cured from EMT6 tumors by a combination approach of adoptive transfer of tumor-sensitized splenocytes and PDT treatment [47]. The group of Preise demonstrated long-lasting protection against rechallenge in immunocompetent mice cured from primary tumors using a vascular-targeted approach of PDT. Interestingly, this approach even resulted in partial cross-protection against a different type of tumor cell used for rechallenge. However, the mechanism underlying this observation still remains to be elucidated [36]. In another study by Sanovic et al., BALB/c mice bearing a s.c. CT26 colon carcinoma were treated with hypericin-PDT, and this treatment yielded a striking 100% of tumor cures, which lasted until the end of the study. Additionally, i.v. challenge of those cured mice with viable CT26 cells showed no development of new tumors, thereby indicating existence of systemic memory immunity. Notably, these results were obtained with a protocol using a low PS dose delivered at a low fluence and low fluence rate [48]. Similar findings were reported by Mroz et al. who demonstrated 95% of cured mice resisting tumor development upon subsequent rechallenge [10]. Reginato and coworkers achieved 90% of cures with a treatment protocol employing BPD and Treg depletion using cyclophosphamide in a CT26 tumor model. Sixty-five percent of these mice rejected the rechallenge. However, with this protocol, another round of Treg depletion prior to rechallenge was necessary to unravel the memory immunity [24]. Interestingly, this group used the same type of tumor model (CT26 colon carcinoma in BALB/c mice) as Sanovic et al., whose studies showed no requirement for Treg depletion for therapeutic success. These differences might be attributed to the use of different PS (hypericin vs BPD) and/or differences in fluence and fluence rate (14 J cm^{-2} @27 mW cm^{-2} vs. 120 J cm^{-2} @100 mW cm^{-2}). Other groups assessed induction of memory immunity by resistance to rechallenge as well and reported results in line with the abovementioned findings [31,43].

The mediators of the adaptive immune response are antigen-specific B and T cells. Upon antigen recognition, B cells produce the antibodies necessary for eliminating extracellular pathogens. Although there are pieces of data pointing to a role for B cells in PDT-induced antitumor immunity [27,36,43], the importance of this humoral response has remained largely uninvestigated. In contrast to that, considerable efforts have been made over the past two decades to elucidate the role of the cellular immune response, i.e., the role of T lymphocytes. The findings regarding this population will be discussed in the following sections.

3.1. CD4^+ T Cells

T cells are divided into several subpopulations. When activated, CD4^+ T helper cells differentiate into distinct lineages, a process which is dependent on the stimuli and cytokines present. Those lineages secrete defined cytokines to assist in clearance of intracellular pathogens and extracellular microorganisms. Furthermore, CD4^+ T helper cells provide help for B cells and CD8^+ cytotoxic T cells for their activation and the generation of memory cells. The best defined T helper cell populations are Th1, Th2, and Th17. Th2 cells and their associated cytokines—IL-4, IL-5, and IL-13—serve in the response to extracellular microorganisms and the induction of the B cell isotype switching. Th1 cells are characterized by production of $\text{IFN}\gamma$ and are crucial for the eradication of intracellular pathogens. $\text{IFN}\gamma$ is known to activate the bactericidal activity of macrophages and increase the expression of MHC I on

normal cells and MHC II on APCs. Thereby it facilitates processing and presentation of endogenous antigens, which makes infected and aberrant cells visible to the immune system. Furthermore, IFN γ promotes activity of natural killer (NK) cells, which recognize and eliminate cells with decreased MHC I expression. Th1 cells have implications in antitumor immunity via activation and regulation of CTL, cross-priming of the immune response by APCs (this enables presentation of intracellular antigens in the context of MHC II), and direct tumor cell-killing through the release of specific cytokines [49]. The third subtype of T helper cells, that is well established by now, are Th17 cells and their signature cytokine IL-17. IL-17 leads to stimulation and de novo generation of neutrophils and is important in the response to certain extracellular bacteria and fungi [50]. In cancer, Th17 cells seem to be able to have opposing roles. There are numerous reports showing eradication of tumors by Th17 cells and a beneficial effect of their abundance in the tumor microenvironment. However, an equally solid body of evidence suggests a role for this subpopulation in tumor progression. This opposing impact of Th17 cells on tumor immunity seems to be attributable to the fact that the fine-tuning of their differentiation and function is highly dependent on a variety of factors; these include the type of tumor, the composition of stimuli leading to their activation (e.g., cytokine composition, T cell receptor signaling strength) and the therapeutic approach applied [51]. Interestingly, Th17 cells share ties with immunosuppressive Treg. In a proinflammatory environment, the decision of whether naïve T cells develop into either Treg or Th17 is dependent on the amount of available TGF- β : at low concentrations it synergizes with IL-6 and/or IL-21 and drives the induction of Th17 cells. At high TGF- β concentrations these cytokines are no longer sufficient to overcome Foxp3 (forkhead box protein 3)-mediated repression of retinoic acid receptor (RAR)-related orphan receptor (ROR) γ t, and the cells differentiate into Treg [52]. Additionally, Th17 cells are able to acquire a Th1-like phenotype with the ability to secrete IFN γ when they are exposed to IL-12 [51]. The role of T helper cells in PDT-mediated immunity is somewhat controversial. Experiments by Kabingu et al. showed no effect of CD4 $^{+}$ T cell depletion on PDT efficiency and induction of systemic antitumor immunity [42]. In contrast to that, other groups found a dependency of treatment outcome on the presence of CD4 $^{+}$ T cells. The group of Korbelik used antibodies for CD4, CD25, and a combination of both to deplete T helper cells, and saw a drop in cures by 30%–50% [29,47]. In line with this are results from others reporting delayed or abrogated tumor growth in naïve mice following adoptive transfer of CD4 $^{+}$ T cells from PDT-cured mice. Further analysis of this CD4 $^{+}$ population showed increased IFN γ secretion upon restimulation, which is indicative for the generation of a Th1 response [36]. However, the precise mechanisms by which CD4 $^{+}$ T cells contribute to PDT outcome remain largely elusive so far. Some light on this was shed by Brackett and coworkers, who showed an increase of Th17 cells and the corresponding signature cytokine IL-17A in the tumor-draining lymph nodes after PDT treatment [23]. In a very recent work Garg et al. found elevated levels of Th1 and Th17 cells in the brain immune contexture of mice treated with an immunogenic cell death (ICD)-based DC vaccine against high-grade glioma (HGG) and subsequently inoculated with the respective glioma cells. Furthermore, splenic T cells from these mice exhibited higher IFN γ production upon restimulation with naïve GL261 cell lysates, thus indicating expansion of localized immunostimulation in the brain to a systemic effect crucial for long-term immunity [14].

3.2. CD8 $^{+}$ T Cells

CD8 $^{+}$ CTL are essential for recognition and elimination of cells that are virally infected or display aberrant self. CTL recognize intracellular peptide bound to MHC class I on the cell surface, and upon activation they exert direct cytolytic effects against the target cell accompanied by the secretion of IFN γ . First evidence for the involvement of CTL came from Korbelik et al. in 1999. This group used an EMT6 mammary carcinoma model in which depletion of CD8 $^{+}$ T cells led to a 50% decrease in cures after PDT compared to unmanipulated mice [47]. Similar results were obtained by different groups using 2-iodo-5-ethylamino-9-diethylaminobenzo-phenothiazinium chloride or Photofrin $^{\text{®}}$ as photosensitizers, albeit Photofrin $^{\text{®}}$ was used in a combination approach with 5-aza-2'-deoxycytidine

to induce the tumor antigen P1A [53,54]. However, presence of P1A was not necessary to sustain long-term immunity. Likewise, adoptive transfer of CD8⁺ lymphocytes from cured animals was sufficient to protect naïve recipients from subsequent challenge with viable cancer cells from the same type [36,54]. It should be noted that this protection did not show a requirement for additional transfer of CD4⁺ T helper cells. A study by Saji et al. further substantiates these findings with an experiment where the transfer of CD8⁺ T cell-depleted splenocytes from PDT-cured mice into naïve recipients conferred protection to rechallenge [35]. Other studies frequently found elevated levels of CD8⁺ T cells after treatment, and closer examination of those cells revealed increased lytic activity against tumor cells in an antigen-specific manner [10,30,31]. On a clinical level, Abdel-Hady et al. were able to show that patients with vulval intraepithelial neoplasia who responded to PDT had increased levels of infiltrating CD8⁺ T cells after treatment [55].

3.3. Regulatory T Cells

Regulatory T cells comprise a unique subset among the CD4⁺ T cell subpopulations. Treg cells display regulatory and suppressive activity towards other immune cells, and especially effector T cells. On the molecular level they are characterized by the constitutive expression of high levels of the transmembrane protein CD25 (IL-2R α chain) [56] and cytotoxic T lymphocyte-associated antigen 4 (CTLA-4) [57] and stable expression of the lineage-specific transcription factor Foxp3 [58,59]. By now, it is well established that Treg are required for immunological tolerance and prevention of excessive inflammatory immune responses. Neonatal thymectomy in mice results in fatal T cell-mediated autoimmunity against various organs due to the lack of regulatory T cells [60]. Mutations in the X chromosome-encoded Foxp3 gene, as in human IPEX patients and Scurfy mice, leads to severe immune dysregulation, polyendocrinopathy, and enteropathy related to an inability to generate Treg and establish tolerance [59,61]. Their origin is either in the thymus (tTreg) in response to recognition of self-antigen during negative selection or in peripheral lymphoid organs (pTreg), where naïve T cells recognize antigens in a tolerogenic environment—like that of commensal bacteria in the gut or the cancer microenvironment—and differentiate into pTreg. tTreg are considered to provide tolerance towards self-antigens that are represented in the thymus, whereas the main function of pTreg is the establishment of tolerance to antigens that are either foreign but not harmful or self-antigens not presented in the thymus during T cell development [62,63]. In cancer it has been shown that Treg are the predominant T cell type accumulating in tumor tissue, and low T effector/Treg ratios correlate with poor prognosis in various tumor types [64–66]. Regulatory T cells employ various mechanisms to suppress effector T cells. Those mechanisms include sequestration of available IL-2 via the high affinity IL-2 receptor, CTLA-4 (CTL-associated protein 4)-mediated sequestration of CD80/86 on APC surfaces, production of inhibitory cytokines like IL-10 and IL-35, production of pericellular adenosine, and direct cytotoxicity of effector T cells by granzyme B and perforin [67]. In the tumor microenvironment, Treg keep effector T cells in an intermediate state via sequestration of IL-2 and production of TGF- β . Withdrawal of IL-2 prevents full activation of effector T cells and ensures continuous availability of IL-2 produced by partially activated T cells, which Treg need for their maintenance but do not produce themselves [68]. TGF- β prevents full cytotoxic effector differentiation of tumor-specific CD8⁺ T cells and keeps memory CD8⁺ T cells in an inactive state [69,70]. The importance of suppression of Treg to increase PDT efficiency has recently been shown in several studies [24,71]. Treg depletion by cyclophosphamide followed by PDT in mice bearing CT26 colon carcinomas led to improved long-term survival and development of memory immunity [24]. It should be mentioned that this need for Treg depletion constitutes sort of a conundrum: lymphocytes have been shown to be especially sensitive to PDT-mediated cell death (see below). Therefore, Treg residing in the tumor microenvironment should be depleted by PDT treatment, thus abolishing the need for external depletion. However, other studies using the same tumor model did not show this requirement. Although there have been substantial differences in the treatment protocols between those studies, the reason for this particular aspect has (to the best of our knowledge) not been addressed so far and clearly needs further elucidation.

A recent study from Garg and coworkers looking at the brain immune contexture in a murine model of HGG showed a shift from Treg towards Th1/Th17/CTL following treatment with an ICD-based DC vaccine in a prophylactic as well as in a curative setting [14]. Zheng et al. found a decrease of Treg induction in vitro and in vivo in response to stimulation/treatment with DC which had been pulsed with PDT-treated Lewis lung carcinoma cells (LLC). This was accompanied by a significant inhibition of tumor growth upon challenge with live LLC cells [40]. In a clinical setting, blood analysis of patients with esophageal squamous cell carcinoma demonstrated that PDT with the PS Photofrin® abolished the suppressive function of peripheral Treg, but had no effect on Treg numbers [72]. Taken together, these studies indicate effects of PDT on Treg, which have to be elucidated in order to harness the potential of PDT to break tumor-promoting immune suppression.

4. Treatment Regimen and Modes of Cell Death

There are still considerable differences in treatment outcomes, limiting the successful translation of PDT into broad clinical application. These differences might be attributed to a variety of parameters including the PS and PS dose used, the drug–light interval, the applied fluence and fluence rate, and the light source itself.

One determinant of the induction of antitumor immunity is the mode of cell death, which is triggered by the applied treatment regimen and can be influenced by any of the parameters mentioned above. An extensive review about the modes and mechanisms of cell death in PDT induced by different PS was published by Bacellar et al. in 2015 [73]. In general, PDT is able to result in apoptosis, necrosis, the so-called immunogenic cell death (ICD), and autophagy. Apoptosis is traditionally considered as a programmed form of cell death which is immunologically silent. The remnants of these “physiologically” dying cells are quickly removed afterwards by phagocytes. Therefore, cells undergoing apoptosis normally do not elicit a strong immune response or a detectable response at all, for that matter. In contrast to that, necrosis is the result of an insult or trauma that leads to rapid cell death. This form of cell death characteristically involves the uncontrolled release of cellular products and the initiation of an inflammatory response in the surrounding tissue, which can lead to severe bystander damage. Although an inflammatory response is necessary for the induction of the immune response, this process can be detrimental for the host when it cannot be resolved by the immune system. In light of these definitions, one would assume that necrotic cells or a mixture of necrotic and apoptotic cells should be more efficient in facilitating the development of a distinct immune response than apoptotic cells. Contrasting this, there are numerous reports demonstrating that apoptotic cells are superior to necrotic cells in inducing antitumor immunity [74–80]. Intensive research in the field of cell death in the following years led to the fairly new concept of ICD. ICD describes an immunogenic form of apoptosis or necrosis. Since the emergence of the concept of ICD it has been shown that tumor cells undergoing immunogenic apoptosis are more potent inducers of antitumor immune responses than cell dying via necrosis or nonimmunogenic apoptosis. Thus, it would be favorable to use and develop PSs which predominantly cause ICD in cancer cells for future approaches. Importantly, so far hypericin is the only PS shown to induce all major molecular and immunological hallmarks of ICD. This includes surface expression of CRT, HSP70, and HSP90 and secretion of ATP—four DAMPs crucial in ICD [80,81].

In an elegant study, Garg et al. demonstrated remarkable prophylactic and therapeutic success using DCs loaded with hypericin–PDT killed tumor cells in a model of HGG. In this case, the induction of antitumor immunity was dependent on the PDT-induced surface exposure of CRT and release of HMGB1 (amongst others). Notably, analysis of glioma cells treated with aminolevulinic acid (ALA)–PDT revealed no significant increase of those two DAMPs [14]. This clearly shows that the type of PS used can influence the determinants of cell death and its impact on subsequent antitumor immunity. Treatment parameters regarding the applied fluence and fluence rate also differ greatly among studies and have considerable effect on therapy outcome. It has been shown that at high-fluence PDT predominantly causes necrosis, while at medium to low fluences apoptosis or a mixture of

apoptosis and necrosis is more prevalent [82]. Analysis of neutrophilia and secretion of cytokines (as a measure for inflammation) induced by different combinations of fluence and fluence rate by Henderson et al. showed that the most inflammatory response was triggered at a low fluence and a low fluence rate. However, the best tumor control was achieved with a high to intermediate fluence at a low fluence rate. This regimen only caused mild inflammation [19]. In a subsequent study, a sequential treatment approach consisting of a first session causing substantial inflammation (low fluence, low fluence rate) followed by a second session for tumor control (high/intermediate fluence, low fluence rate) yielded the best results with respect to control of the primary disease and induction of memory immunity [31]. These results are backed from findings by others indicating that low-dosed or vascular-targeted treatment regimens have better overall therapeutic outcome [36,43,48,83]. Additionally, clinical reports support a beneficial effect for therapy when using milder treatment protocols [45,84]. Another example for the impact of different treatment regimens and the influence they can have on the therapeutic approach comes from comparison of studies from Reginato et al. and Sanovic and coworkers: those two groups used the same tumor model (i.e., subcutaneously growing CT26 tumors in BALB/c mice) but their treatment regimen differed considerably in terms of PS (BPD vs hypericin) and in the fluence and fluence rate applied (120 J cm^{-2} @ 100 mW cm^{-2} vs. 14 J cm^{-2} @ 27 mW cm^{-2}). Still, both groups achieved tumor cures and induction of memory immunity. However, in the system using BPD and a high light dose, depletion of Treg was necessary to induce tumor-specific immunity and unravel memory immunity [24,48].

A different aspect of the PS dose used is the effect on surrounding immune cells. T lymphocytes have been shown to be especially sensitive to PDT-induced death [85,86]. This might actually be beneficial therapy outcome since most of the T cells within the tumor microenvironment are considered to have an immunosuppressive phenotype. These T cells would be destroyed and the area would be repopulated by activated effector T cells. Indeed, it has been shown that shortly after PDT treatment, CD3⁺ lymphocytes (CD3 as part of the T cell receptor is expressed on all T cells) disappeared. About 24 h later, CD3⁺ T cells were present again with levels exceeding those prior to treatment [36,43]. Additionally, unpublished data from our group indicates that DCs show a higher susceptibility to PDT-mediated cell death in a dose-dependent manner with a variety of PSs compared to several different cancer cell lines tested. This raises the possibility that the PS dose used might affect antigen uptake and presentation (due to enhanced killing of antigen-presenting cells) necessary for launching the adaptive immune response.

5. Conclusions

The capability of PDT to effectively cure primary tumors and induce systemic and long-lasting immunity to combat metastases and recurring disease has been shown in numerous studies and a variety of settings over the past two decades. This holds the potential for this particular treatment modality to become a powerful therapeutic option for cancer patients. Recent years have seen a number of improvements to lift limitations given by the nature of PDT. Technical improvements include the development of new light sources to reach solid tumors that are neither superficial nor intraluminal. Furthermore, there are continuous efforts to develop PS which need less energy to be properly excited. This enables the use of light with longer wavelength, which penetrates deeper into tissue. Coupling of PS to antibodies specific for the tumor cells in question is supposed to improve targeting of the PS to the tumor.

With increasing technical progress and improvements of PSs it should be possible to extend the applicability of PDT to a point where it would be a feasible therapy option for a broad spectrum of cancer entities. We believe that comparative analyses of the immunological effects elicited by different parameters of PDT (e.g., PS type and dose, fluence and fluence rate) would greatly enhance the understanding of the induction of antitumor immunity induced by this therapy. This would aid in developing protocols which efficiently fight off the primary tumor and boost the immune system to

recognize and combat distant and recurring disease manifestation while being patient-sparing, easy to handle, and cost-effective.

Conflicts of Interest: The authors declare no conflict of interest.

References

1. Moan, J.; Peng, Q. An outline of the hundred-year history of PDT. *Anticancer Res.* **2003**, *23*, 3591–3600. [[PubMed](#)]
2. Allison, R.R.; Sibata, C.H. Oncologic photodynamic therapy photosensitizers: A clinical review. *Photodiagnosis Photodyn. Ther.* **2010**, *7*, 61–75. [[CrossRef](#)] [[PubMed](#)]
3. Agostinis, P.; Berg, K.; Cengel, K.A.; Foster, T.H.; Girotti, A.W.; Gollnick, S.O.; Hahn, S.M.; Hamblin, M.R.; Juzeniene, A.; Kessel, D.; et al. Photodynamic therapy of cancer: An update. *CA Cancer J. Clin.* **2011**, *61*, 250–281. [[CrossRef](#)] [[PubMed](#)]
4. Dougherty, T.J. An update on photodynamic therapy applications. *J. Clin. Laser Med. Surg.* **2002**, *20*, 3–7. [[CrossRef](#)] [[PubMed](#)]
5. Plaetzer, K.; Krammer, B.; Berlanda, J.; Berr, F.; Kiesslich, T. Photophysics and photochemistry of photodynamic therapy: Fundamental aspects. *Lasers Med. Sci.* **2009**, *24*, 259–268. [[CrossRef](#)] [[PubMed](#)]
6. Brackett, C.M.; Gollnick, S.O. Photodynamic therapy enhancement of anti-tumor immunity. *Photochem. Photobiol. Sci.* **2011**, *10*, 649–652. [[CrossRef](#)] [[PubMed](#)]
7. Kim, G.; Gaitas, A. Extracorporeal photo-immunotherapy for circulating tumor cells. *PLoS ONE* **2015**, *10*, e0127219. [[CrossRef](#)] [[PubMed](#)]
8. Vogl, T.J.; Eichler, K.; Mack, M.G.; Zangos, S.; Herzog, C.; Thalhammer, A.; Engelmann, K. Interstitial photodynamic laser therapy in interventional oncology. *Eur. Radiol.* **2004**, *14*, 1063–1073. [[CrossRef](#)] [[PubMed](#)]
9. Bechet, D.; Mordon, S.R.; Guillemin, F.; Barberi-Heyob, M.A. Photodynamic therapy of malignant brain tumours: A complementary approach to conventional therapies. *Cancer Treat. Rev.* **2014**, *40*, 229–241. [[CrossRef](#)] [[PubMed](#)]
10. Mroz, P.; Szokalska, A.; Wu, M.X.; Hamblin, M.R. Photodynamic therapy of tumors can lead to development of systemic antigen-specific immune response. *PLoS ONE* **2010**, *5*, e15194. [[CrossRef](#)] [[PubMed](#)]
11. Korbelik, M. Cancer vaccines generated by photodynamic therapy. *Photochem. Photobiol. Sci.* **2011**, *10*, 664–669. [[CrossRef](#)] [[PubMed](#)]
12. Gollnick, S.O. Photodynamic therapy and antitumor immunity. *J. Natl. Compr. Cancer Netw.* **2012**, *10*, S40–S43.
13. Mroz, P.; Hashmi, J.T.; Huang, Y.-Y.; Lange, N.; Hamblin, M.R. Stimulation of anti-tumor immunity by photodynamic therapy. *Expert Rev. Clin. Immunol.* **2011**, *7*, 75–91. [[CrossRef](#)] [[PubMed](#)]
14. Garg, A.D.; Vandenberk, L.; Koks, C.; Verschuere, T.; Boon, L.; van Gool, S.W.; Agostinis, P. Dendritic cell vaccines based on immunogenic cell death elicit danger signals and T cell-driven rejection of high-grade glioma. *Sci. Transl. Med.* **2016**, *8*, 328ra27. [[CrossRef](#)] [[PubMed](#)]
15. Kick, G.; Messer, G.; Goetz, A.; Plewig, G.; Kind, P. Photodynamic therapy induces expression of interleukin 6 by activation of AP-1 but not NF-kappa B DNA binding. *Cancer Res.* **1995**, *55*, 2373–2379. [[PubMed](#)]
16. Gollnick, S.O.; Evans, S.S.; Baumann, H.; Owczarczak, B.; Maier, P.; Vaughan, L.; Wang, W.C.; Unger, E.; Henderson, B.W. Role of cytokines in photodynamic therapy-induced local and systemic inflammation. *Br. J. Cancer* **2003**, *88*, 1772–1779. [[CrossRef](#)] [[PubMed](#)]
17. Du, H.; Bay, B.-H.; Mahendran, R.; Olivo, M. Hypericin-mediated photodynamic therapy elicits differential interleukin-6 response in nasopharyngeal cancer. *Cancer Lett.* **2006**, *235*, 202–208. [[CrossRef](#)] [[PubMed](#)]
18. Wei, L.-H.; Baumann, H.; Tracy, E.; Wang, Y.; Hutson, A.; Rose-John, S.; Henderson, B.W. Interleukin-6 trans signalling enhances photodynamic therapy by modulating cell cycling. *Br. J. Cancer* **2007**, *97*, 1513–1522. [[CrossRef](#)] [[PubMed](#)]
19. Henderson, B.W.; Gollnick, S.O.; Snyder, J.W.; Busch, T.M.; Kousis, P.C.; Cheney, R.T.; Morgan, J. Choice of oxygen-conserving treatment regimen determines the inflammatory response and outcome of photodynamic therapy of tumors. *Cancer Res.* **2004**, *64*, 2120–2126. [[CrossRef](#)] [[PubMed](#)]

20. Cecic, I.; Korbelik, M. Mediators of peripheral blood neutrophilia induced by photodynamic therapy of solid tumors. *Cancer Lett.* **2002**, *183*, 43–51. [[CrossRef](#)]
21. De Vree, W.J.; Essers, M.C.; Koster, J.F.; Sluiter, W. Role of interleukin 1 and granulocyte colony-stimulating factor in photofrin-based photodynamic therapy of rat rhabdomyosarcoma tumors. *Cancer Res.* **1997**, *57*, 2555–2558. [[PubMed](#)]
22. Sun, J.; Cecic, I.; Parkins, C.S.; Korbelik, M. Neutrophils as inflammatory and immune effectors in photodynamic therapy-treated mouse SCCVII tumours. *Photochem. Photobiol. Sci.* **2002**, *1*, 690–695. [[CrossRef](#)] [[PubMed](#)]
23. Brackett, C.M.; Muhitch, J.B.; Evans, S.S.; Gollnick, S.O. IL-17 promotes neutrophil entry into tumor-draining lymph nodes following induction of sterile inflammation. *J. Immunol. Baltim. Md 1950* **2013**, *191*, 4348–4357. [[CrossRef](#)] [[PubMed](#)]
24. Reginato, E.; Mroz, P.; Chung, H.; Kawakubo, M.; Wolf, P.; Hamblin, M.R. Photodynamic therapy plus regulatory T-cell depletion produces immunity against a mouse tumour that expresses a self-antigen. *Br. J. Cancer* **2013**, *109*, 2167–2174. [[CrossRef](#)] [[PubMed](#)]
25. Korbelik, M. PDT-associated host response and its role in the therapy outcome. *Lasers Surg. Med.* **2006**, *38*, 500–508. [[CrossRef](#)] [[PubMed](#)]
26. De Vree, W.J.; Essers, M.C.; de Bruijn, H.S.; Star, W.M.; Koster, J.F.; Sluiter, W. Evidence for an important role of neutrophils in the efficacy of photodynamic therapy in vivo. *Cancer Res.* **1996**, *56*, 2908–2911. [[PubMed](#)]
27. Korbelik, M.; Kros, G.; Kros, J.; Dougherty, G.J. The role of host lymphoid populations in the response of mouse EMT6 tumor to photodynamic therapy. *Cancer Res.* **1996**, *56*, 5647–5652. [[PubMed](#)]
28. Gollnick, S.O.; Liu, X.; Owczarczak, B.; Musser, D.A.; Henderson, B.W. Altered expression of interleukin 6 and interleukin 10 as a result of photodynamic therapy in vivo. *Cancer Res.* **1997**, *57*, 3904–3909. [[PubMed](#)]
29. Korbelik, M.; Cecic, I. Contribution of myeloid and lymphoid host cells to the curative outcome of mouse sarcoma treatment by photodynamic therapy. *Cancer Lett.* **1999**, *137*, 91–98. [[CrossRef](#)]
30. Kousis, P.C.; Henderson, B.W.; Maier, P.G.; Gollnick, S.O. Photodynamic therapy enhancement of antitumor immunity is regulated by neutrophils. *Cancer Res.* **2007**, *67*, 10501–10510. [[CrossRef](#)] [[PubMed](#)]
31. Shams, M.; Owczarczak, B.; Manderscheid-Kern, P.; Bellnier, D.A.; Gollnick, S.O. Development of photodynamic therapy regimens that control primary tumor growth and inhibit secondary disease. *Cancer Immunol. Immunother.* **2015**, *64*, 287–297. [[CrossRef](#)] [[PubMed](#)]
32. Dudek, A.M.; Martin, S.; Garg, A.D.; Agostinis, P. Immature, Semi-Mature, and Fully Mature Dendritic Cells: Toward a DC-Cancer Cells Interface That Augments Anticancer Immunity. *Front. Immunol.* **2013**, *4*, 438. [[CrossRef](#)] [[PubMed](#)]
33. Strioga, M.; Schijns, V.; Powell, D.J.; Pasukoniene, V.; Dobrovolskiene, N.; Michalek, J. Dendritic cells and their role in tumor immunosurveillance. *Innate Immun.* **2013**, *19*, 98–111. [[CrossRef](#)] [[PubMed](#)]
34. Jalili, A.; Makowski, M.; Switaj, T.; Nowis, D.; Wilczynski, G.M.; Wilczek, E.; Chorazy-Massalska, M.; Radzikowska, A.; Maslinski, W.; Biały, L.; et al. Effective photoimmunotherapy of murine colon carcinoma induced by the combination of photodynamic therapy and dendritic cells. *Clin. Cancer Res.* **2004**, *10*, 4498–4508. [[CrossRef](#)] [[PubMed](#)]
35. Saji, H.; Song, W.; Furumoto, K.; Kato, H.; Engleman, E.G. Systemic antitumor effect of intratumoral injection of dendritic cells in combination with local photodynamic therapy. *Clin. Cancer Res.* **2006**, *12*, 2568–2574. [[CrossRef](#)] [[PubMed](#)]
36. Preise, D.; Oren, R.; Glinert, I.; Kalchenko, V.; Jung, S.; Scherz, A.; Salomon, Y. Systemic antitumor protection by vascular-targeted photodynamic therapy involves cellular and humoral immunity. *Cancer Immunol. Immunother.* **2009**, *58*, 71–84. [[CrossRef](#)] [[PubMed](#)]
37. Gollnick, S.O.; Brackett, C.M. Enhancement of anti-tumor immunity by photodynamic therapy. *Immunol. Res.* **2010**, *46*, 216–226. [[CrossRef](#)] [[PubMed](#)]
38. Gollnick, S.O.; Owczarczak, B.; Maier, P. Photodynamic therapy and anti-tumor immunity. *Lasers Surg. Med.* **2006**, *38*, 509–515. [[CrossRef](#)] [[PubMed](#)]
39. Kushibiki, T.; Tajiri, T.; Tomioka, Y.; Awazu, K. Photodynamic therapy induces interleukin secretion from dendritic cells. *Int. J. Clin. Exp. Med.* **2010**, *3*, 110–114. [[PubMed](#)]
40. Zheng, Y.; Yin, G.; Le, V.; Zhang, A.; Chen, S.; Liang, X.; Liu, J. Photodynamic-therapy activates immune response by disrupting immunity homeostasis of tumor cells, which generates vaccine for cancer therapy. *Int. J. Biol. Sci.* **2016**, *12*, 120–132. [[CrossRef](#)] [[PubMed](#)]

41. Canti, G.; Lattuada, D.; Nicolin, A.; Taroni, P.; Valentini, G.; Cubeddu, R. Antitumor immunity induced by photodynamic therapy with aluminum disulfonated phthalocyanines and laser light. *Anticancer. Drugs* **1994**, *5*, 443–447. [[CrossRef](#)] [[PubMed](#)]
42. Kabingu, E.; Vaughan, L.; Owczarczak, B.; Ramsey, K.D.; Gollnick, S.O. CD8+ T cell-mediated control of distant tumours following local photodynamic therapy is independent of CD4+ T cells and dependent on natural killer cells. *Br. J. Cancer* **2007**, *96*, 1839–1848. [[CrossRef](#)] [[PubMed](#)]
43. Rocha, L.B.; Gomes-da-Silva, L.C.; Dąbrowski, J.M.; Arnaut, L.G. Elimination of primary tumours and control of metastasis with rationally designed bacteriochlorin photodynamic therapy regimens. *Eur. J. Cancer Oxf. Engl. 1990* **2015**, *51*, 1822–1830. [[CrossRef](#)] [[PubMed](#)]
44. Thong, P.S.-P.; Ong, K.-W.; Goh, N.S.-G.; Kho, K.-W.; Manivasager, V.; Bhuvaneswari, R.; Olivo, M.; Soo, K.-C. Photodynamic-therapy-activated immune response against distant untreated tumours in recurrent angiosarcoma. *Lancet Oncol.* **2007**, *8*, 950–952. [[CrossRef](#)]
45. Kabingu, E.; Oseroff, A.R.; Wilding, G.E.; Gollnick, S.O. Enhanced systemic immune reactivity to a Basal cell carcinoma associated antigen following photodynamic therapy. *Clin. Cancer Res.* **2009**, *15*, 4460–4466. [[CrossRef](#)] [[PubMed](#)]
46. Morrison, S.A.; Hill, S.L.; Rogers, G.S.; Graham, R.A. Efficacy and safety of continuous low-irradiance photodynamic therapy in the treatment of chest wall progression of breast cancer. *J. Surg. Res.* **2014**, *192*, 235–241. [[CrossRef](#)] [[PubMed](#)]
47. Korbelik, M.; Dougherty, G.J. Photodynamic therapy-mediated immune response against subcutaneous mouse tumors. *Cancer Res.* **1999**, *59*, 1941–1946. [[PubMed](#)]
48. Sanovic, R.; Verwanger, T.; Hartl, A.; Krammer, B. Low dose hypericin-PDT induces complete tumor regression in BALB/c mice bearing CT26 colon carcinoma. *Photodiagnosis Photodyn. Ther.* **2011**, *8*, 291–296. [[CrossRef](#)] [[PubMed](#)]
49. Knutson, K.L.; Disis, M.L. Tumor antigen-specific T helper cells in cancer immunity and immunotherapy. *Cancer Immunol. Immunother.* **2005**, *54*, 721–728. [[CrossRef](#)] [[PubMed](#)]
50. Stockinger, B.; Veldhoen, M. Differentiation and function of Th17 T cells. *Curr. Opin. Immunol.* **2007**, *19*, 281–286. [[CrossRef](#)] [[PubMed](#)]
51. Bailey, S.R.; Nelson, M.H.; Himes, R.A.; Li, Z.; Mehrotra, S.; Paulos, C.M. Th17 cells in cancer: The ultimate identity crisis. *Front. Immunol.* **2014**, *5*, 276. [[CrossRef](#)] [[PubMed](#)]
52. Zhou, L.; Lopes, J.E.; Chong, M.M.W.; Ivanov, I.I.; Min, R.; Vitorica, G.D.; Shen, Y.; Du, J.; Rubtsov, Y.P.; Rudensky, A.Y.; et al. TGF-beta-induced Foxp3 inhibits T(H)17 cell differentiation by antagonizing RORgamma function. *Nature* **2008**, *453*, 236–240. [[CrossRef](#)] [[PubMed](#)]
53. Hendrzak-Henion, J.A.; Knisely, T.L.; Cincotta, L.; Cincotta, E.; Cincotta, A.H. Role of the immune system in mediating the antitumor effect of benzophenothiazine photodynamic therapy. *Photochem. Photobiol.* **1999**, *69*, 575–581. [[CrossRef](#)] [[PubMed](#)]
54. Wachowska, M.; Gabrysiak, M.; Muchowicz, A.; Bednarek, W.; Barankiewicz, J.; Rygiel, T.; Boon, L.; Mroz, P.; Hamblin, M.R.; Golab, J. 5-Aza-2'-deoxycytidine potentiates antitumour immune response induced by photodynamic therapy. *Eur. J. Cancer* **2014**, *50*, 1370–1381. [[CrossRef](#)] [[PubMed](#)]
55. Abdel-Hady, E.S.; Martin-Hirsch, P.; Duggan-Keen, M.; Stern, P.L.; Moore, J.V.; Corbitt, G.; Kitchener, H.C.; Hampson, I.N. Immunological and viral factors associated with the response of vulval intraepithelial neoplasia to photodynamic therapy. *Cancer Res.* **2001**, *61*, 192–196. [[PubMed](#)]
56. Sakaguchi, S.; Sakaguchi, N.; Asano, M.; Itoh, M.; Toda, M. Immunologic self-tolerance maintained by activated T cells expressing IL-2 receptor alpha-chains (CD25). Breakdown of a single mechanism of self-tolerance causes various autoimmune diseases. *J. Immunol. Baltim. Md 1950* **1995**, *155*, 1151–1164.
57. Takahashi, T.; Tagami, T.; Yamazaki, S.; Uede, T.; Shimizu, J.; Sakaguchi, N.; Mak, T.W.; Sakaguchi, S. Immunologic self-tolerance maintained by CD25(+)CD4(+) regulatory T cells constitutively expressing cytotoxic T lymphocyte-associated antigen 4. *J. Exp. Med.* **2000**, *192*, 303–310. [[CrossRef](#)] [[PubMed](#)]
58. Fontenot, J.D.; Gavin, M.A.; Rudensky, A.Y. Foxp3 programs the development and function of CD4+CD25+ regulatory T cells. *Nat. Immunol.* **2003**, *4*, 330–336. [[CrossRef](#)] [[PubMed](#)]
59. Khattry, R.; Cox, T.; Yasayko, S.-A.; Ramsdell, F. An essential role for Scurfin in CD4+CD25+ T regulatory cells. *Nat. Immunol.* **2003**, *4*, 337–342. [[CrossRef](#)] [[PubMed](#)]
60. Sakaguchi, S.; Wing, K.; Miyara, M. Regulatory T cells—a brief history and perspective. *Eur. J. Immunol.* **2007**, *37*, S116–S123. [[CrossRef](#)] [[PubMed](#)]

61. Bennett, C.L.; Christie, J.; Ramsdell, F.; Brunkow, M.E.; Ferguson, P.J.; Whitesell, L.; Kelly, T.E.; Saulsbury, F.T.; Chance, P.F.; Ochs, H.D. The immune dysregulation, polyendocrinopathy, enteropathy, X-linked syndrome (IPEX) is caused by mutations of FOXP3. *Nat. Genet.* **2001**, *27*, 20–21. [[PubMed](#)]
62. Sakaguchi, S.; Yamaguchi, T.; Nomura, T.; Ono, M. Regulatory T cells and immune tolerance. *Cell* **2008**, *133*, 775–787. [[CrossRef](#)] [[PubMed](#)]
63. Schmitt, E.G.; Williams, C.B. Generation and function of induced regulatory T cells. *Front. Immunol.* **2013**, *4*, 152. [[CrossRef](#)] [[PubMed](#)]
64. Beyer, M.; Schultze, J.L. Regulatory T cells in cancer. *Blood* **2006**, *108*, 804–811. [[CrossRef](#)] [[PubMed](#)]
65. Nishikawa, H.; Sakaguchi, S. Regulatory T cells in tumor immunity. *Int. J. Cancer J. Int. Cancer* **2010**, *127*, 759–767. [[CrossRef](#)] [[PubMed](#)]
66. Darrasse-Jèze, G.; Podsypanina, K. How numbers, nature, and immune status of foxp3(+) regulatory T-cells shape the early immunological events in tumor development. *Front. Immunol.* **2013**, *4*, 292.
67. Vignali, D.A.A.; Collison, L.W.; Workman, C.J. How regulatory T cells work. *Nat. Rev. Immunol.* **2008**, *8*, 523–532. [[CrossRef](#)] [[PubMed](#)]
68. Roychoudhuri, R.; Eil, R.L.; Restifo, N.P. The interplay of effector and regulatory T cells in cancer. *Curr. Opin. Immunol.* **2015**, *33*, 101–111. [[CrossRef](#)] [[PubMed](#)]
69. Chen, M.-L.; Pittet, M.J.; Gorelik, L.; Flavell, R.A.; Weissleder, R.; von Boehmer, H.; Khazaie, K. Regulatory T cells suppress tumor-specific CD8 T cell cytotoxicity through TGF-beta signals in vivo. *Proc. Natl. Acad. Sci. USA* **2005**, *102*, 419–424. [[CrossRef](#)] [[PubMed](#)]
70. Kalia, V.; Penny, L.A.; Yuzefpolskiy, Y.; Baumann, F.M.; Sarkar, S. Quiescence of memory CD8(+) T cells Is mediated by regulatory T cells through inhibitory receptor CTLA-4. *Immunity* **2015**, *42*, 1116–1129. [[CrossRef](#)] [[PubMed](#)]
71. Castano, A.P.; Mroz, P.; Wu, M.X.; Hamblin, M.R. Photodynamic therapy plus low-dose cyclophosphamide generates antitumor immunity in a mouse model. *Proc. Natl. Acad. Sci. USA* **2008**, *105*, 5495–5500. [[CrossRef](#)] [[PubMed](#)]
72. Reginato, E.; Lindenmann, J.; Langner, C.; Schweintzger, N.; Bambach, I.; Smolle-Jüttner, F.; Wolf, P. Photodynamic therapy downregulates the function of regulatory T cells in patients with esophageal squamous cell carcinoma. *Photochem. Photobiol. Sci.* **2014**, *13*, 1281–1289. [[CrossRef](#)] [[PubMed](#)]
73. Bacellar, I.O.L.; Tsubone, T.M.; Pavani, C.; Baptista, M.S. Photodynamic efficiency: From molecular photochemistry to cell death. *Int. J. Mol. Sci.* **2015**, *16*, 20523–20559. [[CrossRef](#)] [[PubMed](#)]
74. Schnurr, M.; Scholz, C.; Rothenfusser, S.; Galambos, P.; Dauer, M.; Röbe, J.; Endres, S.; Eigler, A. Apoptotic pancreatic tumor cells are superior to cell lysates in promoting cross-priming of cytotoxic T cells and activate NK and gammadelta T cells. *Cancer Res.* **2002**, *62*, 2347–2352. [[PubMed](#)]
75. Scheffer, S.R.; Nave, H.; Korangy, F.; Schlote, K.; Pabst, R.; Jaffee, E.M.; Manns, M.P.; Greten, T.F. Apoptotic, but not necrotic, tumor cell vaccines induce a potent immune response in vivo. *Int. J. Cancer* **2003**, *103*, 205–211. [[CrossRef](#)] [[PubMed](#)]
76. Goldszmid, R.S.; Idoyaga, J.; Bravo, A.I.; Steinman, R.; Mordoh, J.; Wainstok, R. Dendritic cells charged with apoptotic tumor cells induce long-lived protective CD4+ and CD8+ T cell immunity against B16 melanoma. *J. Immunol. Baltim. Md 1950* **2003**, *171*, 5940–5947. [[CrossRef](#)]
77. Bartholomae, W.C.; Rininsland, F.H.; Eisenberg, J.C.; Boehm, B.O.; Lehmann, P.V.; Tary-Lehmann, M. T cell immunity induced by live, necrotic, and apoptotic tumor cells. *J. Immunol. Baltim. Md 1950* **2004**, *173*, 1012–1022. [[CrossRef](#)]
78. Gamrekashvili, J.; Ormandy, L.A.; Heimesaat, M.M.; Kirschning, C.J.; Manns, M.P.; Korangy, F.; Greten, T.F. Primary sterile necrotic cells fail to cross-prime CD8(+) T cells. *Oncoimmunology* **2012**, *1*, 1017–1026. [[CrossRef](#)] [[PubMed](#)]
79. Gamrekashvili, J.; Kapanadze, T.; Han, M.; Wissing, J.; Ma, C.; Jaensch, L.; Manns, M.P.; Armstrong, T.; Jaffee, E.; White, A.O.; et al. Peptidases released by necrotic cells control CD8+ T cell cross-priming. *J. Clin. Invest.* **2013**, *123*, 4755–4768. [[CrossRef](#)] [[PubMed](#)]
80. Gamrekashvili, J.; Greten, T.F.; Korangy, F. Immunogenicity of necrotic cell death. *Cell. Mol. Life Sci.* **2015**, *72*, 273–283. [[CrossRef](#)] [[PubMed](#)]
81. Adkins, I.; Fucikova, J.; Garg, A.D.; Agostinis, P.; Špišek, R. Physical modalities inducing immunogenic tumor cell death for cancer immunotherapy. *Oncoimmunology* **2014**, *3*, e968434. [[CrossRef](#)] [[PubMed](#)]

- 82. Garg, A.D.; Agostinis, P. ER stress, autophagy and immunogenic cell death in photodynamic therapy-induced anti-cancer immune responses. *Photochem. Photobiol. Sci.* **2014**, *13*, 474–487. [[CrossRef](#)] [[PubMed](#)]
- 83. Chen, B.; Xu, Y.; Roskams, T.; Delaey, E.; Agostinis, P.; Vandenheede, J.R.; de Witte, P. Efficacy of antitumoral photodynamic therapy with hypericin: Relationship between biodistribution and photodynamic effects in the RIF-1 mouse tumor model. *Int. J. Cancer J. Int. Cancer* **2001**, *93*, 275–282. [[CrossRef](#)] [[PubMed](#)]
- 84. Thong, P.S.P.; Olivo, M.; Kho, K.-W.; Bhuvaneswari, R.; Chin, W.W.L.; Ong, K.-W.; Soo, K.-C. Immune response against angiosarcoma following lower fluence rate clinical photodynamic therapy. *J. Environ. Pathol. Toxicol. Oncol.* **2008**, *27*, 35–42. [[CrossRef](#)] [[PubMed](#)]
- 85. Hunt, D.W.; Jiang, H.; Granville, D.J.; Chan, A.H.; Leong, S.; Levy, J.G. Consequences of the photodynamic treatment of resting and activated peripheral T lymphocytes. *Immunopharmacology* **1999**, *41*, 31–44. [[CrossRef](#)]
- 86. Fox, F.E.; Niu, Z.; Tobia, A.; Rook, A.H. Photoactivated hypericin is an anti-proliferative agent that induces a high rate of apoptotic death of normal, transformed, and malignant T lymphocytes: Implications for the treatment of cutaneous lymphoproliferative and inflammatory disorders. *J. Invest. Dermatol.* **1998**, *111*, 327–332. [[CrossRef](#)] [[PubMed](#)]



© 2016 by the authors; licensee MDPI, Basel, Switzerland. This article is an open access article distributed under the terms and conditions of the Creative Commons Attribution (CC-BY) license (<http://creativecommons.org/licenses/by/4.0/>).